Blow-up and Global Similarity Solutions for Semilinear Third-Order Dispersive PDEs

Koçak, Huseyin

Award date:
2015

Awarding institution:
University of Bath

Blow-up and Global Similarity Solutions for Semilinear Third-Order Dispersive PDEs

submitted by

Hüseyin Koçak

for the degree of Doctor of Philosophy

of the

University of Bath

Department of Mathematical Sciences

March 2015

SUMMARY

Blow-up and global self-similar solutions of the *semilinear dispersion equation*

$$u_t = u_{xxx} + \mu(|u|^{p-1}u)_{xx} \quad \text{in} \quad \mathbf{R} \times \mathbf{R}_+, \quad p > 1,$$

with sufficiently good initial data $u(x,0) = u_0(x)$ in $\mathbf{R}$, for $\mu = \pm 1$, are studied. This equation represents a kind of shallow water model, where, unlike the classical KdV and mKdV equations, the leading nonlinear operator is of the second order, meaning unstable, stable, and "semi-stable" (e.g., for the term $\pm(u^2)_{xx}$). Actually, such an approximation implies that second-order diffusion-like (or forward and backward "porous medium operators") play a leading and key role in contrast to more standard first-order ones.

There are various numerical and analytical challenges in order to observe admissible profiles due to the highly oscillatory nature of the problem, in contrast to parabolic equations. The classification of the solutions governed by self-similarity is given in terms of the initial data, p and μ, where the numerical experiments play a key role. A reliable numerical algorithm for large step sizes, called an exponentially fitted Runge–Kutta (EFRK) method, is proposed for the corresponding second-order ODE of the first critical exponent $p = p_0 = 2$ and the second Painlevé equation related to the KdV equation.

Lastly, single-point blow-up similarity solutions for nonlinear extension of the problem,

$$u_t = (|u|^n u)_{xxx} \pm (|u|^{p-1}u)_{xx} \quad \text{in} \quad \mathbf{R} \times \mathbf{R}_+, \quad n > 0 \quad \text{and} \quad p > n + 1,$$

is very briefly studied. Although the studies on nonlinear dispersion equations have been popular in the mathematical literature for at least the last fifty years, these third-order equations were not investigated in the literature in the sense of self-similarity.

ACKNOWLEDGEMENTS

I would first like to extend my sincerest gratitude to my supervisors Prof. C. J. Budd and Prof. V. A. Galaktionov. This thesis would not exist without their scientific guidance and also personal support. I will always be very grateful to Prof. Budd for all his kind and great help during the project. It was a great pleasure to have Prof. Galaktionov's deep mathematical insight in the project. Turkish delight and coffee will always be ready whenever you want.

Many thanks go to Prof. J. I. Diaz for his great support during my 6 months visit in the Universidad Complutense de Madrid. It was such a nice academic and personal experience.

I would also like to thank the EU FP7 People Marie Curie ITN 'Fronts and Interfaces in Science and Technology (FIRST)' project (Grant Agreement Number 238702) for sponsoring my PhD.

I would like to say huge thanks to Ray Fernandes, Elvijs Sarkans, Acyr Locatelli, James Clarke, Curdin Ott and Melina Freitag for their great friendship. Another huge thanks go to my officemates, especially for joining my Kinder surprise egg break. A warm thanks also go to all the students and staff of the Department of Mathematical Sciences. I would like to say many thanks to Fehmi, Kağan, Nuray & Mehmet, Murat, Batı, Douglas, Tülay, Mustafa, Osman, Deniz, Özgü, İnan, and also all my teammates in FC Assembly Inn and the departmental football team Big Red Machine, for making my life in Bath easier and fun.

Special thanks go to Utku Erdoğan, Murat Sarı, Adrian Hill, Jonathan Evans, Euan Spence, Manuela Chaves, Ben Boyle for fruitful discussions about the thesis.

There is not such a word to describe my gratitude enough for my dear mother, Rabia Koçak, and my dear father, Osman Koçak. Thank you very much for all your support and patience (iyiki varsınız!).

Last but definitely not least, my biggest thank goes to my dear wife, Hande Koçak. Thank you very much for being the best thing in my life since 20/05/2003 (Seni Çok Fazla Kocaman Büsbüyük Seviyorum!).

To the memory of my friends, Ahmet Erdem (Hacı) and Emel & Özgür Subaşıay, who were school teachers and died in the Van-Turkey earthquake on 23/10/2011.

Contents

Chapter 1

Introduction

1.1 Third-order models to study and methodology

In this thesis we study the blow-up and global similarity solutions of the semilinear dispersion PDE,

$$u_t = u_{xxx} \pm (|u|^{p-1}u)_{xx} \quad \text{in} \quad \mathbf{R} \times \mathbf{R}_+, \quad p > 1, \tag{1.1}$$

with bounded initial data which decays suitably to zero at spatial infinity,

$$u(x,0) = u_0(x) \quad \text{in} \quad \mathbf{R}. \tag{1.2}$$

Asymptotic behaviour of the model equation (1.1) incorporating the third and second-order derivatives with nonlinearity are intriguing since it has well-known "neighbouring" equations, such as the KdV and Cahn-Hilliard equations, which will be mentioned in the next chapter. The '+' case and '−' case will imply the sign of the nonlinear term in PDE (1.1). Considering the equation (1.1) with the initial data (1.2) as a Cauchy problem (CP), we introduce the self-similar solution, which has the form

$$u(x,t) = (\sigma(T-t))^{\alpha}\theta(y,\tau), \quad y = x/(\sigma(T-t))^{\beta}, \quad \tau = -\sigma \ln(\sigma(T-t)), \tag{1.3}$$

where $\sigma = \pm 1$, T is the unknown blow-up time (we will generally take $T = 0$ for convenience), $\alpha < 0$ and $\beta > 0$ are parameters (irrelevant with the initial data, σ and T) to be determined. We study the blow-up self-similar (also known as backward self-similar) solutions as $t \to T^-$ when $\sigma = 1$, and the global self-similar (also known as forward self-similar) solutions as $T < t \to \infty$ when $\sigma = -1$. Indeed, for $\sigma = \pm 1$, we study the asymptotic behaviour, as $\tau \to \infty$, of the solution $\theta = \theta(y, \tau)$ satisfying the rescaled PDE. If θ converges to some steady state as $\tau \to \infty$, then the independent of τ stationary solution $f(y) \equiv \theta(y, \tau)$ satisfies the corresponding rescaled ODE. By substituting (1.3) into (1.1), and equating powers of $(\sigma(T - t))$, we obtain the values of $\alpha < 0$ and $\beta > 0$. Formally, the blow-up solution is called single-point for $\beta > 0$, regional for $\beta = 0$ and global for $\beta < 0$. For proposed equations (1.1), we essentially study the single-point self-similar solutions blowing-up at $t = T$ and the origin $x = 0$, i.e., the blow-up set, which will be described in the next chapter, contains the origin only. Due to strong localization phenomenon in the formation of single-point singularity, in general, the boundary conditions are asymptotically irrelevant. Hence, in this thesis, we mainly focus on the Cauchy problem for (1.1) with (1.2). The first critical exponent $p_0 = 2$ is obtained using mass conservation. As a pleasant surprise, we also find the second critical exponent $p_1 = 3/2$ by conservation of the first moment. The order of the corresponding rescaled ODE can be reduced by integration for p_0 and p_1, in contrast to other critical exponents $p = p_k = 1 + 1/(k + 1)$, $k > 1$. Because of the highly oscillatory tail of solutions for $p > 1$, which is a problem not available for parabolic PDEs, it is not easy to observe reliable similarity profiles analytically and even numerically. A delicate analysis must be done in order to distinguish admissible solutions. Numerical experiments play important role in our study to analyse the problem. A formal instability, invariant subspace behaviour and bifurcation points analyses are also presented. The behaviour of solutions are classified in terms of mass, p and the sign of the nonlinear part.

We have replaced

$$u^p \mapsto |u|^{p-1}u \tag{1.4}$$

in (1.1) for solutions of changing sign. Although (1.4) is irrelevant for the solutions that remain non-negative, this form allows us to also consider solutions that may change sign, and discuss importance of partially or completely negative solutions (which actually have less physical significance) in the Cauchy problem. Nevertheless, we also pay attention to the Cauchy problem for the analytical form

of (1.1)

$$u_t = u_{xxx} \pm (u^p)_{xx} \quad \text{in} \quad \mathbf{R} \times \mathbf{R}_+, \quad p > 1. \tag{1.5}$$

One can see that (1.4) makes no sense when p is odd. It is also worth mentioning that (1.1) is not time-reversible in contrast to the KdV equation, i.e., $(t, x) \mapsto u(t, x)$ solves the '$-$' case of (1.1), but $(t, x) \mapsto u(-t, -x)$ does not also solve the '$-$' case of (1.1). On the other hand, non-time-reversibility is the same for (1.5) when p is odd, but the sign in (1.5) is irrelevant when p is even (via $u \mapsto -u$). We investigate the self-similar solutions of both (1.5) and its *signed* form (1.1), for appropriate values of $p > 1$.

A fully nonlinear extension of the semilinear equation (1.1) can be given as

$$u_t = (|u|^n u)_{xxx} \pm (|u|^{p-1} u)_{xx} \quad \text{in} \quad \mathbf{R} \times \mathbf{R}_+, \quad n > 0 \quad \text{and} \quad p > n + 1. \tag{1.6}$$

For the Cauchy problem, intuitively speaking, a continuous *homotopic deformation* (*homotopy* limit or *homotopy* connection), as $n \to 0^+$, can be performed to connect the semilinear equation (1.1), in order to either use or find its properties, such as admissible highly oscillatory behaviour. We refer to [23, Section 4.2.6] and [48, pp. 1801–1803] for extra details and applications of the solutions of changing sign. We will very briefly discuss the similarity solutions of (1.6) numerically.

1.2 Main results and structure of the thesis

Before moving on to presenting new studies, we begin with a detailed literature review in Chapter 2. We firstly visit some well-studied models of the third-order PDEs with their psychical applications. Finite time blow-up and the role of self-similarity in the evolution PDEs are discussed in Section 2.2. Recent results for "neighbouring" models of the semilinear PDE (1.1), such as the Cahn-Hilliard equation, the semilinear PDE with absorption and the KdV equation, are mentioned in Section 2.2.1.

In Chapter 3, we begin the actual study with the blow-up similarity solutions for the unstable '$-$' case of semilinear PDE (1.1), with the first critical exponent $p = p_0 = 2$, which is determined by using conservation of mass, i.e.

$$u_t = u_{xxx} - (|u|u)_{xx}. \tag{1.7}$$

We also pay attention to the analytical form of the above equation, which is the "semi-stable" case,

$$u_t = u_{xxx} - (u^2)_{xx}. \tag{1.8}$$

After constructing the exact blow-up self-similar form for (1.7) as

$$u(x,t) = (T-t)^{-1/3} f(y), \quad y = x/(T-t)^{1/3}, \tag{1.9}$$

where T is the unknown blow-up time (we take $T = 0$ for convenience), we arrive the following ODE

$$f''' - \frac{1}{3} f - \frac{1}{3} f' y - (|f|f)'' = 0. \tag{1.10}$$

We particularly look for the profiles $f = f(y)$ that are suitably decaying at infinity. On the other hand, by recalling the global self-similarity form

$$u(x,t) = (t-T)^{-1/3} f(y), \quad y = -x/(t-T)^{1/3}, \tag{1.11}$$

for the stable '+' case,

$$u_t = u_{xxx} + (|u|u)_{xx}, \tag{1.12}$$

we arrive at the same ODE (1.10). This actually means that the blow-up similarity profiles of (1.7) will also be representing the global similarity profiles of (1.12). Fortunately, the third-order ODE (1.10) can integrated once for $p = p_0 = 2$ to obtain

$$f'' - \frac{1}{3} y f - (|f|f)' = 0. \tag{1.13}$$

We pay attention to the above second-order ODE with zero integration constant, in order to obtain conservative profiles. However, we also briefly discuss the behaviour when the integration constant is non-zero. After the discussion on the asymptotic and algebraic solutions of the corresponding ODEs, the numerical construction is given. According to the numerical experiments and perturbation results on the second-order ODE, we establish that there exists an unbounded continuous family of blow-up self-similar profiles parameterized by initial mass for the unstable '$-$' case (1.7). However, such an existence result is not valid for large enough negative initial mass for the "semi-stable" case (1.8) (i.e. analytical form of (1.7)). The behaviour of profiles is carefully explained, which is also supported by figures.

In Chapter 4, we study the blow-up similarity solutions of (1.12), i.e. the stable '+' case of semilinear PDE (1.1) with the first critical exponent $p = p_0 = 2$.

Constructing the blow-up similarity form (1.9) for (1.12) and integrating the corresponding ODE once yields

$$f'' - \frac{1}{3}yf + (|f|f)' = 0. \tag{1.14}$$

Similar to the previous chapter, recalling the global similarity form (1.11) for (1.7) yields the same ODE (1.14), which means that the blow-up similarity profiles of (1.12) will be representing the global similarity profiles of (1.7). Numerical and perturbation results suggest the non-existence of blow-up self-similar profiles of (1.12) parameterized by initial mass. A detailed explanation with figures is given in order to classify such behaviour carefully.

Chapter 5 contains an efficient numerical technique, which is called an exponentially fitted Runge-Kutta (EFRK) method, with large step sizes for the prototype of the second-order ODEs studied in this thesis. Derivation of the method with suitable reference sets and parameters is given. We apply the proposed method to the second Painlevé equation, which is related to the KdV equation, and the analytical form of (1.14). We show that the EFRK method is more efficient to catch the certain behaviour of the problem for large step sizes, in comparison to the classical fourth-order Runge-Kutta method. The results of this chapter appear in the paper 'Numerical study of the asymptotic of the second Painlevé equation by a functional fitting method' (with U. Erdoğan, 2014) published in the Mathematical Methods in the Applied Sciences.

In Chapter 6, we study the semilinear dispersion PDE (1.1) for arbitrary values of $p > 1$. Fortunately, we also simplify the rescaled third-order ODE by integration for the second critical exponent $p = p_1 = 3/2$, where the first moment is formally conserved. Existence and non-existence of similarity profiles for $p = p_1 = 3/2$ are numerically obtained, similar to the first critical exponent case $p = p_0 = 2$ in Chapter 3 and 4. We next visit the spectral properties of the rescaled linear operator, which is used in the stability analysis of the linearisation of the rescaled PDE for arbitrary values of $p > 1$. Stability, invariant subspaces and bifurcation points analysis are given, under some assumptions, in order to give characteristics of the observed rescaled solutions. However, such analysis remains open due to the lack of integral calculation for growing oscillatory tails. Algebraic solutions of the rescaled ODE are mentioned, in order to enlighten non-symmetric (to 0) oscillatory tails, which are observed in the numerical results for $p > 1$. The behaviour of the rescaled ODE for arbitrary values of $p > 1$ is

given with figures, which suggest the existence of similarity solutions close to the critical exponents $p = p_k = 1+1/(k+1)$, $k = 2, 3, ...$ Lastly, some aspects on the original semilinear PDE are discussed according to the experiments from analysis of the rescaled ODEs. We also illustrate some numerical results for the original PDE for $p > 1$. For instance, for $p = p_0 = 2$, we observe an admissible non-zero stationary global similarity solution for the '+' case of the rescaled PDE, which is one of the obtained similarity profiles in Chapter 3.

Chapter 7 briefly looks at the similarity solutions of the nonlinear dispersion equation (NDE) (1.6). Firstly, some well-known NDEs are visited. In particular, we study the critical case $p = n + 2$, $n > 0$, where we can simplify the rescaled nonlinear equation by integrating once. We briefly present some aspects, such as existence of the blow-up similarity profiles for the '$-$' case and the non-existence for the '+' case with given initial condition, on the behaviour of similarity profiles of the corresponding ODE, especially as $n \to 0^+$ and $n \to \infty$, by using mathematical and numerical tools. The achieved results in Chapter 3, 4, 6 and 7 are in preparation for publication with C. J. Budd and V. A. Galaktionov.

Chapter 8 concludes with an overview of the achievements and limitations in the thesis. Future possible research topics, with planned ones, are also stated.

Appendix A briefly gives some comments on the similarity solution of the semilinear dispersion equation with absorption, which is studied in [21]. Algebraic solutions and numerical illustrations are given, in order to enlighten previous (and possible future) studies.

Chapter 2

Literature Review

2.1 A general semilinear third-order model and related equations

In recent years, there have been various notable contributions to both the theory and applications of partial differential equations (PDEs) of the form in [1, 2],

$$u_t = u_{xxx} + F(u, u_x, u_{xx}). \tag{2.1}$$

The classical and most studied example is the *generalised Korteweg-de Vries* (gKdV) equation [5],

$$u_t = u_{xxx} + (u^p)_x, \tag{2.2}$$

where $p > 1$ is an integer. We essentially obtain the KdV equation with $p = 2$ and the *modified* KdV (mKdV) equation with $p = 3$. These are completely integrable and have many applications to physics, e.g. the evolution of long waves in shallow water. Birth process of the KdV began with the experiments in long shallow basins by J. S. Russel in 1834 [3], followed by the mathematical investigations by Boussinesq in 1872 [4] and ended with the article by Korteweg and De Vries in 1895 [5]. The best known class of special solutions of the KdV equation are solitary waves (or more precisely, solitons) that are localised (asymptotically constant at infinity) and travel at constant speed without change in its shape (initial profile). Global existence and uniform boundedness for the solutions of the gKdV equation in H^1 (which, from the conservation laws, appears as a

natural space to study the solutions) are well known for $p < 5$, which is called mass-subcritical case [6]. The energy (see (2.38)) for (2.2) is always supercritical, but the mass (L^2-norm, see (2.38)) is supercritical for $p > 5$ [7]. The mass-supercritical case is still very unclear. Blow-up in finite time may occur for $p > 5$, however existence of such blow-up solutions in H^1 is still an open problem. The case $p = 5$ is called mass-critical (L^2-critical) [8] with global existence results for sufficiently small initial mass in [9], and finite time blow-up solutions existence in [10]. Therefore self-similar blow-up solutions may be studied for $p \geq 5$, such as numerical studies in [11, 12, 13, 14, 15]. Let us also mention global well-posedness for small inital data in the homogeneous Besov space (which is slightly larger than the homogeneous Sobolev space) for the gKdV equation (where $u^p \mapsto |u|^{p-1}u$), when $5 \leq p \in \mathbf{R}$ [16]. It is also well known that the KdV equation can be reduced to the second Painlevé equation via similarity form, which is discussed in Chapter 5. The KdV type equations play an important role in understanding linear and nonlinear dispersive behaviour of other more complicated problems. A detailed history and properties of the KdV equation can be found in [17, 18, 19, 20].

Recently, asymptotic large-time and small-time behaviour of the *linear dispersion* equation (*Airy equation*)

$$u_t = u_{xxx} \quad \text{in} \quad \mathbf{R} \times \mathbf{R}_+, \tag{2.3}$$

and self-similar solutions of the *semilinear dispersion* equation

$$u_t = u_{xxx} - |u|^{p-1}u \quad \text{in} \quad \mathbf{R} \times \mathbf{R}_+, \quad p > 1, \tag{2.4}$$

were studied in [21]. A class of similarity solutions called very singular solutions (VSSs) for $1 < p < p_0$, where the critical *Fujita* exponent $p = p_0 = 4$, were discussed. Additionally, Hermitian spectral theory for the *linear dispersion* equation was developed in [21], in order to enlighten bifurcations, branching and asymptotic behaviour of the related semilinear and nonlinear equations, such as

$$u_t = (|u|^n u)_{xxx} \quad \text{and} \quad u_t = (|u|^n u)_{xxx} - |u|^{p-1}u \quad \text{in} \quad \mathbf{R} \times \mathbf{R}_+, \tag{2.5}$$

where $n > 0$ and $p > n + 1$ are fixed exponents [22]. Global self-similar solutions governed by *nonlinear eigenfunctions* for the first equation and very singular similarity solutions for the second equation of (2.5) respectively were studied in

[22]. Moreover, studies on higher-odd-order analogies of (2.3), (2.4) and (2.5) can also be found in [21, 22].

A third-order PDE with a quadratic operator

$$u_t = \alpha u_{xxx} + \beta(u_x)^2 + \gamma u^2, \tag{2.6}$$

is studied in [23, Chapter 4], in order to obtain exact periodic solutions via an invariant subspaces (trigonometric one) method. For $\alpha = \beta = \gamma = 1$, essentially for the *KdV equation with source*, an explicit self-similar solution appears as

$$u(x,t) = \frac{1}{T-t}\,\cos^2\left[\frac{1}{2}(x-t)\right], \tag{2.7}$$

where $T > 0$ is the finite blow-up time. This is called a *blow-up soliton solution* that moves with constant unit speed and blows-up as $t \to T^-$ everywhere excluding the points $x_k = T + \pi(2k+1)$, $k = 0, \pm 1, \pm 2, ...$, where $u(x, T^-) = 0$ [23]. Blow-up problems for higher odd-order type of (2.6) are still open.

Studies on the model equations incorporating odd and even-order derivatives with nonlinearity are also intriguing. Let us cite a nonlinear dispersive-dissipative entity $DD(k,m,n)$ [24]

$$u_t + a(u^m)_x + (u^n)_{xxx} = \mu(u^k)_{xx}, \quad a, \mu = \text{const.}, \tag{2.8}$$

which is a combination of the fully nonlinear variant of the KdV equation $K(m,n)$ [25]

$$u_t + a(u^m)_x + (u^n)_{xxx} = 0, \tag{2.9}$$

and a family of fully nonlinear Burgers equation $B(m,k)$

$$u_t + a(u^m)_x = \mu(u^k)_{xx}. \tag{2.10}$$

A brief discussion about nonlinear dispersion equations (NDEs) will be given in Chapter 7. A classic example of $DD(k,m,n)$ is the *KdV-Burgers* (KdVB) equation,

$$u_t + uu_x + bu_{xxx} = \mu u_{xx}, \tag{2.11}$$

which is not integrable in contrast to both the KdV equation ($\mu = 0$) and Burgers equation ($b = 0$). The KdvB equation arises as a model equation in many different scientific applications, such as the propagation of waves on liquid-filled elastic

tubes [26], the behaviour of magneto-acoustic waves in a cold plasma in the presence of effective electron-ion collisions [27], the flow of liquids containing gas bubbles [28], turbulence [29] and ferroelectricity [30, 31]. Another example is the *Sharma-Tasso-Olver* (STO) equation [32, 33],

$$u_t + \alpha(u^3)_x + \frac{3}{2}\alpha(u^2)_{xx} + \alpha u_{xxx} = 0, \tag{2.12}$$

which is integrable and appears in some scientific applications, especially with multi-kink solutions [34, 35]. Let us briefly point out the right hand side of (2.8) via following the *porous medium equation* (PME),

$$u_t = \mu(|u|^{k-1}u)_{xx}, \tag{2.13}$$

where $k > 1$ and $\mu = \pm 1$. It is called *forward in time* when $\mu = 1$ and *backward in time* PME when $\mu = -1$. In the case of $\mu = 1$, a general existence theory for the non-negative solution $u(x,t)$ of (2.13) with suitable initial data in $L^p(\mathbf{R})$, $1 \leq p \leq \infty$, is well established [36]. For $\mu = -1$, the problem is not well-posed and the solution $u(x,t)$ or its derivatives blow-up in arbitrarily small times [37]. It is also worth mentioning that (2.13) is called the *Fast Diffusion equation* (FDE) when $0 < k < 1$, which is also well investigated. Although the general even-order problems are more studied than the general odd-order problems in the literature, we also refer to a number of papers as a guide on the theory and applications of the odd-order PDEs; see [38, 39, 40, 41, 42, 43, 44, 45] and [23, Chapter 4].

Roughly speaking, such linear PDEs containing both odd and even-order (with suitable signs) derivatives generally display both dispersive and dissipative behaviour, but not always [46, pp. 234–237]. For instance, let us consider the linear dispersion equation (or Airy equation) (2.3), allowing solutions to be complex-valued, and assume it has a *plane wave* solution

$$u(x,t) = A\exp\left(i[kx - \omega t]\right), \tag{2.14}$$

where A is the amplitude, k (real valued) is the wave number which equals $2\pi/\lambda$, where λ is the wavelength, and ω (real or complex-valued) is the angular frequency which equals $2\pi/T$, where T is the period. Substituting (2.14) into (2.3) yields

$$\omega = \omega(k) = k^3, \tag{2.15}$$

which is called the *dispersion relation* for the Airy equation. We thus have the solution $u(x,t) = A\exp(ik[x-k^2t])$. Informally, dispersion means that waves of different frequencies move at different velocities. $c_p = \omega/k = k^2$ is called the *phase velocity*, which means higher frequency waves have a faster phase velocity than lower frequency ones for this equation. $c_g = \mathrm{d}\Re(w)/\mathrm{d}k = 3k^2 = 3c_p$ is known as the *group velocity*, which means velocity of the wave envelope or a wave packet (contains a range of different frequencies) is different from the phase velocity of the individual component. One can also see that both velocities are always in a rightward direction for the Airy equation. A wave which has equal group and phase velocities, i.e., $c_p = c_g$ (or $w = const \cdot k$), is called non-dispersive. Let us now consider the following linear equation

$$u_t = u_{xxx} + u_{xx}. \tag{2.16}$$

Substituting (2.14) into (2.16) leads to $\omega = \omega(k) = k^3 - ik^2$. We thus obtain the solution $u(x,t) = A\exp(ik[x-k^2t])\exp(-k^2t)$, which decays exponentially as $t \to +\infty$, for real values of k. The first term $\exp(ik[x-k^2t])$ is known as a dispersive term and the second one $\exp(-k^2t)$ is called dissipative term. One can see that the real part of $\omega(k)$ is affected by odd-order spatial derivatives and the imaginary part is affected by even-order spatial derivatives in such PDEs with real coefficients. For small amplitude or high frequency solutions of the semilinear equations, a similar analysis can be done by using the dispersion relation of the linear component of such equations.

The competition between dispersion, dissipation and nonlinearity rarely exhibits a fruitful interaction (with appropriate parameters), such as KdVB and STO equations, which describe nonlinear wave phenomena in the medium appearing in various scientific problems. Solitons are pleasant as an example of nonlinear terms with appropriate parameters in such PDEs cancelling the nonlinear dispersive behaviour of the medium [46]. However the mix of different entities such as dispersive and dissipative behaviour with nonlinearity usually turns into blow-up behaviour, which will be studied for the given PDEs in this thesis. Rosenau [24] has roughly described the difference between the conservation laws of a dispersive system and a dissipative system, according to their relation to the initial startup at all times, via a quote from Archilochus - *"The fox knows many things, but the hedgehog knows one big thing"*. The fox is identified with a dispersive system and the hedgehog with a dissipative system. This

thesis puts both the fox and the hedgehog in the same bag. From a mathematical point of view, we focus on such PDEs involving the third and second-order (with appropriate signs) derivatives with nonlinearity, in order to study blow-up and global self-similar solutions. We refer to [21, 22, 24, 47] for fruitful discussions on the analogy between odd and even-order PDEs.

In the next section, we describe self-similarity in the finite time blow-up solutions of the PDEs.

2.2 Finite time blow-up and self-similarity

Firstly, let us briefly address local existence (in time), global existence, finite time blow-up (global non-existence) and other types of blow-up mentioned in [49, 56], for a given function space in the study of evolution equations, considering the Cauchy Problem for (1.1) and (1.2). If a solution (classical or weak) $u(x,t)$ of the problem exists on $\mathbf{R}\times(0,T)$, for some $T<\infty$, it is known to be a *local* solution. If we call the maximal existence time T_{max}, the solution is called *global* when $T_{max}=\infty$. Namely, it exists for all time, $0<t<\infty$. However, if $T_{max}<\infty$, we say that the solution *blows-up in finite time* or does not exist for all time. It is worth mentioning that if a solution is global (exists for all $0<t<\infty$) but blows-up at infinity, it is called *infinite-time blow-up*. Also, if a solution blows-up at $t=0$, we say that it is an *instantaneous blow-up*. In the case of instantaneous blow-up, when $u(x,t)\equiv\infty$ in $\mathbf{R}\times(0,T)$ for all $T>0$, it is known as *non-existence of the local solution*.

Next, we address the *blow-up set* for a solution $u(x,t)$ in $\mathbf{R}\times(0,T)$ that blows-up at a time $T>0$ as in [49],

$$B(u_0)=\{x\in\mathbf{R}:\exists\ \{x_n\}\to x\ ,\ \{t_n\}\to T^{-}\text{ such that }u(x_n,t_n)\to\infty\}. \quad (2.17)$$

We say that it is a *single-point blow-up* when $B(u_0)$ contains a single point or a *finite-point blow-up* with a finite number of points, a *regional blow-up* when the measure of $B(u_0)$ is finite and positive, e.g. a bounded localization domain, and a *global blow-up* when $B(u_0)=\mathbf{R}$. These types of blow-up are also known as LS-regime, S-regime and HS-regime of blow-up, respectively [49, 50]. Additionally, The single-point and regional blow-up solutions are called *localized*. An example of the single-point, regional and global blow-up can be seen in Figure 2-1.

Another case of the blow-up solution is whether it is possible to have a non-

trivial extension of the solution beyond blow-up, i.e., for $t > T$. If the solution can be continued (or a continuation exists) for some $t > T$, it will be called *incomplete blow-up*. Otherwise, we say that it is a *complete blow-up*, i.e., $u(x,t) \equiv \infty$ in $\mathbf{R} \times (T, +\infty)$. In the case of incomplete blow-up, the solution $u(x,t)$ may continue as bounded immediately after T, which is known to be *peaking blow-up* or may blow-up again, which is called *multiple blow-up*. Each illustration in Figure 2-1 is also an example of the peaking blow-up.

Remark 2.1. *The existence can be discussed in different function spaces. Blow-up may occur in a function space but not in another one. For example, a weak L^1 solution may globally exist while a classical solution blows-up [51]. If a solution blows-up for all choices of function space, we say that it is an* essential blow-up *which generally appears in the case of complete blow-up.*

Remark 2.2. *Blow-up of derivatives of the solution is another aspect. Finite-time blow-up and global non-existence are not equivalent when the spatial derivative blows-up* (gradient blow-up) *[52] or the time derivative* (extinction or quenching) *[49] blows-up in a finite time while the solution stays bounded. It is also worth mentioning that a free boundary may develop an unbounded derivative (i.e. vertical cusp), while the solution of the free boundary problem (FBP) is still regular, e.g. Stefan problem in [53].*

The basic and natural questions for a blow-up mechanism (or singularity formation) in nonlinear evolution problems, such as when, where and how the blow-up occurs, are well studied with detailed fruitful answers and examples in [47, 49, 50, 54, 55, 56, 57, 58].

This thesis focuses on the finite time blow-up solutions of (1.1) and (1.2). More precisely, we suppose that the solution $u(x,t)$ of the problem exists for all $0 < t < T$ and blows-up at the finite time T in the $L^\infty - norm$, i.e.,

$$\sup_x |u(x,t)| \to \infty \quad \text{as} \quad t \to T^-. \tag{2.18}$$

Finite time blow-up phenomena occur in various nonlinear evolution PDEs, such as parabolic, hyperbolic, dispersion and Schrödinger equations, for physical models [22, 47, 59, 60, 61, 62, 63, 64, 65, 66]. Several techniques have been used in order to prove finite time blow-up, such as Kaplan's eigenvalue method [67], concavity method [68], nonlinear capacity method [42], comparison (via maximum principle) method [69], integral representation method [58, Section 5.4], Ground

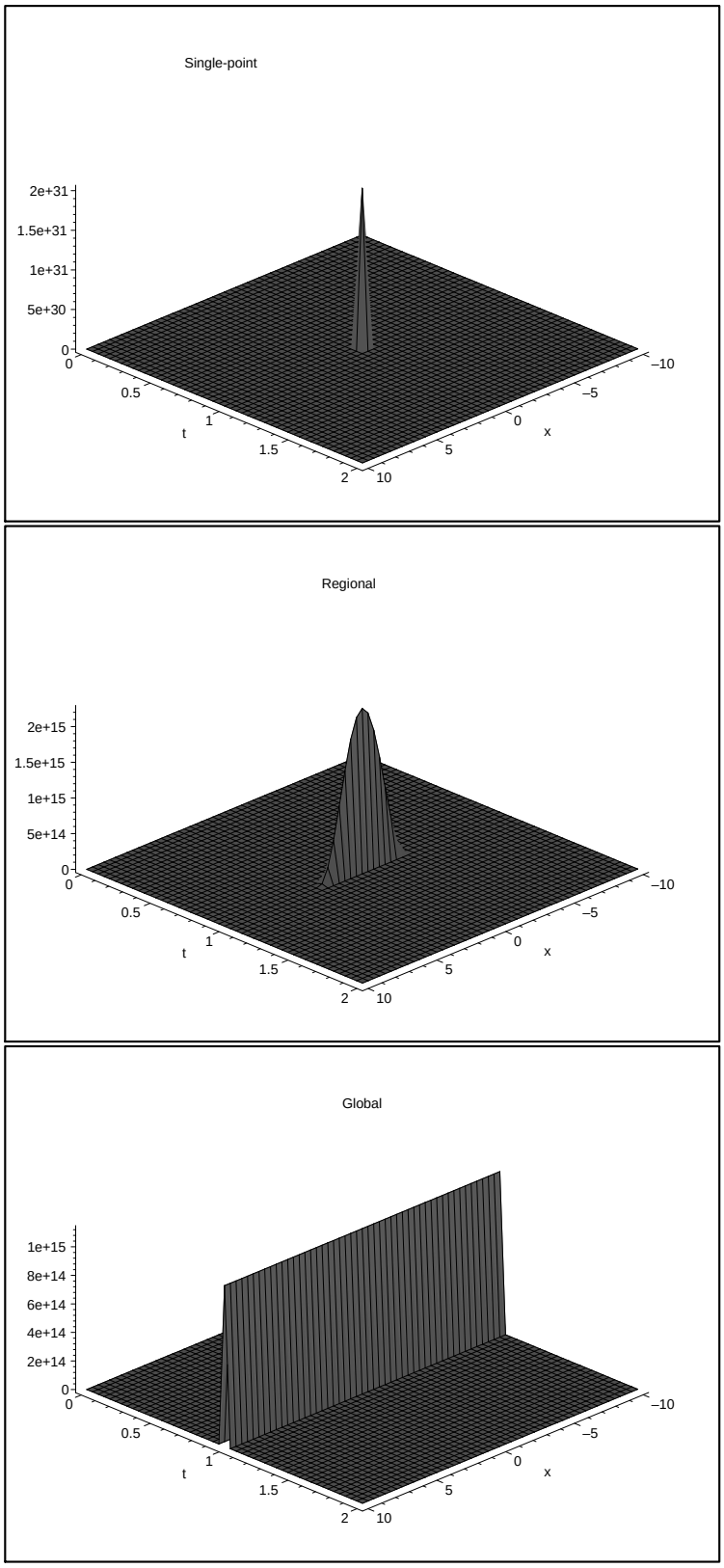

Figure 2-1: *An illustration of the single-point, regional and global blow-up where* $T = 1$.

State (with appropriate ansatz) based method [10, 65] and others [54, 70, 71]. We study the finite time blow-up solutions of the problem via the idea of self-similarity [72, 73].

Similarity solutions arise as a useful tool for analysing and even solving nonlinear problems. There are various techniques, such as travelling waves and other group-invariant methods, of reducing the number of independent variables in order to simplify the problem. However, self-similar solutions are more prevalent in dealing with blow-up. More precisely, self-similarity allows transforming the original PDE into a simpler ordinary differential equation (ODE) with respect to blow-up point, which is relatively easy to be solved numerically or sometimes analytically. Before giving details of the role of self-similarity in finite time blow-up, we visit the following fundamental equations. Let us start with a first-order ODE [57],

$$u_t = |u|^{p-1}u, \quad t > 0; \quad u(0) = u_0, \tag{2.19}$$

where $1 < p < \infty$. One can see that the stationary solution $u = 0$ is unstable. It is known that the solution

$$u(t) = \pm(p-1)^{-1/(p-1)}(T-t)^{-1/(p-1)}, \quad T = T(u_0) = \frac{1}{p-1}|u_0|^{1-p}, \tag{2.20}$$

exists for $0 < t < T$, and also $u(t) \to \infty$ if $u_0 > 0$ and $u(t) \to -\infty$ if $u_0 < 0$, as $t \to T^-$. Therefore we say that the non-trivial solution $u(t)$ blows-up at the finite time $T > 0$ like $(T-t)^{-1/(p-1)}$. The exponent $1/(p-1)$ is called the (algebraic) blow-up rate. A more elementary form of (2.19) can be written as

$$u_t = f(u), \quad t > 0; \quad u(0) = u_0, \tag{2.21}$$

where f is positive and continuous, and $u_0 > 0$. The *Osgood* criterion [74],

$$\int_1^\infty \frac{\mathrm{d}u}{f(u)} < \infty, \tag{2.22}$$

is the necessary and sufficient condition for the occurrence of blow-up in finite time [49].

Remark 2.3. *When we change the sign of the nonlinear part, namely when we consider $u_t = -|u|^{p-1}u$, where $t > 0$, it is also well known that all solutions are global and bounded as $t \to \infty$ with $(T+t)^{-1/(p-1)}$.*

We now take the *heat equation*,

$$u_t = \Delta u \quad \text{in} \quad \mathbf{R}^N \times \mathbf{R}_+, \tag{2.23}$$

with the initial data $u(x,0) = u_0(x)$ in $\mathbf{R}^N$, where Δ is the N-dimensional Laplacian. The suitably defined solution of the problem exists globally in time, and is given by

$$u(x,t) = (4\pi t)^{-N/2} \int_{\mathbf{R}^N} u_0(y) \exp\left(-|x-y|^2/4t\right) \mathrm{d}y, \tag{2.24}$$

which decays like $t^{-N/2}$ as $t \to +\infty$. The exponent $N/2$ is called the decay rate.

A combination of (2.19) and (2.23) yields one of the classical and most studied blow-up problem, which is an initial value problem (IVP) for the semilinear parabolic equation,

$$\begin{aligned} u_t &= \Delta u + |u|^{p-1}u \quad \text{in} \quad \mathbf{R}^N \times \mathbf{R}_+, \\ u(x,0) &= u_0(x) \qquad\quad \text{in} \quad \mathbf{R}^N, \end{aligned} \tag{2.25}$$

where $p > 1$. Early results of (2.25) by Fujita [71] show that all nontrivial nonnegative (i.e. for the initial data $u_0 \geq 0$) solutions blow up in finite time if the blow-up rate $1/(p-1)$ is greater than the decay rate $N/2$, i.e., $1 < p < 1 + 2/N$. On the other hand, there exist both global in time (for sufficiently 'small' initial data) and blow-up nontrivial nonnegative solutions if the blow-up rate is smaller than the decay rate, i.e., $p > 1 + 2/N$. Therefore, $p_0 = p = 1 + 2/N$ is known to be the *Fujita critical exponent*. Later it has been shown by Hayakawa (for $N = 1, 2$) [75] and others (for higher N) [76, 77] that p_0 belongs to the blow-up case, where all nontrivial nonnegative solutions cannot be global.

Fujita-type critical exponents, p_0, have been widely used in the studies of the finite time blow-up for various even and odd-order PDEs [21, 47, 62, 63]. However, it is not generally easy to define the blow-up rate for certain problems. Self-similarity arises here as an useful technique determining the blow-up rate. We suppose the non-trivial blow-up self-similar solutions of (2.25) have the form

$$u(x,t) = (T-t)^{\alpha}\theta(y,\tau), \quad y = x/(T-t)^{\beta}, \quad \tau = -\ln(T-t), \tag{2.26}$$

where $\alpha < 0$ and $\beta > 0$ parameters, and T is the unknown blow-up time. Sub-

stituting (2.26) into (2.25) and equating powers of $(T-t)$ yield

$$\alpha = -\frac{1}{p-1} \quad \text{and} \quad \beta = \frac{1}{2}, \tag{2.27}$$

where $1/(p-1)$ is accurately the blow-up rate for (2.25). One can see that (2.26) reduces the blow-up behaviour as $t \to T^-$ to the asymptotic behaviour of $\theta = \theta(y, \tau)$, as $\tau \to \infty$, where θ satisfies

$$\theta_\tau = \mathbf{A}(\theta) \equiv \Delta_y \theta - \frac{1}{2} y \cdot \nabla_y \theta - \frac{1}{p-1}\theta + |\theta|^{p-1}\theta. \tag{2.28}$$

θ_τ converges to 0 when θ converges to a suitable stationary solution as $\tau \to \infty$ in a certain sense. Thus the right hand side of (2.28) is independent of τ. Namely, an independent of τ non-trivial stationary solution $f(y) \equiv \theta(y, \tau)$ of (2.28) satisfies $\mathbf{A}(f) = 0$, as $\tau \to \infty$. However, non-existence of the exact non-trivial self-similar solutions has been well-known for $p > 1$, when $N < 3$ and for $1 < p \le p_s = (N+2)/(N-2)$ when $N \ge 3$ [78]. In this case, there exist only three trivial constant stationary solutions,

$$f \equiv 0 \quad \text{and} \quad f \equiv \pm(p-1)^{-1/(p-1)}. \tag{2.29}$$

On the other hand, the generic stable asymptotic behaviour of blow-up can be given locally by the following *approximate* self-similarity [49],

$$u(x,t) \approx ((p-1)(T-t))^{-1/(p-1)} f(\eta), \quad \eta = \frac{x}{((T-t)\,|\ln(T-t)|)^{1/2}},$$

where

$$f(\eta) = (1 + c\eta^2)^{-1/(p-1)}, \quad c = (p-1)/4p.$$

Namely, the corresponding rescaled ODE of the original PDE has no non-trivial stationary solution with suitably decay rate at infinity. Let us point out that large classes of PDEs generally have exact self-similar blow-up solutions in contrast to problem (2.25), e.g. higher order generalization of (2.25) for $N = 1$ in [64, 79],

$$u_t = (-1)^{m+1} D_x^{2m} u + |u|^{p-1} u, \quad p > 1. \tag{2.30}$$

Surely, the existence of stationary self-similar profiles does not prove the existence of admissible self-similar solutions of the PDE; however, the non-existence of stationary self-similar profiles means the non-existence of exact self-similar

solutions of the PDE.

Furthermore, it is known that continuation after blow-up for (2.25) is not possible, where complete blow-up occurs. However, it is shown in [80] that the blow-up is incomplete for $p > p_s$, when $N > 2$, under some assumptions. We refer to [49, 58, 81] for all detailed current results with other critical exponents for the problem (2.25). On the other hand, both incomplete and complete self-similar blow-up solutions for (2.30), when $m = 2$, can be found in [59] as fruitful examples.

Remark 2.4. *The technique governed by (2.26) does not always work. For instance, if one replaces $|u|^{p-1}u$ with e^u in (2.25), it can be seen that the blow-up rate is not algebraic. Therefore the exact form of self-similar solutions for exponential nonlinearity can be given as $u(x,t) = -\ln(T-t)+\theta(y,\tau)$. In addition, it is known that approximate self-similar solutions also appear for exponential nonlinearity. Let us also mention that one of the first studies on incomplete blow-up solutions for the parabolic equations can be found in [82], where they particularly focused on exponential nonlinearity in three dimensions.*

2.2.1 Some recent results for "neighbouring" models

More detailed discussions with recent results for the heat equation (2.23) and its higher order generalizations, such as (2.30), can be found in the above mentioned references. The self-similar fundamental solution and spectral theory of the linear dispersive equation (2.3) will be mentioned in Chapter 6. Here, we would first like to visit recent results of the "neighbouring" fourth-order semilinear parabolic equation,

$$u_t = -\Delta\left(\Delta u + |u|^{p-1}u\right) \quad \text{in} \quad \mathbf{R}^N \times \mathbf{R}_+, \quad p > 1, \tag{2.31}$$

which is known as the limit unstable Cahn-Hilliard equation [61]. Considering the Cauchy problem for (2.31) with bounded and integrable initial data $u(x,0) = u_0(x)$, which in most cases decays exponentially at spatial infinity, the blow-up and global similarity solutions of the problem are well studied in [61], particularly for $N = 1$. An exact similarity form was introduced as

$$u(x,t) = (\sigma(T-t))^{-1/2(p-1)} f(y), \quad y = x/(\sigma(T-t))^{1/4}, \quad \tau = -\sigma \ln(\sigma(T-t)), \tag{2.32}$$

where an independent of τ stationary solution $f = f(y)$ satisfies

$$\mathbf{A}(f) \equiv -\Delta\left(\Delta f + |f|^{p-1}f\right) - \frac{\sigma}{4}y \cdot \nabla f - \frac{\sigma}{2(p-1)}f = 0 \quad \text{in} \quad \mathbf{R}^N. \tag{2.33}$$

[61] focused on the radial and suitable decaying (exponential in most cases) solutions, as $y \to \infty$, hence the conditions were imposed as

$$f'(0) = 0, \quad f'''(0) = 0 \quad \text{and} \quad f(y) \to 0 \quad \text{as} \quad y \to \infty. \tag{2.34}$$

In the case of the first critical exponent $p = p_0 = 1 + 2/N$ (conservation in mass case), a countable discrete set of blow-up similarity solutions ($\sigma = 1$) and an unbounded continuous family of global similarity solutions ($\sigma = -1$) parameterized by mass and decaying as $t \to \infty$ were established. It has also been observed in [61] that the family of blow-up similarity solutions is countable and the global similarity for odd solutions is continuous for the second critical exponent $p = p_1 = 1+2/(N+1)$, where the first moment of the solutions is conserved. A sequence of critical exponents $p = p_k = 1 + 2/(N + k)$, $k = 0, 1, 2, ...$, was also detected, which yields bifurcation of similarity solutions at $p = p_k$. Also, under certain assumptions, the set of exponentially decaying similarity profiles was expected to be countable for $p \neq p_0, p_1$ according to the formal analytical and numerical progress in [61]. In short, either decaying in time (global) or blow-up solutions may exist in all cases of $p > 1$, i.e., the absence of the critical Fujita exponent [79]. In addition to that, [61] very briefly mentioned that at the same critical exponents $p = p_k$ the blow-up cannot occur for the limit stable Cahn-Hilliard equation,

$$u_t = -\Delta\left(\Delta u - |u|^{p-1}u\right) \quad \text{in} \quad \mathbf{R}^N \times \mathbf{R}_+, \quad p > 1. \tag{2.35}$$

So a unique classical decaying in time solution is expected for the Cauchy problem.

Let us now visit the semilinear dispersive equation (2.4), which is studied in [21] as the Cauchy Problem with sufficiently good initial data $u(x, 0) = u_0(x)$. [21] introduced self-similar solutions of the very singular type in the form

$$u(x, t) = t^{-1/(p-1)}f(y), \quad y = x/t^{1/3}, \tag{2.36}$$

where f satisfies the ODE

$$f''' + \frac{1}{p-1} f + \frac{1}{3} f' y - |f|^{p-1} f = 0 \quad \text{in} \quad \mathbf{R}. \tag{2.37}$$

Unlike our model (1.1) and the Cahn-Hilliard equation, the rescaled ODE (2.37) cannot be integrated for the critical Fujita exponent $p = p_0 = 4$, which was obtained in [21] by linearised stability analysis of the trival zero solution of (2.4). According to the numerical results via boundary value problem (BVP) solver supplied by *MatLab* taking $f(y_0) = 0$, $f'(y_0) = 0$ and $f(y_1) = 0$, where $y_0 < 0$ and $y_1 > 0$ are boundary points, [21] did not manage to find any reliable admissible profiles, which have nondecaying and/or asymmetric to $f = 0$ oscillatory tails, for $p \leq p_0 = 4$. On the other hand, under certain assumptions, a countable number of subcritical pitch-fork bifurcations was analytically expected at $p = p_k = 1 + 3/(1+k)$, $k = 0, 1, 2, ...$ in [21]. However, a full justification of such behaviour is not easy and remains open due to the highly oscillatory tail of the profiles. In contrast to studies in [21], we will be able to classify similarity profiles for the critical exponents numerically using IVP solvers for the rescaled ODE of (1.1). However, our invariant subspace behaviour and bifurcation point analysis will remain formal. This will be detailed in Chapter 6. We would like to refer Appendix A for new comments on the semilinear dispersion PDE (2.4).

We would like to recall the Cauchy problem for the gKdV equation,

$$u_t + u_{xxx} + (u^p)_x = 0, \quad p > 1,$$

with the initial condition $u(x, 0) = u_0(x)$. As we have stated before, both the KdV ($p = 2$) and the mKdV ($p = 3$) equation are completely integrable and have infinitely many conservation laws for appropriate u_0 (u_0 and its derivatives have fast decay at infinity). For general $p > 1$, the gKdV equation formally has three conserved (in time) quantities

$$\int u \mathrm{d}x, \tag{2.38a}$$

$$\int u^2 \mathrm{d}x, \tag{2.38b}$$

$$\int \frac{1}{2} u_x^2 - \frac{1}{p+1} u^{p+1} \mathrm{d}x, \tag{2.38c}$$

which are conservation of mass, L^2-norm (L^2 mass) and energy, respectively. The conservation of energy is known from Hamiltonian structure of the equation

similar to the nonlinear Schrödinger equation (NLSE). From the conservation of L^2 mass and energy, H^1 appears as a natural space to study solutions, i.e., these two conservation laws can control the H^1 norm. For $p < 5$, using the Gagliardo-Nirenberg inequality [8]

$$\forall v \in H^1(\mathbf{R}), \quad \int |v|^{p+1} \leq C(p) \left(\int v^2 \right)^{\frac{p+3}{4}} \left(\int v_x^2 \right)^{\frac{p-1}{4}}, \tag{2.39}$$

all solutions in H^1 are global and uniformly bounded in time with suitable decay and smooth data, regardless the amount of L^2 mass [10]. A family of explicit soliton solutions of the gKdV for $p > 1$ is well known, such as [6, 8]

$$u(x,t) = c^{\frac{1}{p-1}} Q(c^{\frac{1}{2}}(x - x_0 - ct)),$$

where $c > 0$ and $Q > 0$ (called the ground state) is the solution of the ODE

$$Q_{xx} + Q^p = Q, \quad Q \in H^1(\mathbf{R}), \quad \text{i.e.,} \quad Q(x) = \left(\frac{p+1}{2\cosh^2(\frac{p-1}{2}x)} \right)^{\frac{1}{p-1}}.$$

For the critical case $p = 5$, the L^2 mass of the initial condition plays a critical role. If L^2 mass is sufficiently small, i.e., $\int u_0^2 < \int Q^2$, then the solution is known to be global (in time) and uniformly bounded in H^1 using the inequality (2.39) and the properties of the ground state Q [9, 83]. On the other hand, assuming $\int Q^2 < \int u_0^2 < \int Q^2 + \alpha_0$, for some small $\alpha_0 > 0$, and $\int \frac{1}{2} u_{0x}^2 - \frac{1}{6} {u_0}^6 < 0$, the existence of solutions blowing-up in finite or infinite time in H^1 is known [10]. The supercritical case $p > 5$ is still very unclear in terms of the blow-up solutions. Here, solitons are known to be unstable [84]. It is natural to expect singularities for large initial mass, however there is no rigorous evidence yet. So there is no obstruction to blow-up self-similar solutions for $p \geq 5$. Since the explicit blow-up similarity solutions (in H^1) are not known yet, in contrast to NLSE, we refer to numerical observations [11, 12, 13, 14]. It is also worth mentioning a current study constructing the self-similar solutions for the slightly super-critical gKdV in L^{p+1} with derivative in L^2 [15].

The above studies for the gKdV equation are mainly focused on smooth and regular initial data with fast decay as $|x| \to \infty$. Here, a natural question appears: Are there any other initial data yielding finite time blow-up in the Cauchy problem? A solution (or its derivative) that does not decay has not been studied

extensively. Here, we would like to point out the following two results. Let us first recall the mKdV equation,

$$u_t = u_{xxx} - 6u^2 u_x. \tag{2.40}$$

The blow-up similarity solutions of (2.40) have the form,

$$u(x,t) = (3(T-t))^{-1/3} f(y), \quad y = x/(3(T-t))^{1/3},$$

where $T > 0$ is a given finite blow-up time, and $f = f(y)$ decays suitably and has the following asymptotics

$$f(y) \sim \begin{cases} C\,\mathrm{airy}(y) & \text{as} \quad y \to \infty, \\ d|y|^{-1/4} \sin\left(\frac{2}{3}|y|^{3/2} - \frac{3}{4}d^2 \log(|y|) - \theta_0\right) & \text{as} \quad y \to -\infty, \end{cases} \tag{2.41}$$

where $|C| < 1$, d and θ_0 are constants depending on C [89]. The existence of such solutions are known from the Hastings and McLeod results in [88], by following the properties of the second Painlevé equation [109],

$$\frac{\mathrm{d}^2 f}{\mathrm{d}y^2} = yf + 2f^3 \quad \text{in} \quad \mathbf{R}. \tag{2.42}$$

Here, airy(y) is the Airy function and is a solution of $f'' = yf$. Note that $f(y)$ has exponential fast decay, as $y \to \infty$, and oscillatory slow decay, as $y \to -\infty$, and also its derivatives grow. Such behaviour will be a guide to analysing and classfying the behaviour of our problem. More details for the Airy function can be found in Chapter 3, by setting $y \mapsto 3^{-1/3}y$. A detailed discussion about the second Painlevé equation will be given in Chapter 5 with numerical results. Let us now recall the KdV equation,

$$u_t + u_{xxx} + uu_x = 0, \tag{2.43}$$

with the initial condition $u(x,0) = u_0(x) = u_0$. An interesting result for the Cauchy problem of the KdV equation was recently proposed by Pohozaev, using the nonlinear capacity method. If the initial function u_0 satisfies

$$u_0(x) \sim \begin{cases} A_+ x^\alpha \cos(x^\beta) & \text{as} \quad x \to \infty, \\ A_- |x|^\alpha \exp(-|x|^\beta) & \text{as} \quad x \to -\infty, \end{cases} \tag{2.44}$$

with $\beta > 0$, $\alpha > \beta + 1$ and $A_+ > 0$, then the Cauchy problem for the KdV equation (2.43) with this inital data has a blow-up solution in the appropriate class $W_{\varphi,loc}(\mathbf{R}^2_+)$, where $\varphi(x,t)$ is the test function [47]. We refer to [47, Chapter 7] for more details and fruitful discussions.

Chapter 3

Existence of the Blow-up Similarity Profiles for the Unstable '−' Case with the First Critical Exponent

In this Chapter we focus on the blow-up self-similar solutions for the following PDE of the form (1.1), which is the unstable '−' case,

$$u_t = u_{xxx} - (|u|^{p-1}u)_{xx}, \quad p > 1, \tag{3.1}$$

with appropriate initial data (1.2) in the case of the first critical exponent, $p = p_0 = 2$, which will be determined by conservation of mass. We also pay attention to the unsigned form (obviously, when this makes sense for solutions of changing sign),

$$u_t = u_{xxx} - (u^p)_{xx}, \quad p > 1. \tag{3.2}$$

We observe that there exists an unbounded continuous family of blow-up self-similar solutions parameterized by initial mass for (3.1) when $p = p_0 = 2$. However, such existence is bounded by large enough negative initial mass for (3.2) ("semi-stable"). Let us also mention that if we use the reflections,

$$x \mapsto -x \quad \text{and} \quad t \mapsto -t, \tag{3.3}$$

we obtain another PDE of (1.1), which is the stable '+' case,

$$u_t = u_{xxx} + (|u|^{p-1}u)_{xx}, \quad p > 1. \tag{3.4}$$

Therefore the blow-up similarity profiles of (3.1) will also represent the global similarity profiles of (3.4), which will be discussed later on. Namely, the existence of an unbounded continuous family of blow-up self-similar solutions implies the existence of an unbounded continuous family of global self-similar solutions. Moreover, the global similarity profiles of the equation (3.1) will represent the blow-up similarity profiles of the equation (3.4) via the reflections (3.3), which will be mentioned in Chapter 4.

Recalling the similarity form (1.3) as

$$u_S(x,t) = (\sigma(T-t))^{\alpha} f(y), \quad y = x/(\sigma(T-t))^{\beta}, \tag{3.5}$$

and substituting (3.5) into (1.1) yields following ODE:

$$\begin{aligned} \mathbf{A}_{\pm}(f) \equiv & (\sigma(T-t))^{\alpha-3\beta} f''' \pm (\sigma(T-t))^{\alpha p-2\beta} (|f|^{p-1} f)'' \\ & + \sigma\alpha(\sigma(T-t))^{\alpha-1} f - \sigma\beta(\sigma(T-t))^{\alpha-1} f' y = 0. \end{aligned} \tag{3.6}$$

By equating powers of $(\sigma(T-t))$, we obtain the parameters that make the ODE independent of t as

$$\alpha = -\frac{1}{3(p-1)} < 0 \quad \text{and} \quad \beta = \frac{1}{3} > 0. \tag{3.7}$$

3.1 Blow-up self-similarity and the rescaled equation

According to (3.5) and (3.7), with $\sigma = 1$, we construct an exact blow-up self-similar solutions of (3.1) as

$$u_-(x,t) = (T-t)^{-1/3(p-1)} f(y), \quad y = x/(T-t)^{1/3}, \tag{3.8}$$

where $t < T$ and the function $f = f(y)$, $f \not\equiv 0$, solves the following third-order ODE,

$$\mathbf{A}_-(f) \equiv f''' - \frac{1}{3(p-1)} f - \frac{1}{3} f' y - (|f|^{p-1} f)'' = 0 \quad \text{in} \quad \mathbf{R}. \tag{3.9}$$

We will particularly pay attention to a suitable decay condition (say, exponential) as $y \to \infty$, which will be detailed later on.

Without loss of generality, the blow-up self-similar variables for general solutions of (3.1) and the initial data (1.2) with finite blow-up time $T > 0$ are given

as in (1.3) by

$$u(x,t) = (T-t)^{-1/3(p-1)}\theta(y,\tau), \quad y = x/(T-t)^{1/3}, \quad \tau = -\ln(T-t), \quad (3.10)$$

where $t \in (0,T)$ and the new variable $\tau \in (-\ln T, \infty)$. The rescaled solution $\theta(y,\tau)$ satisfies the third-order equation with the same operator as in (3.9)

$$\theta_\tau = \mathbf{A}_-(\theta) \quad \text{for} \quad \tau > \tau_0 = -\ln T, \quad \theta(y,\tau_0) = \theta_0(y) \equiv T^{1/3(p-1)}u_0(yT^{1/3}). \quad (3.11)$$

We suppose that the solution $u(x,t)$ blows-up at the finite time T in the L^∞ form, i.e,

$$\sup_x |u(x,t)| \to \infty \quad \text{as} \quad t \to T^-,$$

and its blow-up set,

$$B(u_0) = \{x \in \mathbf{R} : \exists\ \{x_n\} \to x\ ,\ \{t_n\} \to T^- \text{ such that } u(x_n,t_n) \to \infty\},$$

contains the origin, $0 \in B(u_0)$. For an arbitrary point $x_0 \in B(u_0)$, we may use the spatial scaling

$$y = (x-x_0)/(T-t)^{1/3}.$$

We are mainly interested in all possible equilibria of $\mathbf{A}_-$ for $\tau \gg 1$. Therefore, by choosing (or reducing T to) $T = 0$ in (3.8) for convenience, we pay attention to the behaviour as $t \to T^-$ that is given by following exact self-similar blow-up solution,

$$u_{BL}(x,t) = (-t)^{-1/3(p-1)}f(y), \quad y = x/(-t)^{1/3}, \quad (3.12)$$

where an independent of the variable τ suitable stationary solution $f(y)$ satisfies the ODE (3.9). It is one of the most natural and the simplest way in the blow-up phenomena as we discussed in Chapter 2.

3.1.1 Global similarity pattern profiles

If we construct the exact global similarity solutions of (3.4) as in (3.5) with $\sigma = -1$ and $x \mapsto -x$, then we have

$$u_{GL}(x,t) = (t-T)^{-1/3(p-1)}f(y), \quad y = -x/(t-T)^{1/3}, \quad (3.13)$$

for $t > T$, where $f(y)$ satisfies the same ODE (3.9) and $T = 0$ again for convenience. Therefore, $f(y)$ describes both blow-up self-similar profiles of (3.1) and global self-similar profiles of (3.4).

3.2 Conservation law: the first critical exponent

If we assume that the solution $u(x,t)$ is integrable (a formal assumption), we have that (1.1) is conservative in mass:

$$\frac{\mathrm{d}}{\mathrm{d}t}\int_{\mathbf{R}} u(x,t)\mathrm{d}x = 0. \tag{3.14}$$

For the exact similarity solutions (3.5), we have

$$\int_{\mathbf{R}} u_S(x,t)\mathrm{d}x = (\sigma(T-t))^{\alpha+\beta}\int_{\mathbf{R}} f(y)\mathrm{d}y, \tag{3.15}$$

which satisfies (3.14) for non-zero rescaled mass, $\int f \neq 0$, only if

$$\alpha+\beta = -\frac{1}{3(p-1)} + \frac{1}{3} = 0 \quad \Rightarrow \quad p = p_0 = 2, \tag{3.16}$$

where p_0 is the first critical exponent. On the other hand, by using (3.15), we also have that the similarity profile f has zero mass for other values of $p > 1$ (see Chapter 6), i.e.,

$$\text{for any} \quad p \neq p_0, \quad \int f = 0. \tag{3.17}$$

Our aim is to study the similarity solutions of the third-order ODE (3.6) with different values of $p > 1$, remembering the conservation law. We expect to face some numerical and analytical difficulties due to both slow decaying highly oscillatory and fast exponential decay nature of fundamental solutions, and also asymmetry property. Fortunately, it can be easily seen that we can integrate (3.6) once for the first critical exponent $p = p_0 = 2$. The rest of this chapter focuses on the blow-up self-similar profiles of the '−' case with analytical and signed form for the first critical exponent. The next chapter will pay attention to the blow-up self-similar profiles of the '+' case, when $p = p_0 = 2$.

3.3 Asymptotic behaviour at infinity for $p = p_0 = 2$

The conservative case $p = p_0 = 2$ plays an important role in our study, in order to enlighten the general values of p. In the case of $p = p_0 = 2$, the equation (3.9) becomes

$$f''' - \frac{1}{3}f - \frac{1}{3}f'y - (|f|f)'' = 0, \tag{3.18}$$

which can be integrated once with the zero integration constant (kind of a " zero-flux condition at infinity", actually meaning an Airy-type radiation condition at infinity to be discussed later on) to give

$$f'' - \frac{1}{3}yf - (|f|f)' = 0 \quad \text{for} \quad y \in \mathbf{R}, \quad f(y) \to 0 \quad \text{as} \quad y \to \infty, \tag{3.19}$$

where we will particularly pay attention to exponentially decaying solutions, as $y \to \infty$, according to the conservation law (3.14). So, this zero integration constant setting removes $f(y) = -1/y$ and $f(y) = -y^2/12 + c_0$ (c_0 is any real number) satisfying the analytical form of (3.18),

$$f''' - \frac{1}{3}f - \frac{1}{3}f'y - (f^2)'' = 0, \tag{3.20}$$

which are not admissible solutions for the conservative case with finite mass. Moreover, $f(y) = -1/y - y^2/12$ is an explicit solution for the analytical form of (3.19), which is also not admissible. We expect to see in the figures for the analytical form that $f(y) = -1/y$ will cause blow-up (become infinite) for large enough negative inital mass. On the other hand, profiles of the analytical form asymptote to the parabola $f(y) = -y^2/12 + c_0$ for the critical value of negative initial mass. For large values of positive initial mass, we also expect to see the effect of $f(y) = -y^2/12 + c_0$, which will be detailed in Section 3.4.1.

By a local analysis, one can see that $\pm 1/y$ for $y < 0$ and $\pm y^2/12 \mp c_0$, $c_0 > 0$, for $|y| < \sqrt{12c_0}$, satisfy the signed equation (3.18). The effect of such explicit solutions to the corresponding ODEs will be displayed. We do not expect to have any singularities for the signed form since $\pm 1/y$ is not effective for $y > 0$. On the other hand, for large enough positive and negative initial mass, we will see the effect of $\pm y^2/12 \mp c_0$, $c_0 > 0$, for $|y| < \sqrt{12c_0}$, which will be detailed in Section 3.4.2. We will also discuss the behaviour of (3.19) when the integration constant is non-zero, where $\pm 1/y$, for $y < 0$, will yield asymmetric (to 0) oscillatory tails.

It will be a guide to analysing admissible behaviour of such third-order ODEs when $1 < p \neq p_0$, which will be discussed in Chapter 6.

The unique admissible solution of the linear part of (3.19),

$$f'' - \frac{1}{3} y f = 0, \tag{3.21}$$

is the *Airy function*, $\mathrm{Ai}(y)$, where $f(y) = \mathrm{Ai}(y)$. The Airy function is one of the special functions with a turning point, where the behaviour changes from exponential to oscillatory (changing sign). Asymptotic behaviour of $\mathrm{Ai}(y)$ is given by [23, pp. 198],

$$f(y) \sim \begin{cases} y^{-1/4} \exp\left(-a_0 y^{3/2}\right) & \text{as} \quad y \to +\infty, \\ |y|^{-1/4} \sin\left(a_0 |y|^{3/2} + A\right) & \text{as} \quad y \to -\infty, \end{cases} \tag{3.22}$$

where $a_0 = \frac{2}{9}\sqrt{3}$ and A is a constant. We also refer to [21, Section 2] for detailed asymptotic expansions and spectral properties of the Airy equation (3.21) by using the reflection $y \mapsto -y$, which will be briefly mentioned in Chapter 6. In Figure 3-1, we display $f(y)$, $|f(y)|$, $f'(y)$, $f''(y)$, $f(y)f'(y)$ and $|f(y)|f'(y)$, where $f(y) = \mathrm{Ai}(y)$. It is well known that $f(y) = \mathrm{Ai}(y)$ is bounded and in $L^1_{loc}(\mathbf{R})$, and also $\int\limits_{\mathbf{R}} f(y) < \infty$. The oscillatory tail of $\mathrm{Ai}^{(k)}(y)$ as $y \to -\infty$, where $k = 1, 2, ...$ is the order of derivative, grows faster as k increases.

According to exponentially decaying behaviour in (3.22) as $y \to \infty$, with respect to the conservation of mass condition (3.14), we consider a one-parameter family of functions with reasonable regularity properties,

$$f(y) = C\,\mathrm{Ai}(y)(1 + o(1)) \quad \text{as} \quad y \to \infty, \quad C = const. \neq 0. \tag{3.23}$$

In order to obtain an admissible solution of (3.19), we will use the exponentially decaying function (3.23) while shooting from $y = \infty$. Therefore, all admissible self-similar profiles f will have the asymptotic behaviour (3.23). For $y \ll -1$, we will also keep in mind that the oscillatory tail must be decaying and symmetric to 0 because of the finite mass condition.

In short, we try to explore admissible blow-up similarity profile $f = f(y, C)$ of the following second-order ODE,

$$f'' - \frac{1}{3} y f - (|f|f)' = 0, \quad -\infty < y < \infty, \tag{3.24}$$

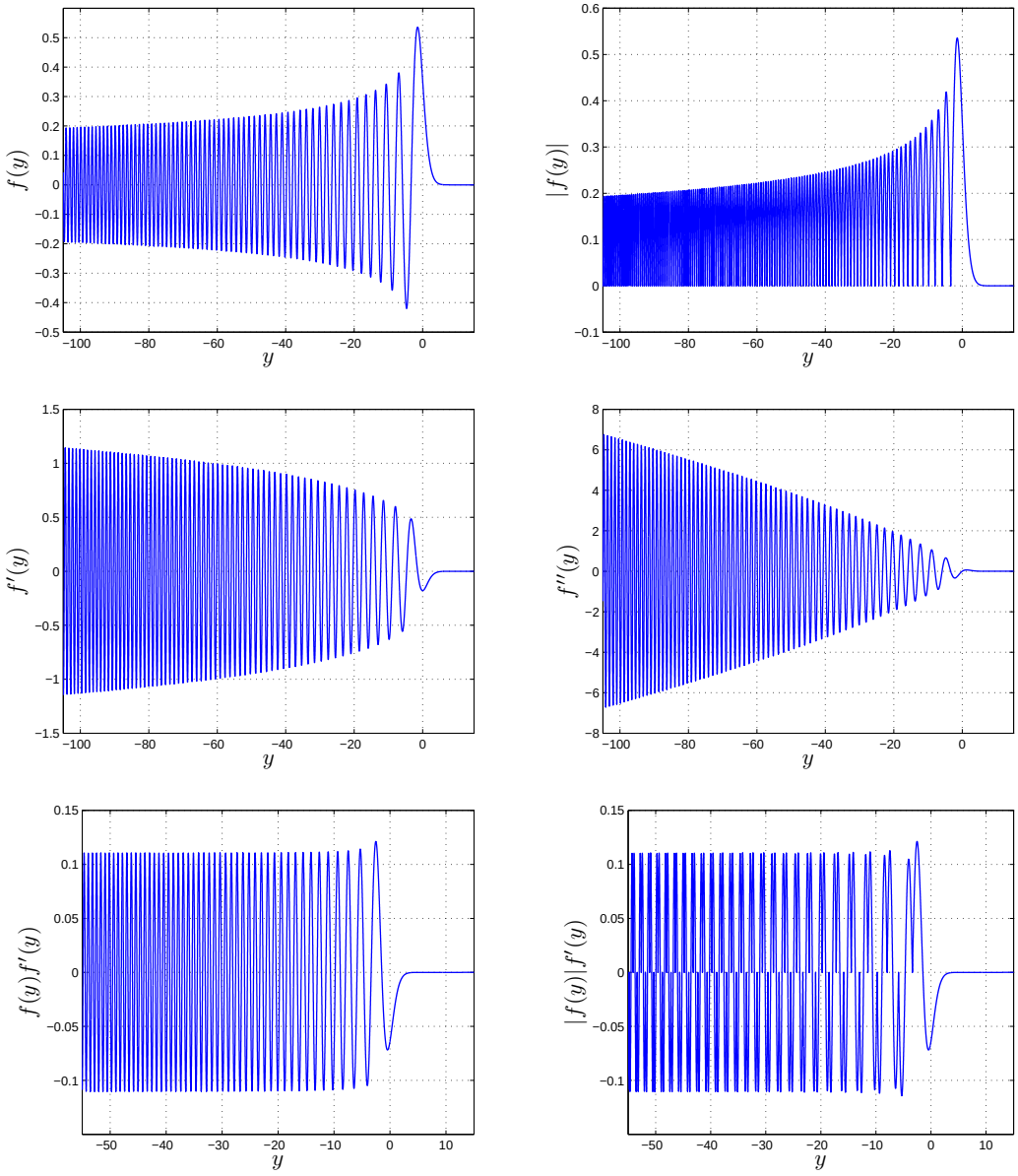

Figure 3-1: *The behaviour of* $f(y)$, $|f(y)|$, $f'(y)$, $f''(y)$, $f(y)f'(y)$ *and* $|f(y)|f'(y)$ *for* $f(y) = \mathrm{Ai}(y)$.

with the boundary condition,

$$f(y, C) \sim C\,\mathrm{Ai}(y) \quad \text{as} \quad y \to \infty, \tag{3.25}$$

where $\mathrm{Ai}(y)$ is the Airy function and $C \neq 0$ varies from $-\infty$ to ∞. Actually, the right-hand conditions are constructed as $f(y_0, C) = C\mathrm{Ai}(y_0)$ and $f'(y_0, C) = C\mathrm{Ai}'(y_0)$, where $y_0 > 0$ is far enough initial point and C is a non-zero real number, which will be detailed in the following section. We classify the solutions of (3.24) and its unsigned form in terms of the values of C (i.e. initial mass).

3.4 Numerical construction of the blow-up similarity profiles

The problem (3.24) and (3.25) can be roughly generalised in the form of

$$f''(y) = G(y, f(y), f'(y)), \quad f(y_0) = f_0, \quad f'(y_0) = f_1. \tag{3.26}$$

Therefore it is not easy to find any specific reliable method and most of the numerical methods for such ODEs are incapable for this problem because of having y, f and f'. Another difficulty is the robust nature of the problem due to strong oscillatory slow decay, as $y \to -\infty$, and the fast exponential decay, as $y \to \infty$.

We have mainly used the *MatLab-R2010b ode45*, *ode15s* solvers to obtain the solutions of the problem (3.19) and (3.25). Additionally, the *Maple-16 rkf45* solver and a two stage exponentially-fitted Runge-Kutta (EFRK) method with two parameters [85, 86] have been used in order to check reliability of the results presented here. Abilities of computing closed form solutions of the differential equations and setting *Digits* to higher than 16 are the advantages of the *Maple-16*. The advantage of the EFRK method is that we can catch the long-time behaviour of the problem even for large step sizes, $h = 0.1$, in y, which will be discussed in Chapter 5. However, the most important advantage of the *MatLab-R2010b* is the computational time. We have set *AbsTol* and *RelTol* to $1e-20$, and *Digits* to 16. We have assigned $\mathrm{Ai}(y) = \mathrm{airy}(3^{-1/3}y)$ and $\mathrm{Ai}'(y) = 3^{-1/3}\,\mathrm{airy}(1, 3^{-1/3}y)$, where $\mathrm{airy}(y)$ is the classical Airy function as a solution of $f'' - yf = 0$ according to the *MatLab* and $\mathrm{airy}(1, y) = \mathrm{airy}'(y)$. We have chosen a far enough inital point on the right-hand side as $y_0 = 15$ in order to have a non-negligible initial

condition. As an example of the values of the initial conditions at $y_0 = 15$ for $C = 1$, *MatLab* calculates $f(15, 1) = \mathrm{Ai}(15) = 3.045738545051102e - 11$ and $f'(15, 1) = \mathrm{Ai}'(15) = -6.860334475160123e - 11$. Obviously, we should increase *Digits* and decrease Error Tools for even large initial points. We would like to mention that we obtain the same behaviours by choosing $y_0 = 20, 25$ and setting *AbsTol* to $1e - 30$.

In the following sections, we focus on the analytical and signed forms of (3.1) regarding to above mentioned numerics, respectively.

3.4.1 Blow-up similarity profiles of the analytical form

Let us firstly consider the unsigned form of (3.24),

$$f'' - \frac{1}{3}yf - (f^2)' = 0, \quad -\infty < y < \infty, \tag{3.27}$$

with the boundary condition (3.25),

$$f(y, C) \sim C\,\mathrm{Ai}(y) \quad \text{as} \quad y \to \infty,$$

where $C \neq 0$ varies from $-\infty$ to ∞. It follows from (3.25) (and Figure 3-1) that $f(y, C) > 0$ increases, while $f'(y, C) < 0$ decreases when $C > 0$, and $f(y, C) < 0$ decreases, while $f'(y, C) > 0$ increases when $C < 0$, as y decreases from ∞. Similar to studies on the second order ODE [87, 88, 89] if we divide the (y, f) plane into four regions, any solution $f = f(y, C)$ of (3.27) will be strictly convex in the regions (1) $f > 0, y/3 + 2f' > 0$ and (3) $f < 0, y/3 + 2f' < 0$, and strictly concave in the regions (2) $f > 0, y/3 + 2f' < 0$ and (4) $f < 0, y/3 + 2f' > 0$. Based on these properties and the numerical experiments (see figures below), we construct the solutions of the problem as C varies from $-\infty$ to ∞ and make the following conjecture.

Conjecture 3.1. *Let C be a non-zero arbitrary real number and $f = f(y, C)$ be the solution of (3.27) with boundary condition (3.25). There exists a unique C^* such that*

- *If $C < C^*$, then $f(y, C)$ has a pole (becomes infinite) at a finite y^* depending on C,*

$$f(y, C) \sim (y^* - y)^{-1} \quad \text{as} \quad y \downarrow y^*. \tag{3.28}$$

  $f(y, C)$ is a concave and monotonically increasing negative solution in (y^*, ∞),

i.e. $f(y,C) < 0, f'(y,C) > 0, f''(y,C) < 0$ *for* $y \in (y^*, \infty)$. *Additionally,* $y^* \to \infty$ *as* $C \to -\infty$, *monotonically.*

- *If* $C > C^*$, *then* $f(y,C)$ *exists for all* $y \in \boldsymbol{R}$ *and cannot be monotone as the behaviour changes from exponential to oscillatory at the turning point like Airy functions.* $f(y,C)$ *approaches* $C\,\mathrm{Ai}(y)$ *as* $C \to 0$.

- *If* $C = C^*$, *then* $f(y,C)$ *asymptotes to the parabola* $y/3 + 2f' = 0$, *as* $y \to -\infty$.

According to our numerical calculations, with the mentioned methods, we obtain

$$C^* \approx -0.5911. \tag{3.29}$$

It is worth mentioning that in the absence of rigorous numerical convergence argument, it is not easy to establish exact lower and upper bounds on C^*. The approximate bounds on C^*, which will be displayed in figures, are obtained with the mentioned methods and settings in Section 3.4. Comparing to the second Painlevé equation with $|C| < 1$, which is mentioned in Chapter 2, behaviour in Conjecture 3.1 is interesting. We will justify some of these results by perturbation theory later on. Here, let us first describe the behaviour of solutions depending on the values of C in detail, which is supported by figures.

In Figure 3-2, we show the behaviour of $f = f(y,C)$ when C close to C^*. One can see in Figure 3-3 that f remains close to the parabola $y/3+2f' = 0$ for an ever increasing range of y, as $C \to C^*$. As $C \to C^{*+}$, the global minimum (essentially the first 'pit' with the first extremum point) of f decreases by remaining very close to the parabola, and all the extrema, zeros and the turning point of f move towards $-\infty$.

Figure 3-4 displays the profile f with different values of $C < C^*$. f cannot enter the region (3) and always remains in the region (4) (see Figure 3-5), which is always concave. As $C \to C^{*-}$, the singularity point y^* decreases monotonically while f remains close to the parabola $y/3 + 2f' = 0$ for an ever longer range of y. On the other hand, y^* increases monotonically as $C \to -\infty$. Moreover, $f(y,C') > f(y,C'')$ and $f'(y,C') < f'(y,C'')$ for $C^* > C' > C''$. According to *MatLab*, the singularity point y^* is close to $-6.16, -3.88, -1.61, 0.037, 1.54, 5.29$ for $C = -0.591107, -0.6, -1, -2.7, -10, -1000$, respectively. The dependence of y^* on C is an open problem.

In Figure 3-6 we show blow-up similarity profiles f, which are admissible, for

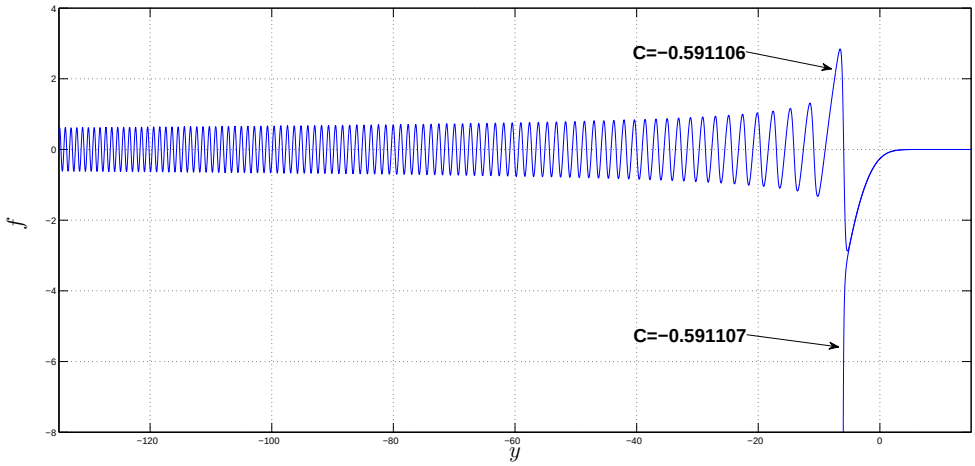

Figure 3-2: *The profile* $f = f(y, C)$ *of (3.27) and (3.25) for* $C = -0.591106 > C^*$ *and* $C = -0.591107 < C^*$.

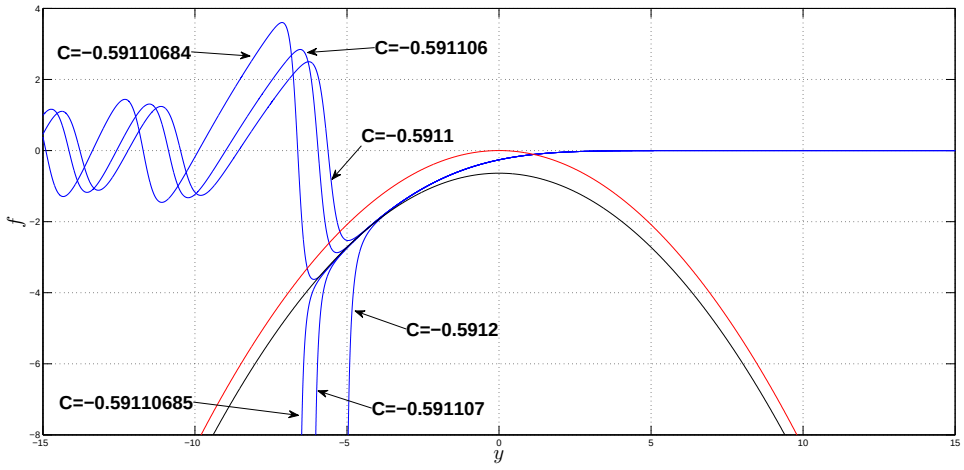

Figure 3-3: *The behaviour of* f *when* C *close to* C^*, *red parabola:* $-y^2/12$, *black parabola:* $-y^2/12 - 0.637$.

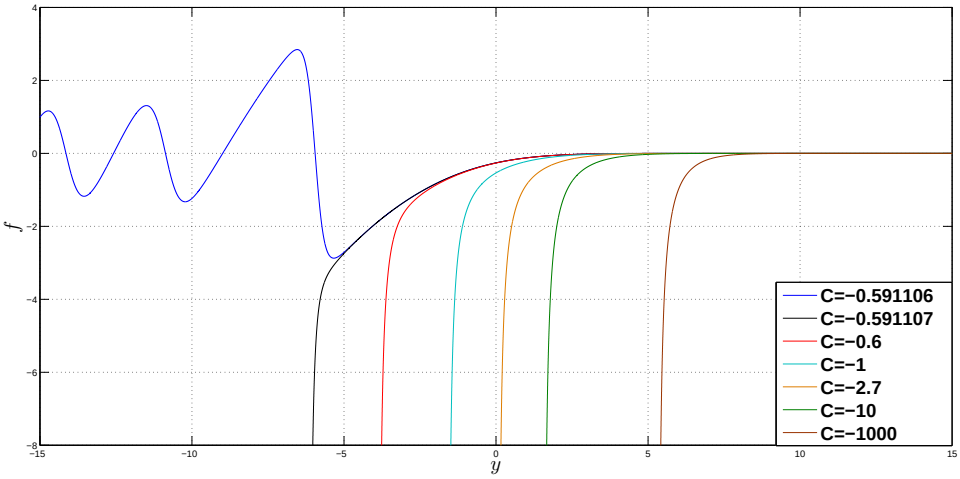

Figure 3-4: *The profile f for the different values of $C < C^*$.*

different non-zero values of $C > C^*$. For $0 > C > C^*$, convexity is large enough to turn $f = f(y, C)$ up from the turning point (essentially the first extremum point) $y_* < 0$, which makes $f' = f'(y_*, C) = 0$. Thus f passes from region (4) to region (3). Then it crosses the line $f = 0$, enters region (2), has a maximum and turns back. Then it crosses the line $f = 0$, enters region (3), has a minimum, turns back and so on. On the other hand, for $C > 0$, concavity is large enough to turn $f = f(y, C)$ down from the turning point (essentially the first extremum point) and f passes from region (1) to region (2). Then it crosses the line $f = 0$, enters region (3), has a minimum and turns back. Then it crosses the line $f = 0$, enters (2), has a maximum, turns back and so on. Therefore f becomes oscillatory from the turning point for any non-zero values of $C > C^*$. As $y \to -\infty$, $y/3 + 2f' \to -\infty$ (see Figure 3-7), which yields sufficiently ever increasing convexity of f in region (3) and concavity in region (2) for bounded f. As a result, the oscillation damps to zero and becomes more rapid, i.e. both the amplitude and the wavelength asymptotically tend to zero, as $y \to -\infty$. As $C > 0$ increases, the maximum (essentially the first 'hump' with the first extremum point) of f increases. Moreover, Figure 3-8 displays that, for $C \gg 1$, the first 'hump', or the global maximum, remains very close to the parabola $y/3 + 2f' = 0$ and the turning point gets very close to $y = 0$. We would like to point out that the symmetry of the oscillatory tail still occurs at 0 for $C \gg 1$, which is not expected for the original third-order ODE (see Chapter 6).

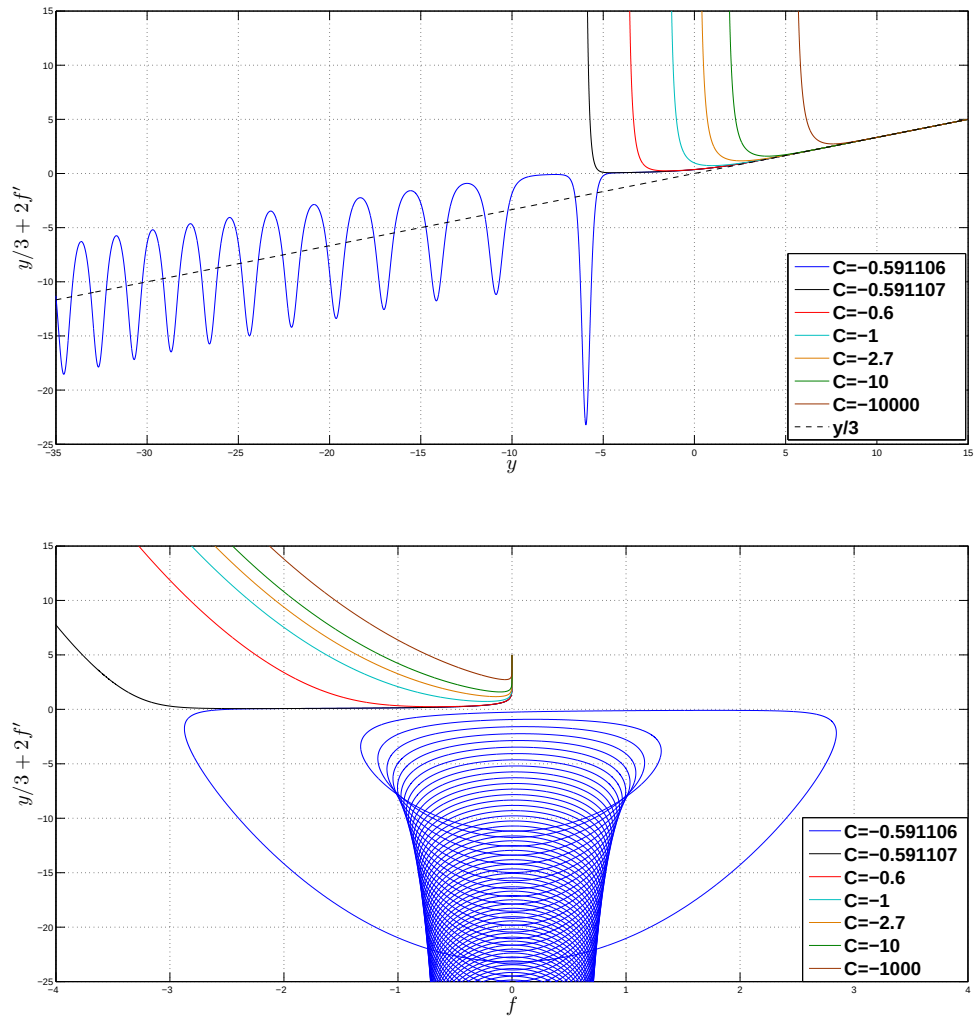

Figure 3-5: *$(y, y/3+2f')$ and $(f, y/3+2f')$ plots for the different values of $C < C^*$.*

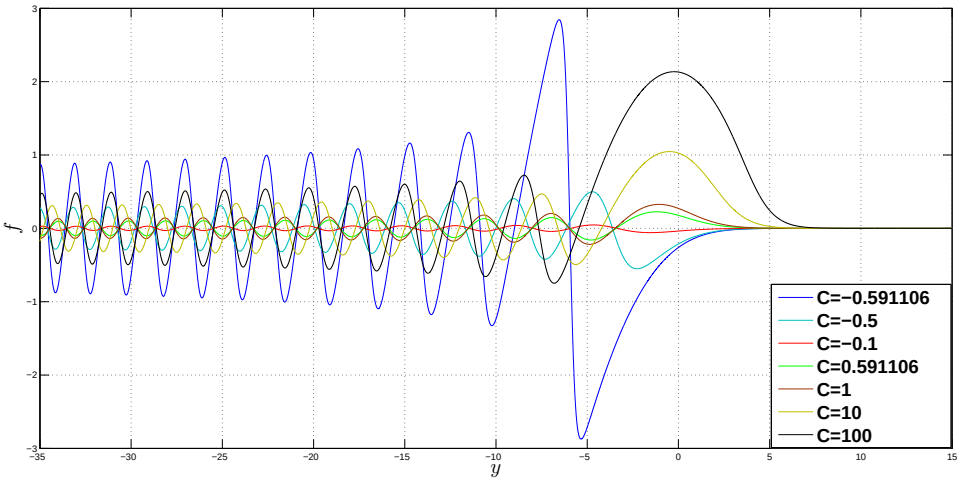

Figure 3-6: *The blow-up similarity profile f for the different non-zero values of $C > C^*$.*

3.4.1.1 Perturbation results

We now justify some of these results by using perturbation theory. In particular, for $0 < |C| \ll 1$ and $|C| \gg 0$. If we set $f = Cg$, for $0 < |C| \ll 1$ in (3.27), we have the following rescaled ODE

$$g'' - \frac{1}{3}yg - C(g^2)' = 0, \quad \text{in} \quad \mathbf{R}. \tag{3.30}$$

According to the classical continuous dependence in ODE theory [90], as $C \to 0$, we have

$$f(y, C) = C(\mathrm{Ai}(y) + o(1)), \quad \text{uniformly in} \quad \mathbf{R}. \tag{3.31}$$

Similarly, the first and second derivatives of f converge. Figure 3-9 displays that $f(y, C)$ cannot be monotone and approaches $C\,\mathrm{Ai}(y)$, as $C \to 0^+$ and $C \to 0^-$.

If we perform the scaling $f(y) = Cg(z)$, $y = z/C$, for $C > 0$ in the problem (3.27) and (3.25), we have the following perturbed ODE

$$g'' - (g^2)' = \frac{1}{3C^3}zg, \quad \text{for} \quad z < z_0, \quad g(z_0) = g_0, \quad g'(z_0) = g_1, \tag{3.32}$$

where $z_0 > 0$, $g_0 > 0$ and $g_1 < 0$. For the sufficiently large values of $C > 0$, we have the following unperturbed ODE

$$(g' - g^2)' = 0, \quad \text{for} \quad z < z_0, \quad g(z_0) = g_0, \quad g'(z_0) = g_1, \tag{3.33}$$

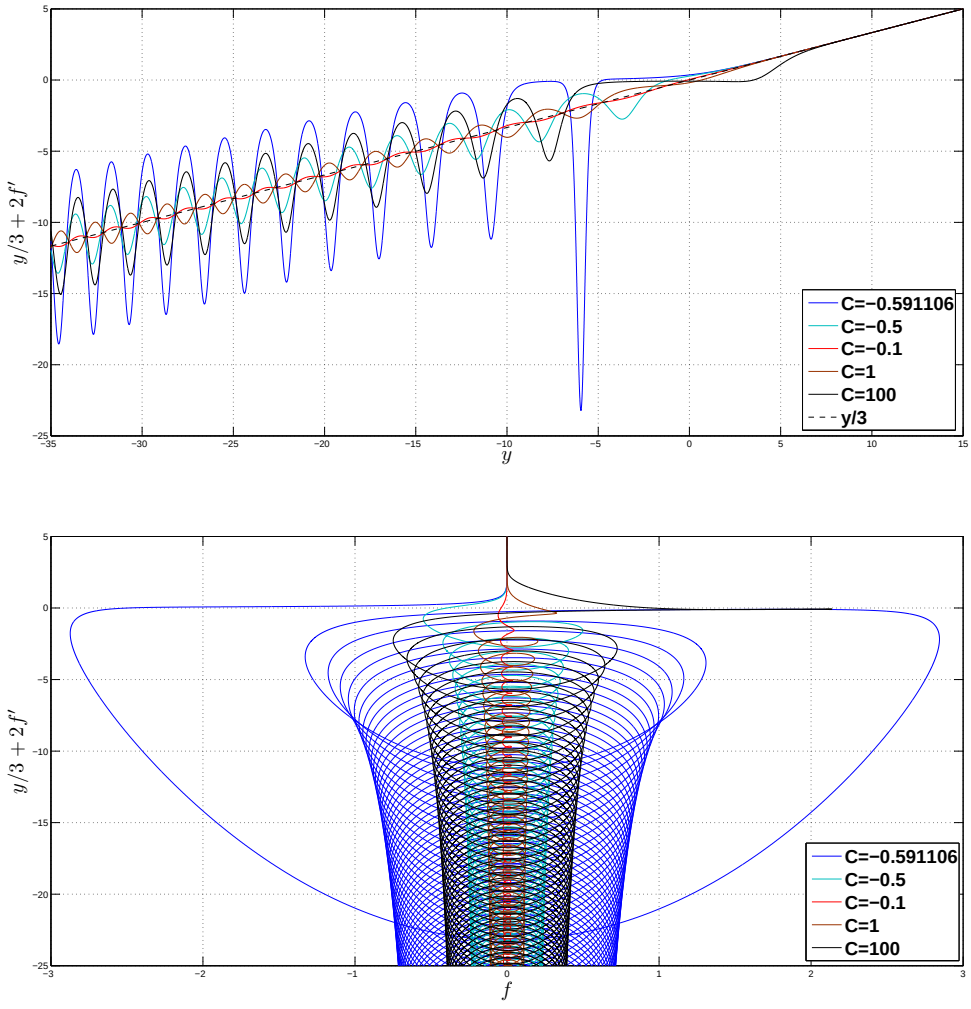

Figure 3-7: $(y, y/3+2f')$ *and* $(f, y/3+2f')$ *plots for* $C > C^*$.

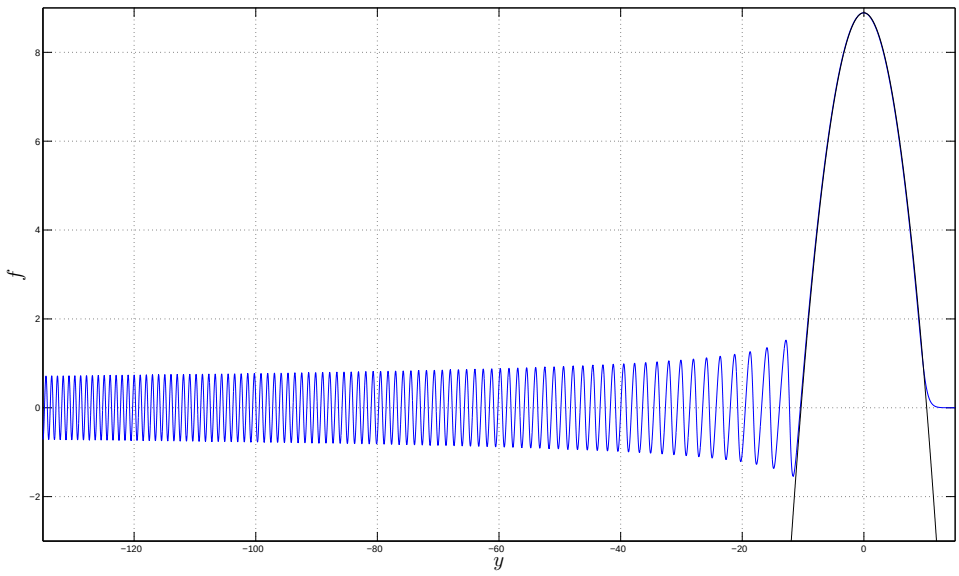

Figure 3-8: *The blow-up similarity profile f for $C = 10^6$ (blue) with parabola $-y^2/12+8.89$ (black)*

which doesn't have a pole for $g_0 > 0$ and $g_1 < 0$, as z decreases from z_0. On the other hand, for $C < 0$, let us set $f(y) = -Cg(z)$, $y = -z/C$, we have

$$g'' - (g^2)' = -\frac{1}{3C^3} zg, \quad \text{for} \quad z < z_0, \quad g(z_0) = g_0, \quad g'(z_0) = g_1, \tag{3.34}$$

where $g_0 < 0$ and $g_1 > 0$. For sufficiently large values of $C < 0$, we have the following unperturbed ODE

$$(g' - g^2)' = 0, \quad \text{for} \quad z < z_0, \quad g(z_0) = g_0, \quad g'(z_0) = g_1, \tag{3.35}$$

which is a classic blow-up problem. It becomes infinite (has a pole) for $g_0 < 0$ and $g_1 > 0$, as z decreases from z_0.

3.4.1.2 Non-zero integration constant

We now focus on the problem (3.27) that has non-zero integration constant, i.e.

$$f'' - \frac{1}{3} yf - (f^2)' = A, \quad -\infty < y < \infty, \tag{3.36}$$

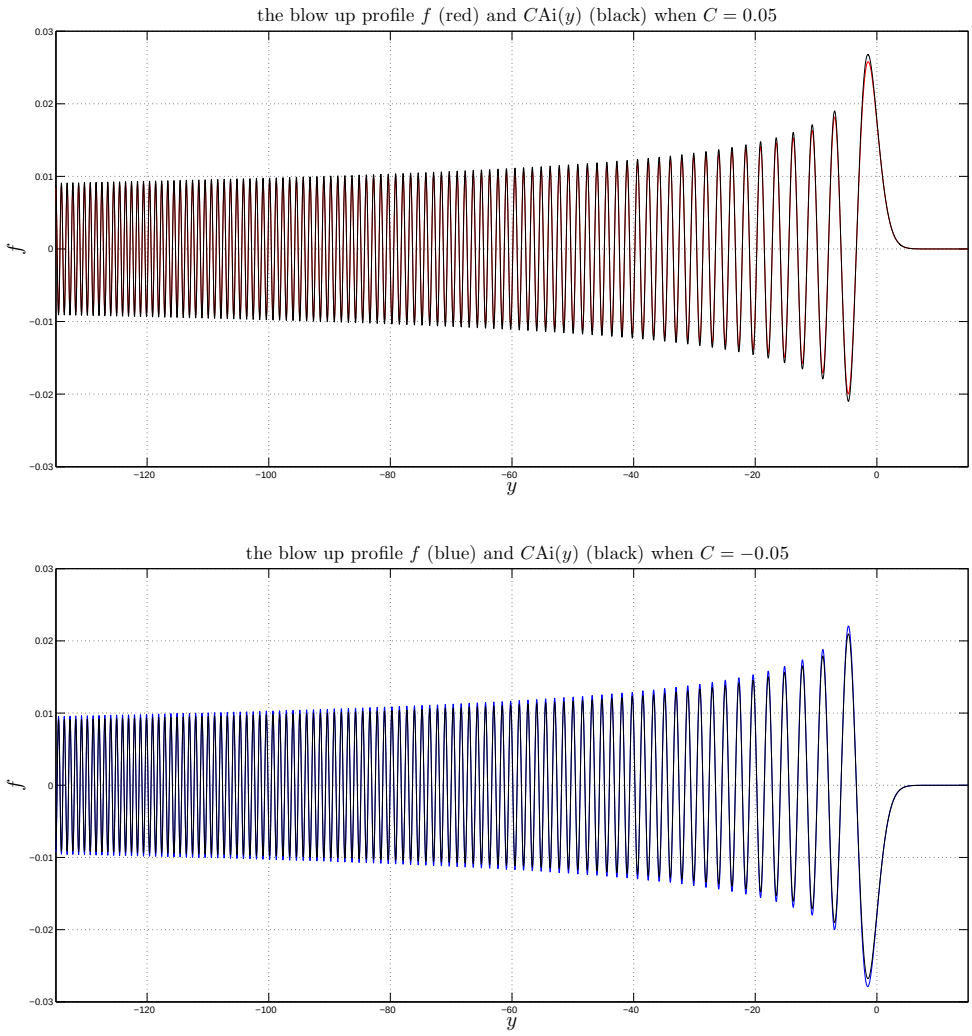

Figure 3-9: *The blow-up similarity profile* f *and* $C\mathrm{Ai}(y)$ *when* $C = -0.05$ *and* $C = 0.05$

with the same boundary condition (3.25),

$$f(y, C) \sim C\,\mathrm{Ai}(y) \quad \text{as} \quad y \to \infty,$$

where $0 \neq A \in \mathbf{R}$ is the constant of integration. We expect to see the effect of $-1/y$, as $y \to -\infty$, according to our discussion in Section 3.3. In Figure 3-10, one can see that oscillatory tails are positive dominant, so they are not symmetric to 0. Symmetry of tail occurs as close to 0 as algebraic decay rate $A \to 0$. Such profiles are bounded, but not admissible regarding to the finite mass condition. We would also like to inform that oscillatory tails of bounded profiles are not symmetric to 0 or not decaying for the values of $C \gg 1$ and $C \ll -1$. Therefore, when we cannot integrate the rescaled ODE for arbitrary values of $1 < p \neq p_0$, we must remember the conditions for admissible bounded profiles, such as decaying and symmetric (to 0) oscillatory tail, for $y \ll -1$. Additionally, let us use the following singular data in order to see the effect clearly,

$$f(y, C) \sim -1/y + C\,\mathrm{Ai}(y) \quad \text{as} \quad y \to \infty. \tag{3.37}$$

The behaviour of the profile f of (3.36) with (3.37) can be found in Figure 3-11.

3.4.2 Blow-up similarity profiles of the signed form

By going back to (3.24), we now consider the signed case,

$$f'' - \frac{1}{3}yf - (|f|f)' = 0, \quad -\infty < y < \infty,$$

with the boundary condition (3.25)

$$f(y, C) \sim C\,\mathrm{Ai}(y) \quad \text{as} \quad y \to \infty.$$

We restrict our attention to $C > 0$, since the solution $f(y, -C)$ is symmetric to $f(y, C)$ with respect to the y-axis, i.e. $f(y, -C) = -f(y, C)$. Similar to the previous case, according to (3.25) (and Figure 3-1), one can see that $f(y, C) > 0$ increases, while $f'(y, C) < 0$ decreases for $C > 0$, as y decreases from ∞. Let us divide the (y, f) plane into four regions, any solution f of (3.24) will be strictly convex in the regions (1) $f > 0, y/3 + 2\,\mathrm{sgn}(f)f' > 0$ and (3) $f < 0, y/3 + 2\,\mathrm{sgn}(f)f' < 0$, and strictly concave in the regions (2) $f > 0, y/3 + 2\,\mathrm{sgn}(f)f' < 0$ and (4) $f < 0, y/3 + 2\,\mathrm{sgn}(f)f' > 0$. According to these features and numerical

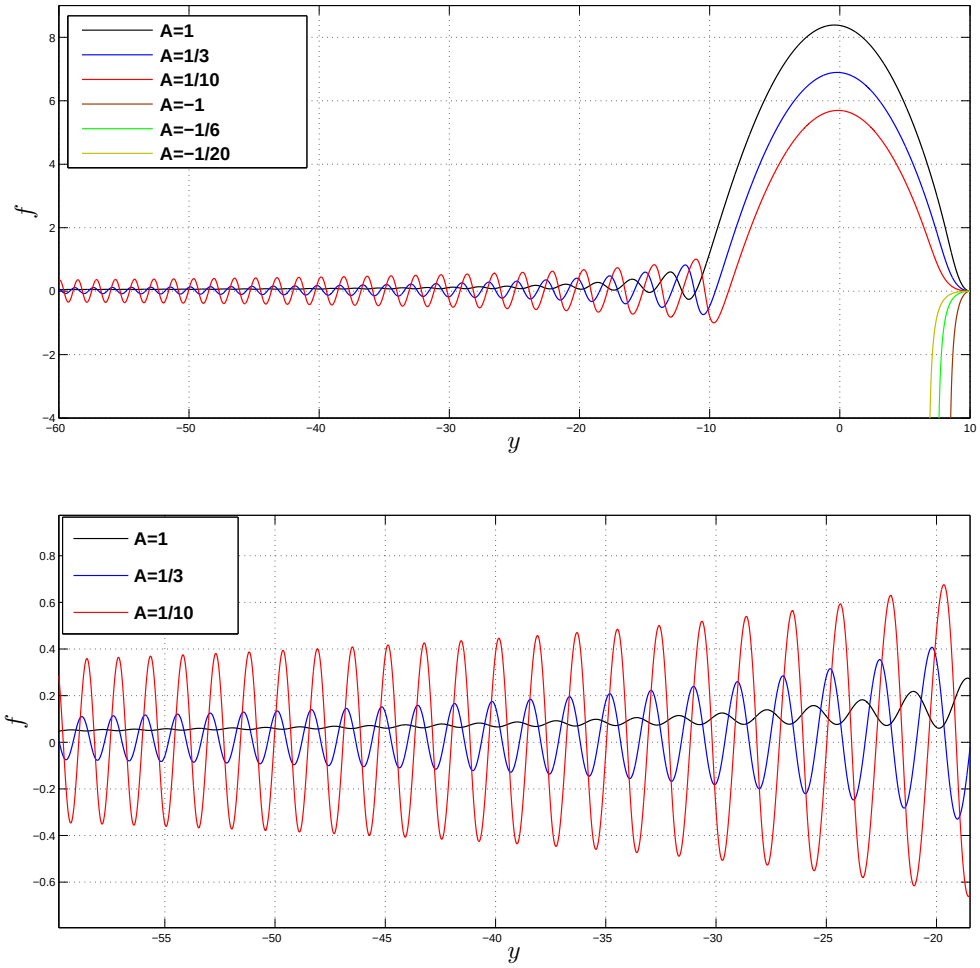

Figure 3-10: *The profile f of (3.36) with (3.25) for different values of A when $C = 1$ and $y_0 = 10$, and the tail.*

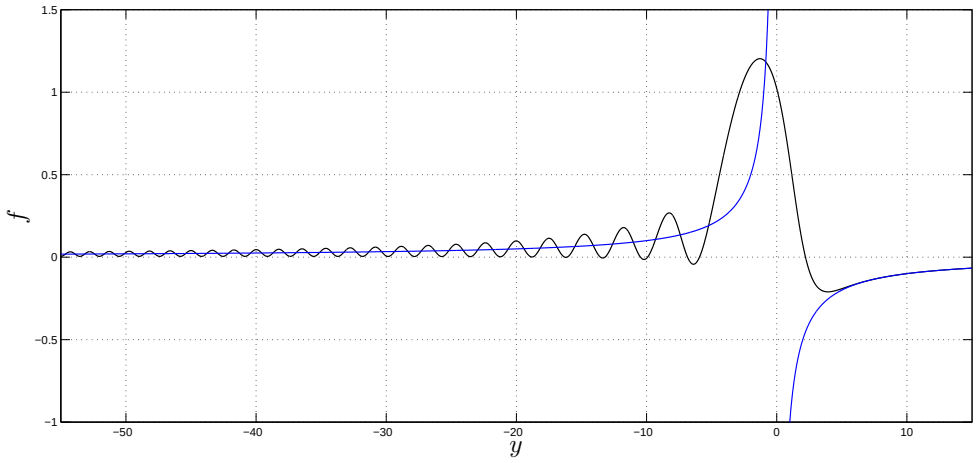

Figure 3-11: *The behaviour of f for (3.36) with (3.37) when $A = 1/3$ and $C = 1$ (black), and $-1/y$ (blue).*

calculations, we construct the solutions of the mentioned problem as C varies from 0 to ∞ and make the following conjecture.

Conjecture 3.2. *For any $C \in \boldsymbol{R}_+$, the solution $f = f(y, C)$ of (3.24) and (3.25) exists for all $y \in \boldsymbol{R}$ and cannot be monotone as the behaviour changes from exponential to oscillatory at the turning point, similar to Airy functions. Additionally, $f(y, C)$ approaches $C\,\mathrm{Ai}(y)$ as $C \to 0$.*

Similar to the previous section, one can also see from the local properties of the equation (3.24) that it does not admit blow-up at finite y for large values of $C > 0$ and cannot be monotone. We will justify such results in detail in the next perturbation results section.

Now, let us explain the conjecture and illustrate in detail the behaviour of the solutions, according to the values of $C > 0$. Figure 3-12 displays the blow-up similarity profile $f = f(y, C)$ of (3.24) and (3.25), for the different values of $C > 0$. As an example, we show general view and 'tail' of f when $C = 0.5$, for $y \ll -1$, in Figure 3-13.

For any $C > 0$, concavity is large enough to turn $f = f(y, C)$ down from the turning point (essentially the first extremum point) and f passes from region (1) to region (2). Then it crosses the line $f = 0$, while $y/3 + 2f' = 0$ changes as decreased by jumping at the line $f = 0$, enters region (3), has a minimum and turns back. Then it crosses the line $f = 0$, while $y/3 + 2f' = 0$ changes as decreased by jumping the line $f = 0$, enters region (2), has a maximum, turns

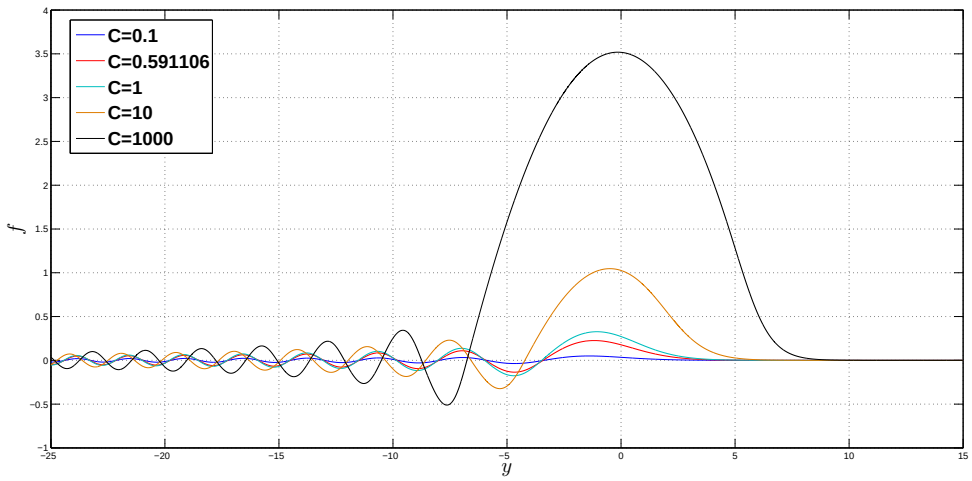

Figure 3-12: *The blow-up similarity profile f for the different values of $C > 0$*

back and so on. Therefore f becomes oscillatory from the turning point for any $C > 0$. As $y \to -\infty$, $y/3 + 2\,\mathrm{sgn}(f)f' \to -\infty$ (see Figure 3-14), which yields sufficiently ever increasing convexity of f in region (3) and concavity in region (2), for bounded f. Also, $y/3 + 2f' = 0$ changes as decreased while crossing the line $f = 0$ each times. As a result, the oscillation rapidly damps to zero compared to the analytical form in the previous section and becomes stronger, i.e. both the amplitude and the wavelength tend to zero, as $y \to -\infty$. As $C > 0$ increases, the maximum (essentially the first 'hump' with the first extremum point) of f increases. Moreover, Figure 3-15 displays that, for $C \gg 1$, the first 'hump', or the global maximum, remains very close to the parabola $y/3 + 2f' = 0$ and the turning point gets very close to $y = 0$.

3.4.2.1 Perturbation results

Similar to the previous section, if we rescale (3.24) by setting $f = Cg$ for $0 < C \ll 1$, we arrive at the following rescaled ODE

$$g'' - \frac{1}{3}yg - |C|(|g|g)' = 0, \quad \text{in} \quad \mathbf{R}.$$

As $C \to 0^+$, we have

$$f(y, C) = C(\mathrm{Ai}(y) + o(1)) \quad \text{uniformly in} \quad \mathbf{R}. \tag{3.38}$$

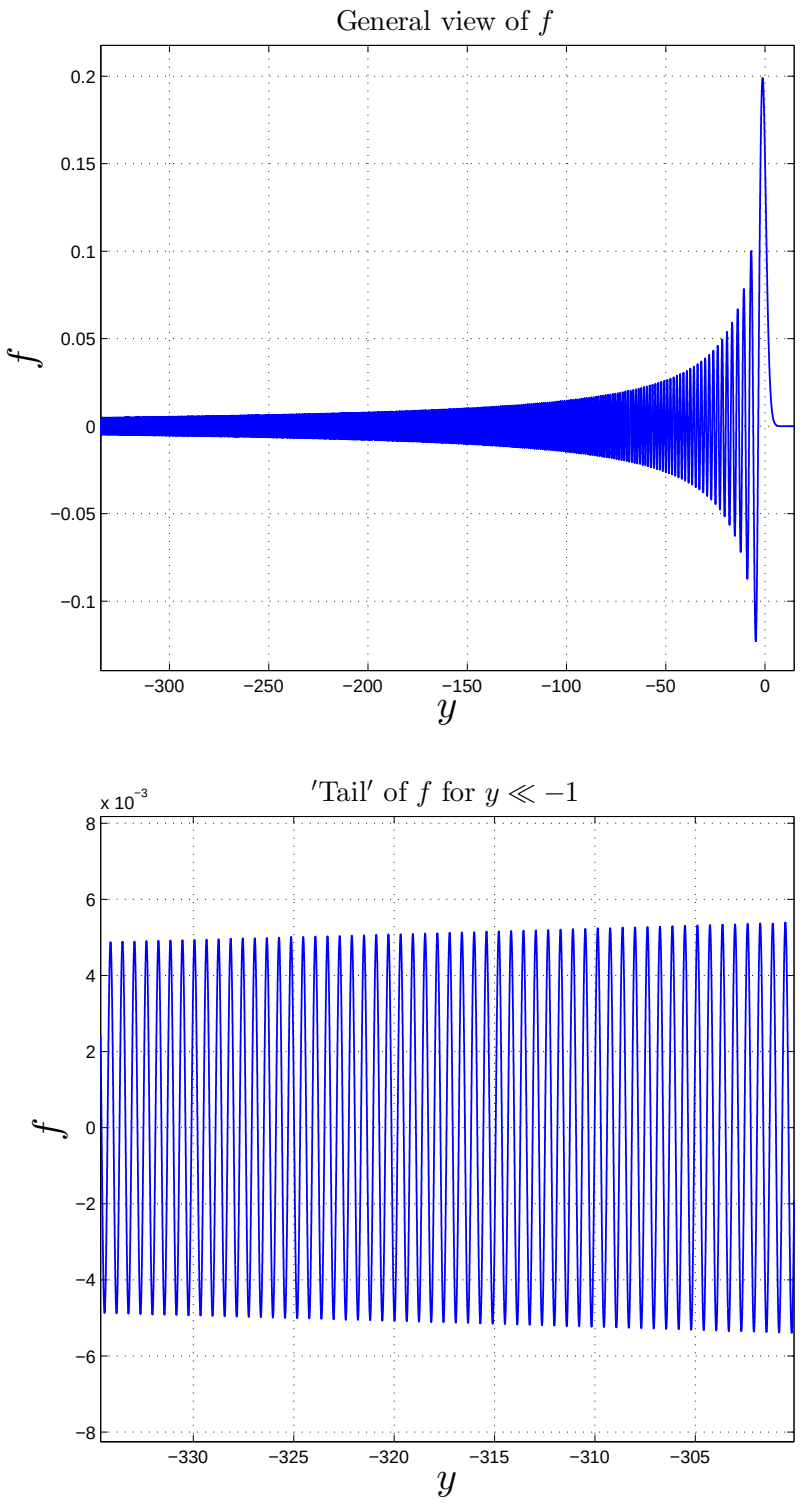

Figure 3-13: *General view and 'tail' of blow-up similarity profile f when $C = 0.5$*

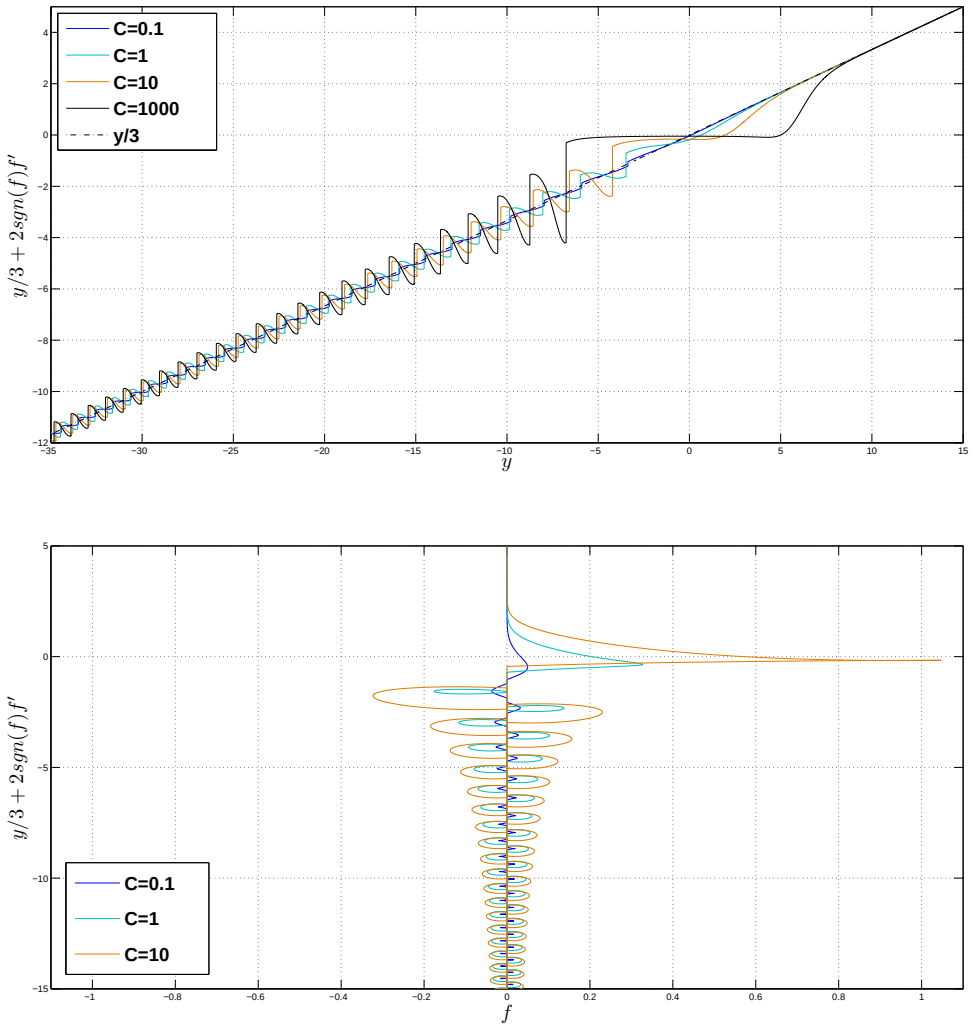

Figure 3-14: $(y, y/3 + 2\,\mathrm{sgn}(f)f')$ *and* $(f, y/3 + 2\,\mathrm{sgn}(f)f')$ *plots for the different values of* $C > 0$

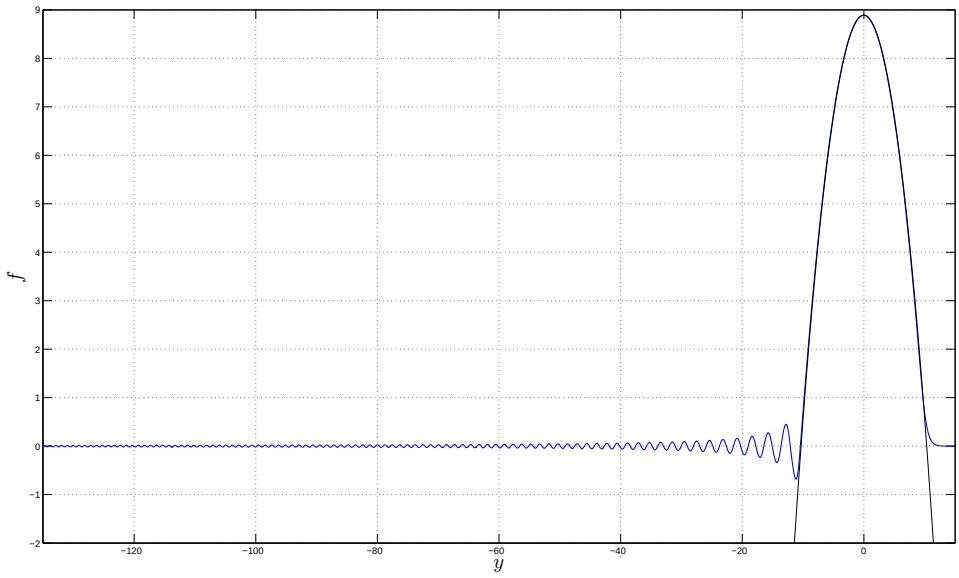

Figure 3-15: *The behaviour of blow-up singularity profile f for $C = 10^6$ (blue) and parabola $-y^2/12 + 8.89$ (black)*

Figure 3-16 displays that $f = f(y, C)$ approaches $C\,\mathrm{Ai}(y)$ and indicates that it cannot be monotone, as $C \to 0^+$.

We now perform the scaling $f(y) = Cg(z)$, $y = z/C$ for $C > 0$ in the problem (3.24) and (3.25), so we have the following perturbed ODE

$$g'' - (|g|g)' = \frac{1}{3C^3} zg, \quad \text{for} \quad z < z_0, \quad g(z_0) = g_0, \quad g'(z_0) = g_1,$$

where $z_0 > 0$, $g_0 > 0$ and $g_1 < 0$. For sufficiently large values of $C > 0$, we have the following unperturbed ODE:

$$(g' - |g|g)' = 0, \quad \text{for} \quad z < z_0, \quad g(z_0) = g_0, \quad g'(z_0) = g_1,$$

which doesn't have a pole for $g_0 > 0$ and $g_1 < 0$, as z decreases from z_0.

3.4.2.2 Non-zero integration constant

Similar to the previous section, let us now consider (3.24) with non-zero integration constant A and the same boundary condition (3.25). We restrict our attention to $A \in \mathbf{R}_+$, as the oscillatory tail of the profile will be negative dominant when $A < 0$, for same values of C. We display the behaviour of f for

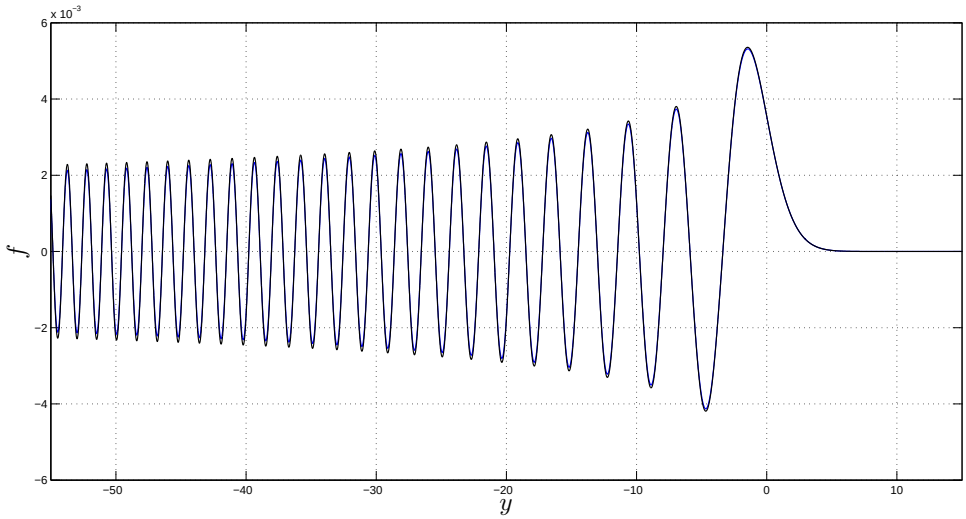

Figure 3-16: *The behaviour of blow-up similarity profile f for $C = 0.01$ (blue) and* $0.01\mathrm{Ai}(y)$ *(black)*

$A = 1, 1/3, 1/10$, when $C = 1$, in Figure 3-17. All profiles are bounded but not admissible according to the conservation law. Symmetry of tails occur close to 0, as $A \to 0^+$.

3.5 Summary

In this chapter, regarding the numerical and perturbation results, we have represented the blow-up profiles of the '−' case with the analytical and signed form for suitable values of C, when $p = p_0 = 2$. We have observed the existence of an unbounded continuous family of exponentially decaying blow-up self-similar solutions parameterized by C (i.e. initial mass) for (3.1), when $p = p_0 = 2$. However, such existence is valid when $C > C*$ for (3.2). Recall that the blow-up self-similar profiles of the '−' case also represent the global self-similar profiles of the '+' case. In Section 6.5, numerical simulations to the rescaled PDE will show that the non-zero stationary global solution for the '+' case of the rescaled PDE is one of the presented admissible similarity profiles in this chapter. However, Section 6.5 will not be able to give stable evolution of a non-zero stationary blow-up similarity solution for the '−' case of the rescaled PDE due to the unstable porous medium operator.

One can also see that the blow-up similarity profile of the signed form damps

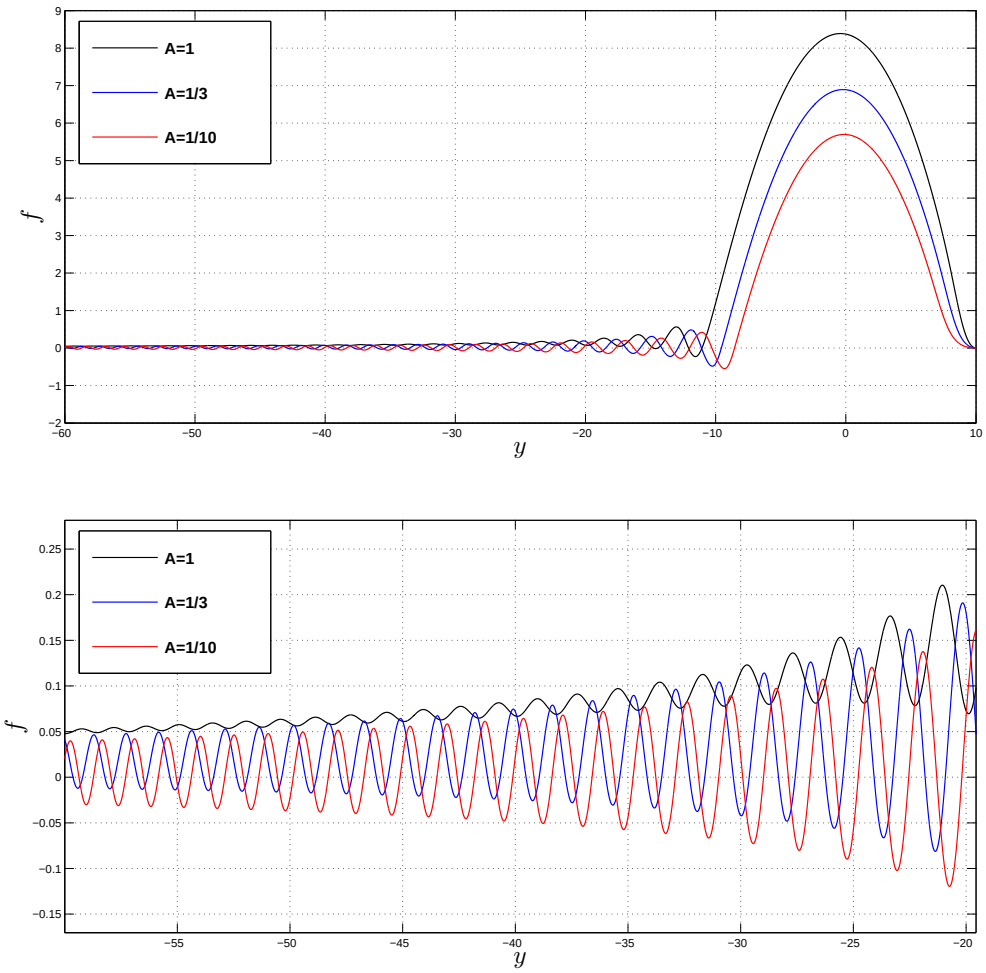

Figure 3-17: *The profile f of (3.24) with (3.25) for different values of A when $C = 1$ and the tail.*

to zero faster than the analytical form for the same value of C, see Figure 3-18. Unlike the '−' case, signed form of the '+' case yields poles (becomes unbounded), which will be discussed in the next chapter.

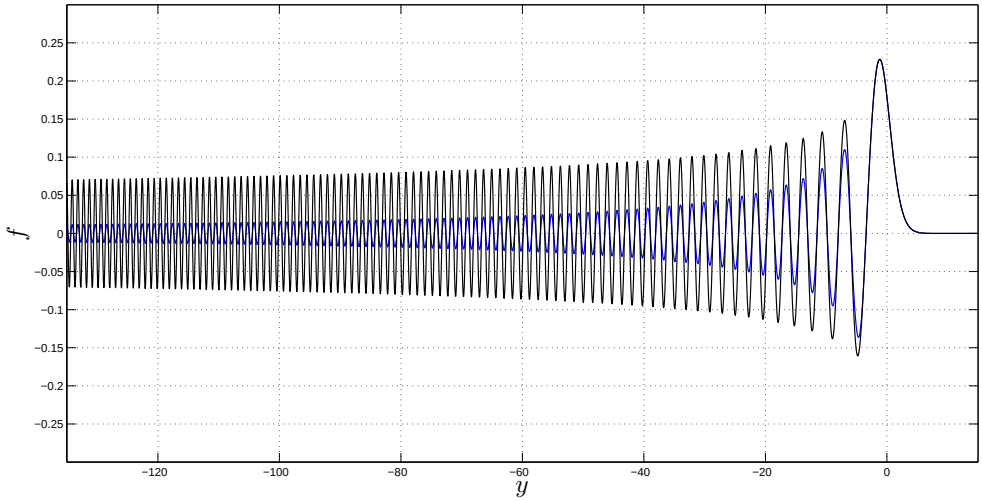

Figure 3-18: *The behaviour of blow-up similariy profile f of (3.27) (black) and (3.24) (blue) when $C = 0.6$*

Chapter 4

Non-Existence of the Blow-up Similarity Profiles for the Stable '+' Case with the First Critical Exponent

We now study the blow-up self-similar solutions of the '+' case (3.4),

$$u_t = u_{xxx} + (|u|^{p-1}u)_{xx}, \quad p > 1.$$

with suitable initial data (1.2) for the first critical exponent $p = p_0 = 2$. We observe the non-existence of blow-up self-similar profiles of (3.4) parameterized by initial mass (again by C), when $p = p_0 = 2$. Note that such a non-existence blow-up result is not that formal: it is known that even the linear dispersion equation can create a blow-up δ-type singularity in finite time (e.g., take the fundamental Airy solution backward in time).

As we mentioned in the previous Chapter, the blow-up similarity profiles of the '+' case (3.4) will represent the global similarity profiles of the '−' case (3.1)

$$u_t = u_{xxx} - (|u|^{p-1}u)_{xx}, \quad p > 1,$$

which will be discussed later on.

4.1 Blow-up self-similarity and the rescaled equation

If we propose an exact blow-up similarity solution of (3.4) as

$$u_+(x,t) = (T-t)^{-1/3(p-1)} f(y), \quad y = x/(T-t)^{1/3}, \tag{4.1}$$

where $t < T$, then the function f, $f \not\equiv 0$, solves the following third-order ODE

$$\mathbf{A}_+(f) \equiv f''' - \frac{1}{3(p-1)} f - \frac{1}{3} f' y + (|f|^{p-1} f)'' = 0 \quad \text{in} \quad \mathbf{R}, \tag{4.2}$$

according to (3.6) with $\sigma = 1$. Similar to the previous chapter, we will pay attention to the profiles with the suitable decay condition, as $y \to \infty$

4.1.1 Global similarity pattern profiles

Let us now construct the exact global self-similar solutions of (3.1) as in (3.5) with $\sigma = -1$ and $x \mapsto -x$, for $t > T$,

$$u_{GL}(x,t) = (t-T)^{-1/3(p-1)} f(y), \quad y = -x/(t-T)^{1/3},$$

then $f(y)$ satisfies the same ODE (4.2), where we take $T = 0$ again for convenience. Hence, $f(y)$ implies both blow-up self-similar profiles of (3.4) and global self-similar profiles of (3.1).

4.2 Asymptotic behaviour at infinity for $p = p_0 = 2$

If we consider $p = p_0 = 2$ according to the conservation in mass (3.15) for (3.4), then the ODE (4.2) becomes

$$f''' - \frac{1}{3} f - \frac{1}{3} f' y + (|f| f)'' = 0, \tag{4.3}$$

which can be integrated once with the zero integration constant to give

$$f'' - \frac{1}{3} y f + (|f| f)' = 0 \quad \text{for} \quad y \in \mathbf{R}, \quad f(y) = 0 \quad \text{as} \quad y \to \infty, \tag{4.4}$$

where again we will take particularly interest in exponentially decaying solutions as $y \to \infty$. This removes $f(y) = 1/y$ and $f(y) = y^2/12 + c_0$ (c_0 is any real number) which satisfy the analytical form of (4.3),

$$f''' - \frac{1}{3}f - \frac{1}{3}f'y + (f^2)'' = 0. \tag{4.5}$$

Additionally, $f(y) = 1/y + y^2/12$ is an explicit solution for the analytical form of (4.4), which is also not admissible because of the growth. By a local analysis, one can see that $\pm 1/y$ for $y > 0$ and $\pm y^2/12 \mp c_0$, $c_0 \geq 0$, for $|y| > \sqrt{12c_0}$ satisfy the signed equation (4.3).

Similar to the previous analysis in Chapter 3, the unique admissible solution of the linear part of the operator in (4.4), is the *Airy function* $\mathrm{Ai}(y)$. So we will analyse the behaviour of the solutions, f, for the following second-order ODE,

$$f'' - \frac{1}{3}yf + (|f|f)' = 0, \quad -\infty < y < \infty, \tag{4.6}$$

with the boundary condition,

$$f(y, C) \sim C\,\mathrm{Ai}(y) \quad \text{as} \quad y \to \infty, \tag{4.7}$$

where $\mathrm{Ai}(y)$ is the Airy function and $C \neq 0$ is an arbitrary real number.

4.3 Numerical construction of blow-up similarity profiles

We use the same notations and methods described in Section 3.4 of the previous chapter. In the following sections, we first analyse the analytical form and then signed form of (4.6), regarding to the proposed numerics.

4.3.1 Blow-up similarity profiles of the analytical form

We first consider the analytical form of (4.6),

$$f'' - \frac{1}{3}yf + (f^2)' = 0, \quad -\infty < y < \infty, \tag{4.8}$$

with the boundary condition (4.7),

$$f(y, C) \sim C\,\mathrm{Ai}(y) \quad \text{as} \quad y \to \infty.$$

As we mentioned in Chapter 1, the sign of the nonlinear part is irrelevant when p is even for the analytical form. If $g(y, C)$ has the same properties described in Conjecture 3.1, then $f(y, C) \equiv -g(y, -C)$, i.e. $f(y, C)$ is symmetric to $g(y, -C)$ with respect to the y-axis. However, we will also briefly display the behaviour of the problem (4.8) and (4.7) while C varies from $-\infty$ to ∞, in order to enlighten the signed form, which will be discussed in the next section. In addition, we use this equation and the second Painlevé equation to show the efficiency of EFRK method, which will be discussed in Chapter 5.

Similar to analysis in the previous Chapter, if we divide the (y, f) plane into four regions, any solution f of (4.8) will be strictly convex in the regions (1) $f > 0, y/3 - 2f' > 0$ and (3) $f < 0, y/3 - 2f' < 0$, and strictly concave in the regions (2) $f > 0, y/3 - 2f' < 0$ and (4) $f < 0, y/3 - 2f' > 0$. According to these properties and numerics, the following conjecture can be given according to Section 3.4.1

Conjecture 4.1. *Let C be a non-zero arbitrary real number and $f = f(y, C)$ be the solution of (4.8) with boundary condition (4.7). There exists a unique C^* such that*

- *If $C > C^*$, then $f(y, C)$ has a pole (becomes infinite) at a finite y^* depending on C,*

$$f(y, C) \sim (y - y^*)^{-1} \quad \text{as} \quad y \downarrow y^*. \tag{4.9}$$

  $f(y, C)$ is a convex and monotonically decreasing positive solution in (y^*, ∞), i.e. $f(y, C) > 0, f'(y, C) < 0, f''(y, C) > 0$ for $y \in (y^*, \infty)$. Additionally, $y^* \to \infty$ as $C \to \infty$, monotonically.

- *If $C < C^*$, then $f(y, C)$ exists for all $y \in \boldsymbol{R}$ and cannot be monotone as the behaviour changes from exponential to oscillatory at the turning point very much like Airy functions. $f(y, C)$ approaches $C\,\mathrm{Ai}(y)$ as $C \to 0$.*

- *If $C = C^*$, then $f(y, C)$ asymptotes to the parabola $y/3 - 2f' = 0$ as $y \to -\infty$.*

$C^* \approx 0.5911$ is known regarding to proposed numerical construction in Section 3.4. Let us also give the following two figures in order to be a guide to decaying

oscillatory tail, when $C < C^*$, for signed form (4.6) and numerical studies in Chapter 5. Figure 4-1 displays the profile $f = f(y, C)$ when C close to C^*. One can see the behaviour of f for the different values of $0 < C < C*$ in Figure 4-2.

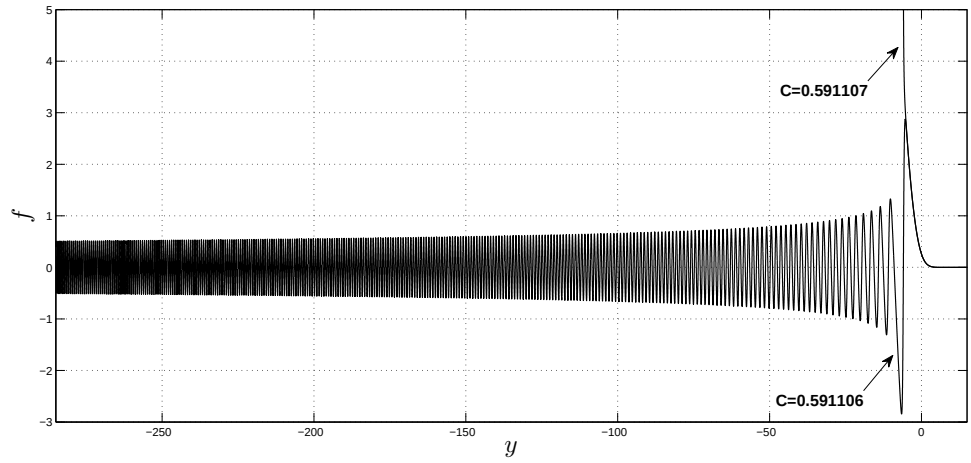

Figure 4-1: *The similarity profile* $f = f(y, C)$ *of (4.8) and (4.7) for* $C = 0.591106 < C^*$ *and* $C = 0.591107 > C^*$.

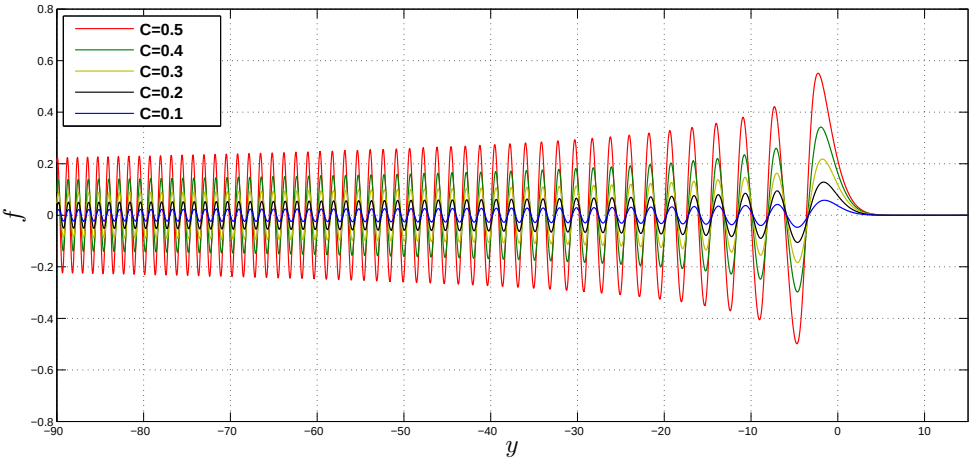

Figure 4-2: *The behaviour of blow-up similarity profile* f *for* $0 < C < C^*$.

4.3.2 Blow-up similarity profiles of the signed form

We now consider the signed form (4.6),

$$f'' - \frac{1}{3}yf + (|f|f)' = 0, \quad -\infty < y < \infty,$$

with the boundary condition

$$f(y, C) \sim C\,\mathrm{Ai}(y) \quad \text{as} \quad y \to \infty.$$

We restrict our attention to $C > 0$ since the solution $f(y, -C)$ is symmetric of $f(y, C)$ with respect to the y-axis, i.e. $f(y, -C) = -f(y, C)$. Similar to the previous section, according to (4.7) (and Figure 3-1), one can see that $f(y, C) > 0$ increases, while $f'(y, C) < 0$ decreases for $C > 0$, as y decreases from ∞. Let us divide the (y, f) plane into four regions, any solution f of (3.19) will be strictly convex in the regions (1) $f > 0, y/3 - 2\,\mathrm{sgn}(f)f' > 0$ and (3) $f < 0, y/3 - 2\,\mathrm{sgn}(f)f' < 0$, and strictly concave in the regions (2) $f > 0, y/3 - 2\,\mathrm{sgn}(f)f' < 0$ and (4) $f < 0, y/3 - 2\,\mathrm{sgn}(f)f' > 0$. According to these features and numerical studies, we construct the solutions of the mentioned problem as C varies from 0 to ∞ and propose the following conjecture.

Conjecture 4.2. *Let $C \in \boldsymbol{R}_+$ and $f = f(y, C)$ be the solution of (4.6) with boundary condition (4.7). There exists a unique C_k^*, $k = 0, 1, 2, \ldots$ such that*

- *If $C > C_0^*$, then $f(y, C)$ has a pole (becomes infinite) at a finite y_0^* depending on C,*

  $$f(y, C) \sim (y - y_0^*)^{-1} \quad \text{as} \quad y \downarrow y_0^*. \tag{4.10}$$

  $f(y, C)$ is a convex and monotonically decreasing positive solution in (y_0^*, ∞). Moreover, $y_0^* \to \infty$ as $C \to \infty$, monotonically.

- *If $C_k^* < C < C_{k-1}^*$, $k = 1, 2, 3, \ldots$, then $f(y, C)$ has a pole (becomes infinite) at a finite point y_k^* depending on C,*

  $$f(y, C) \sim (-1)^k (y - y_k^*)^{-1} \quad \text{as} \quad y \downarrow y_k^*, \tag{4.11}$$

  and cannot be monotone in (y_k^*, ∞) since f has k local extrema due to the changing behaviour from exponential to oscillatory at the turning point. $y_k^* \to -\infty$ as $C \to 0^+$ (or as $k \to \infty$).

- *If* $C = C_k^*$, $k = 0, 1, 2, ...$,*then* $f(y, C)$ *asymptotes to the parabola* $y/3 - 2(-1)^k f' = 0$, *as* $y \to -\infty$.

Let us explain the conjecture and display the behaviour of the problem in detail, and then justify some of them by using perturbation results. We firstly introduce the sets

$$S_0 = \{C > 0 : f(y, C) \text{ is monotonically decreasing in } (y_0^*, \infty)\}, \tag{4.12}$$

and, for any $k = 1, 2, ...,$

$$S_k = \{0 < C < C_{k-1}^* : f(y, C) \text{ has at most } k \text{ local extrema in } (y_k^*, \infty)\}. \tag{4.13}$$

According to numerics, we have that $S_0 \neq \emptyset$ and bounded from below by

$$C_0^* = \inf S_0 \approx 0.5911. \tag{4.14}$$

For any $k = 1, 2, ...,$ we also have that $S_k \neq \emptyset$ and bounded from below by

$$C_1^* = \inf S_1 \approx 0.5, \tag{4.15}$$

$$C_2^* = \inf S_2 \approx 0.4412, \tag{4.16}$$

and so on. As k increases, $C_{k-1}^* - C_k^*$ decreases. We would like to remind the reader that the above values are determined by the numerical construction mentioned in Section 3.4 in order to give an idea about the behaviour of f for different values of C.

Figure 4-3 shows the different values of $C > 0$ for f. It can be seen that f is monotone decreasing for $C > C_0^*$ and cannot be monotone for $C < C_0^*$ in (y_k^*, ∞), $k = 0, 1, 2, ...$

Similar to the first case of the analytical form, for $C > C_0^*$, f cannot enter region (2) and always remains in region (1), where f is always convex and positive, see Figure 4-4. The solution f of the signed form for $C > C_0^*$ will be same with the solution of analytical form for $C > C^*$ since f stays always positive in region (1). The singularity point y_0^* decreases monotonically while f remains close to the parabola $y/3 - 2f' = 0$ for an ever increasing range of y as $C \to C_0^{*+}$. Moreover, y_0^* increases monotonically as $C \to \infty$.

We display the behaviour of f when C is close to C_k^*, for $k = 0, 1, 2$, in Figure 4-5. As $C \to C_k^{*-}$, for $k = 0, 1, 2, ...,$ the last extremum of f grows longer

and moves towards $-\infty$, by remaining very close to the parabola $y/3-2(-1)^k f' = 0$. We cannot say that y_k^* monotonically decreases as $C_k^* < C < C_{k-1}^*$ decreases, when $k = 1, 2, ...$ However, one can see that, for $k = 1, 2, ...,$ all the zeros and extrema of f move towards the left as $C \to C_{k-1}^{*-}$ and move towards the right as $C \to C_k^{*+}$.

Now, we explain the behaviour of f for $C < C_0^*$, which is displayed in Figure 4-3 and 4-6. Let us first start with the profiles have one local extremum in (y_1^*, ∞). For $C_1^* < C < C_0^*$, concavity is large enough to turn f down from the first extremum point. Thus f passes from region (1) to region (2), crosses the line $f = 0$ and enters region (4) since $y/3 - 2\,\mathrm{sgn}(f)f'$ changes (jumps) from $y/3 - 2\,\mathrm{sgn}(f)f' < 0$ to $y/3 - 2\,\mathrm{sgn}(f)f' > 0$, at the line $f = 0$ (see Figure 4-6 and 4-3). Then f cannot enter region (3) and remains in region (4). Therefore $f \to -\infty$ and $y/3 - 2\,\mathrm{sgn}(f)f' \to \infty$, as $y \to y_1^*$, which yields a pole at a finite y_k^* for f, in contrast to the signed form of the '$-$' case in Chapter 3.

We next explain the profiles have two local extrema in (y_2^*, ∞). For $C_2^* < C < C_1^*$, concavity is large enough to turn f down from the first extremum point. Thus f passes from region (1) to region (2) and crosses the line $f = 0$, while $y/3 - 2\,\mathrm{sgn}(f)f'$ changes as increased by jumping at the line $f = 0$. Then f has a minimum at the second extremum point, enters region (3), turns back, crosses the line $f = 0$ and enters region (1) since $y/3 - 2\,\mathrm{sgn}(f)f'$ changes from $y/3-2\,\mathrm{sgn}(f)f' < 0$ to $y/3-2\,\mathrm{sgn}(f)f' > 0$ at the line $f = 0$. Then f cannot enter region (2) and remains in region (1). Thus $f \to \infty$ and $y/3 - 2\,\mathrm{sgn}(f)f' \to \infty$, as $y \to y_2^*$.

Finally, let us generalise above discussions and consider the profiles have k local extrema in (y_k^*, ∞). So, for $C_k^* < C < C_{k-1}^*$, $k = 3, 4, ...,$ f has k local extrema by entering regions (2) and (3) after crossing the line $f = 0$. On the other hand, $y/3 - 2\,\mathrm{sgn}(f)f'$ changes as ever increased (jumps) at the line $f = 0$ each time. This ever increasing (jumping) behaviour at $f = 0$ doesn't produce sufficiently ever increasing concavity of f in region (2) and convexity in region (3), for unbounded f. After changing region (turning) at the k-th extremum point, f crosses the line $f = 0$, remains in the same behaviour of the region due to $y/3-2\,\mathrm{sgn}(f)f'$ changes (jumps) from $y/3-2\,\mathrm{sgn}(f)f' < 0$ to $y/3-2\,\mathrm{sgn}(f)f' > 0$ at the line $f = 0$. Thus $f \to (-1)^k\infty$ and $y/3 - 2\,\mathrm{sgn}(f)f' \to \infty$, as $y \to y_k^*$, see Figure 4-6 and 4-3. In other words, solutions in this range are oscillatory, that have k local extrema, where the amplitude of oscillations increases (in contrast to the signed form of the '$-$' case in Chapter 3) and the wavelength tends to zero

as $y \to y_k^*$. The dependence of y_k^* on C is an open problem.

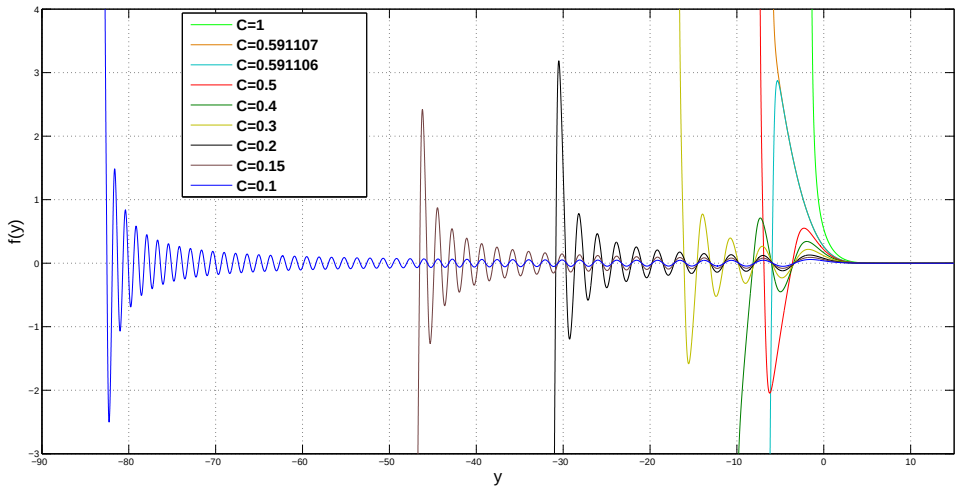

Figure 4-3: *The profile f for the different values of C*

4.3.2.1 Perturbation results

It has already been mentioned that $y_k^* \to -\infty$ as $C \to 0^+$. Additionally, if we set $f = Cg$ in (4.6), we have the following ODE

$$g'' - \frac{1}{3}yg + |C|(|g|g)' = 0, \quad y_k^* < y < \infty. \tag{4.17}$$

Similar to the previous chapter, one can see that f cannot be monotone for $0 < C \ll 1$. In Figure 4-7, we show that all zeros of $f(y, C)$ get very close to the all zeros of $C\,\mathrm{Ai}(y)$, and $f(y, C)$ remain close to $C\,\mathrm{Ai}(y)$ for an ever increasing range of y as $C \to 0^+$.

If we now set $f(y) = Cg(z)$ and $y = z/C$, for $C > 0$, in the problem (4.6) and (4.7), then we have the following perturbed ODE

$$g'' + (|g|g)' = \frac{1}{3C^3}zg, \quad \text{for} \quad z < z_0, \quad g(z_0) = g_0, \quad g(z_0) = g_1, \tag{4.18}$$

where $g_0 > 0$ and $g_1 < 0$. For sufficiently large values of $C > 0$, we arrive at the unperturbed ODE

$$(g' + (|g|g))' = 0, \quad \text{for} \quad z < z_0, \quad g(z_0) = g_0, \quad g(z_0) = g_1, \tag{4.19}$$

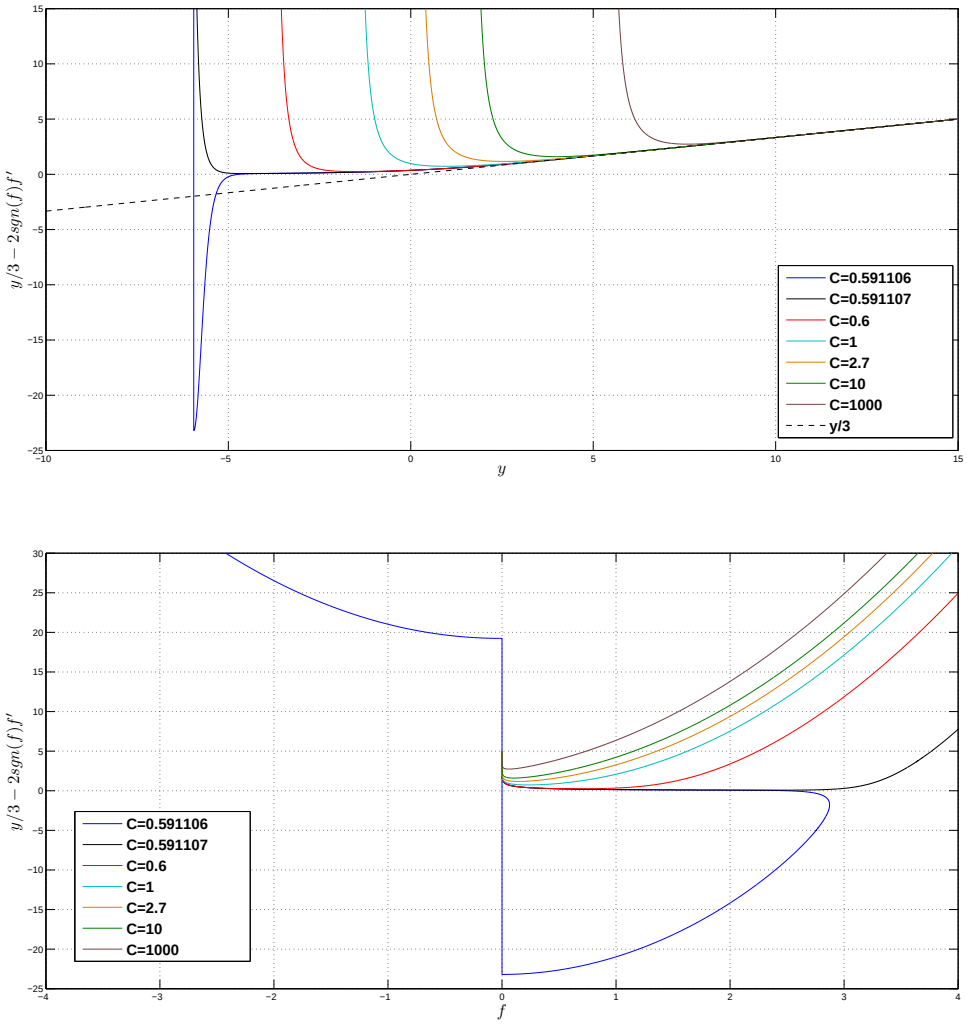

Figure 4-4: $(y, y/3 - 2\,\mathrm{sgn}(f)f')$ *and* $(f, y/3 - 2\,\mathrm{sgn}(f)f')$ *plots for the different values of* $C > C_0^*$

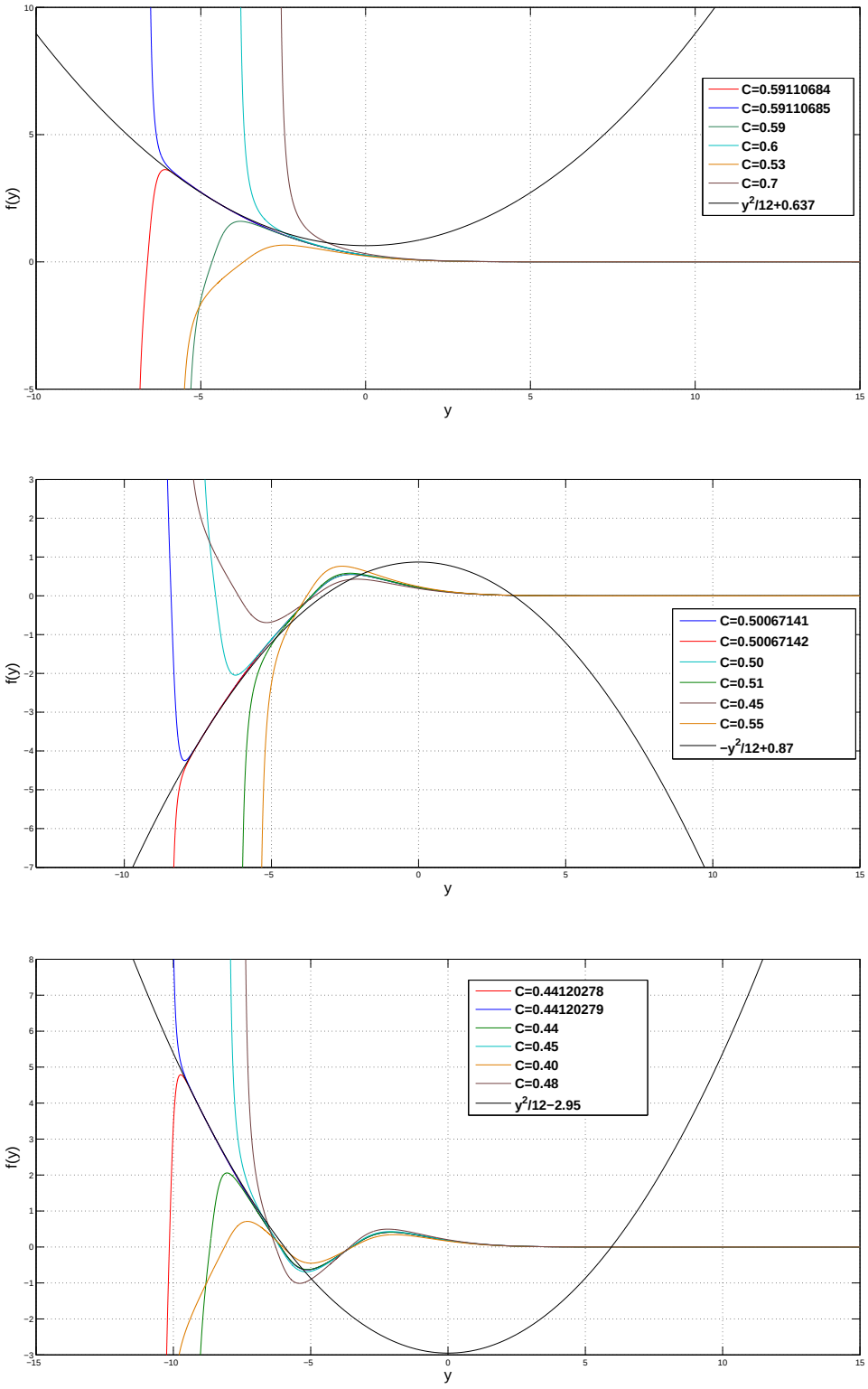

Figure 4-5: *The behaviour of f when C close to C_k^* for $k = 0, 1, 2$.*

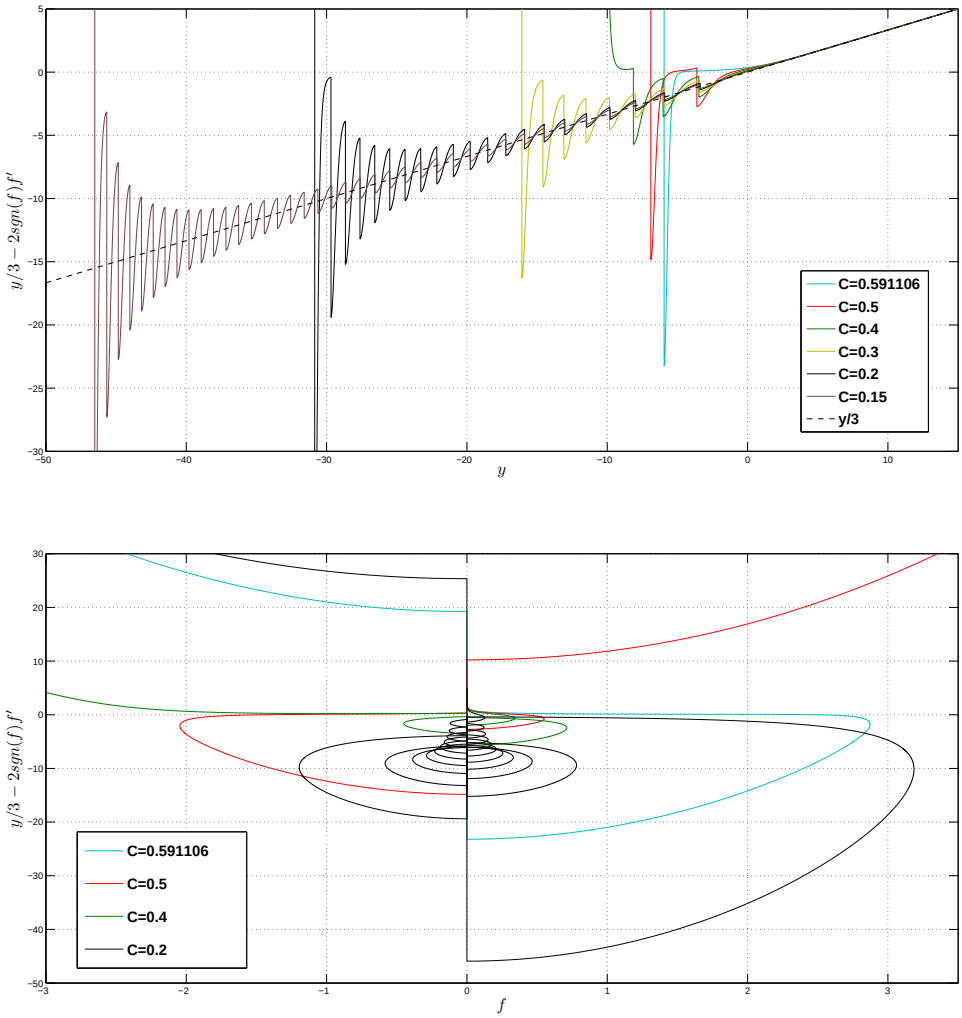

Figure 4-6: $(y, y/3 - 2\,\mathrm{sgn}(f)f')$ *and* $(f, y/3 - 2\,\mathrm{sgn}(f)f')$ *plots for the different values of* $C < C_0^*$.

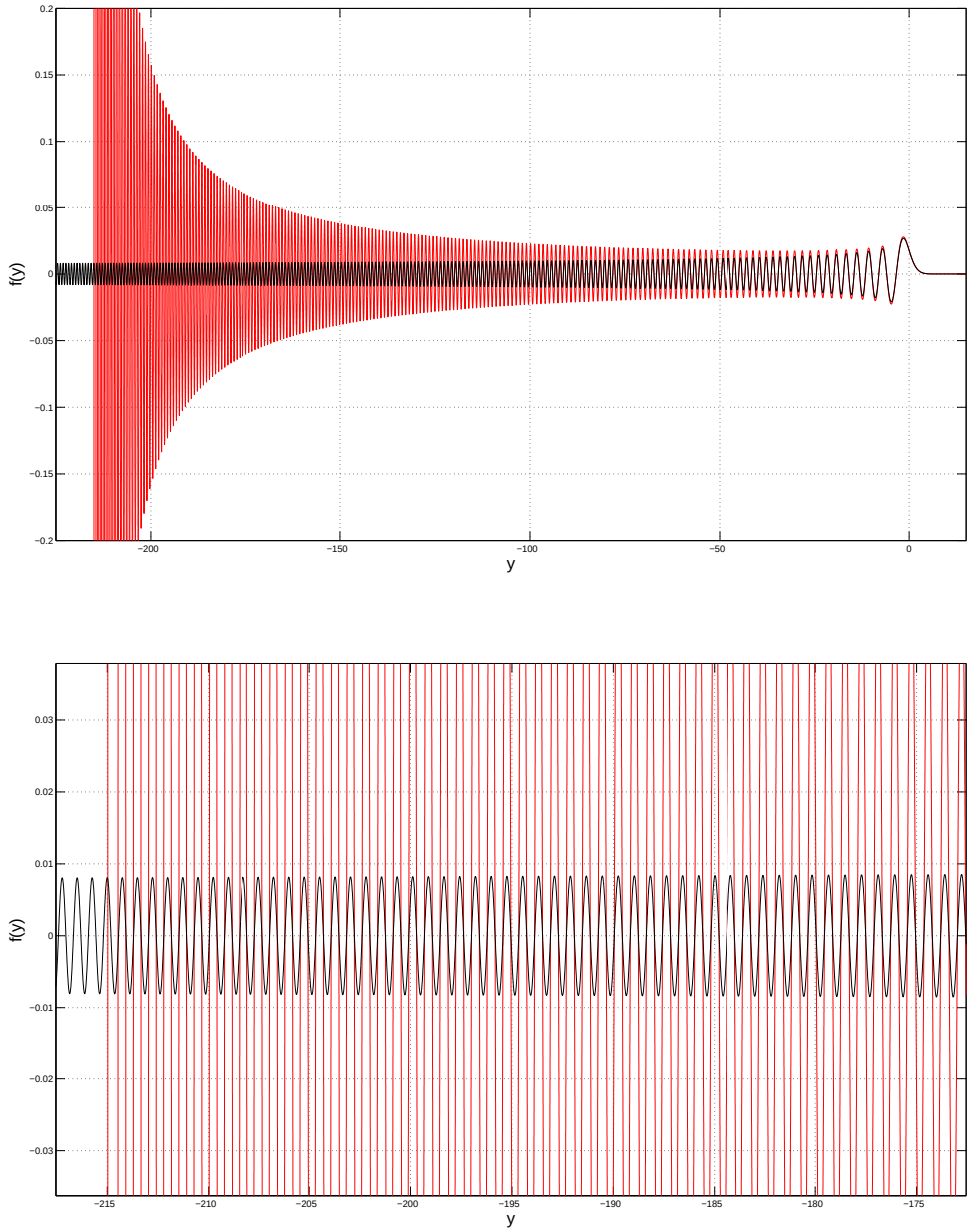

Figure 4-7: *The behaviour of f for $C = 0.05$ (red) and $0.05\mathrm{Ai}(y)$ (black)*

which is another classic blow-up problem. It becomes unbounded for $g_0 > 0$ and $g_1 < 0$, as z decreases from z_0.

4.3.2.2 Non-zero integration constant

We now consider the problem (4.6) with the non-zero integration constant, i.e.

$$f'' - \frac{1}{3}yf + (|f|f)' = A, \quad -\infty < y < \infty, \tag{4.20}$$

with the same boundary condition (4.7),

$$f(y, C) \sim C\,\mathrm{Ai}(y) \quad \text{as} \quad y \to \infty,$$

where $A > 0$ is the constant of integration. In Figure 4-8, we display the behaviour of f, for some values of A, when $C = 0.1$ and $y_0 = 10$, which are unbounded.

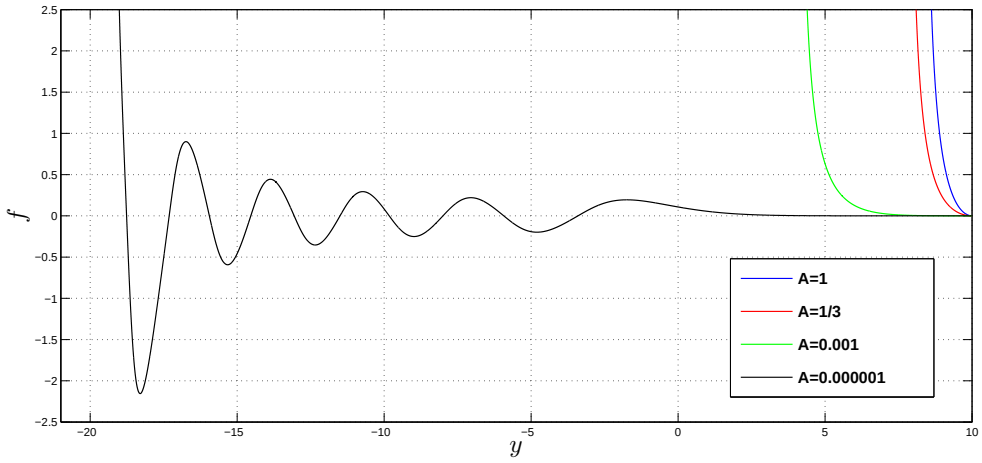

Figure 4-8: *The behaviour of f for (4.20) with (4.7), when $A = 1, 1/3, 10^{-3}, 10^{-6}$, $C = 0.1$ and $y_0 = 10$.*

4.4 Summary

In this chapter we have investigated the blow-up similarity solutions of the '+' case. We would like to point out that the blow-up self-similar profiles of the '+' case implies the global self-similar profiles of the '−' case. We have mentioned

admissible blow-up similarity profiles of the analytical form for appropriate values of C, such as $C < C^*$. Moreover, we observe the non-existence of exponentially decaying blow-up similarity profiles for the signed form with the proposed numerical construction. In Section 6.5, according to the non-existence result, we will discuss the large-time behaviour of the rescaled PDE, which cannot convergence to a non-zero stationary solution.

In summary, for the first critical case $p = p_0 = 2$, we list the existence and non-existence results obtained by using numerical and perturbation techniques in Chapter 3 and 4 for the similarity solutions of

$$f'' - \frac{\sigma}{3} f y \pm (|f|f)' = 0 \tag{4.21}$$

with the boundary condition,

$$f(y, C) \sim C\,\mathrm{Ai}(y) \quad \text{as} \quad y \to \infty, \tag{4.22}$$

in Table 4.1, where $C \neq 0$ varies from $-\infty$ to ∞ and $C^* \approx 0.5911$.

	$-(\lvert f\rvert f)'$	$+(\lvert f\rvert f)'$	$-(f^2)'$	$+(f^2)'$
Blow-up similarity ($\sigma = 1$)	$\forall C$	$\nexists C$	$C > -C^*$	$C < C^*$
Global similarity ($\sigma = -1$)	$\nexists C$	$\forall C$	$C < C^*$	$C > -C^*$

Table 4.1: *A summary table for the existence results obtained for the similarity solutions of 4.21 with 4.22 in Chapter* 3 *(red) and Chapter* 4 *(black).*

Chapter 5

An exponentially fitted Runge-Kutta method for Airy-type IVPs

There are many numerical techniques for the integration of ODEs. However, there is not a specific method that works well for general ODEs, since a method may behave differently for a decaying or oscillating solution. In this chapter, we use a numerical method for a prototype of the second-order ODEs, which have appeared in this thesis. If we generalise the initial value problems that we have studied in Chapter 3 and 4, we have

$$f''(y) = kyf(y) + N(f(y), f'(y)), \quad f(y_0) = f_0, \quad f'(y_0) = f_1, \tag{5.1}$$

where N is continuously differentiable respect to f and f', y_0 is an initial point, f_0 and f_1 are real values and $k \neq 0$ is a constant. It can be seen in previous chapters that there are numerical challenges in order to catch both long time oscillatory slow decaying and exponential fast decaying behaviour of the solutions depending on C. In particular, any small change in C may cause a pole in the solution. In this chapter, we propose a reliable two stage exponentially fitted Runge-Kutta method [85, 86, 91] in order to catch all kind of behaviour of (5.1), even for relatively large step sizes compared to the classical Runge-Kutta methods. We propose a two-parameter reference set to solve (5.1) and use local truncation errors to determine these 'fitting' parameters in each step. Since computational cost is much more than the classic IVP solver of *MatLab*, which is used in the previous chapters, this method is only used in this chapter for proposed examples.

This technique is an extension of pre-existing work [91, 97, 102] to the Airy-

type initial value problems (5.1) by using a two stage Runge Kutta method. The results of this chapter appear in the papers 'Numerical study of the asymptotic of the second Painlevé equation by a functional fitting method' (with U. Erdoğan, 2014) published in the Mathematical Methods in the Applied Sciences, and, partially, in 'A reliable scheme with large time steps for second order initial value problems' (with U. Erdoğan, 2014) submitted.

5.1 A two stage exponentially fitted Runge-Kutta method with two parameters

Exponentially fitted Runge-Kutta methods (EFRK) are of great interest recently [91, 92, 93, 94, 95, 96]. They are designed for highly oscillatory and stiff problems. Each method has to be tailored with respect to the nature of the problem under consideration. The proposed method in this chapter will be constructed on a two stage Runge-Kutta (RK) formula.

The main issues in the construction of multi-stage EFRK methods are the determination of the reference sets for internal and external stages and selection of the parameters. All the classical integrators have in common that they are exact for some degrees of polynomials. The polynomial reference sets might not be the best for the oscillatory and decaying character of the solution of the equation (5.1). The classical exponentially-trigonometrically fitted methods can integrate exactly $f''(y) \mp w^2 f(y) = 0$, for the problem $f''(y) = G(f(y))$, with the reference set $\{e^{wy}, e^{-wy}\}$ or $\{\sin(wy), \cos(-wy)\}$. However, these reference sets do not work for the problem $f''(y) = G(f(y), f'(y))$, e.g. $f'' - kf' + c = 0$ cannot be integrated by $\{e^{wy}, e^{-wy}\}$ or $\{\sin(wy), \cos(-wy)\}$, when $k \neq 0$ [97]. In order to reflect the effect of f' and y in (5.1), we use two parameters rather than one parameter as in [98, 99, 100]. We propose $\{e^{\lambda_1 y}, e^{\lambda_2 y}\}$ for internal stage and $\{1, e^{\lambda_1 y}, e^{\lambda_2 y}\}$ for external stage of RK method. Our aim is to effectively catch the oscillatory and exponential behaviours of (5.1) according to the parameters λ_1 and λ_2 that might be real or complex.

In the next section a two stage EFRK method with two parameters is introduced step by step. The numerical examples section includes the second Painlevé equation with Hastings-McLeod solution and the equation (4.8) with initial condition (4.3.1) discussed in Chapter 4.

5.2 Derivation of the Method

The derivation of a two stage EFRK method is given in [85, 86, 91] for $f''(y) = G(y, f(y))$. For the completeness of the chapter, we give the detailed derivation of the proposed method for the problem (5.1) with some additional arguments.

5.2.1 Derivation of the coefficients

Let us consider the equation

$$f' = G(y, f). \tag{5.2}$$

The coefficients of the EFRK will be determined by the exact integration of (5.2) for exponential and/or trigonometrical functions. We propose a two stage Runge Kutta (RK) method for (5.2) with the internal and external stages as

$$\begin{aligned} F_1 &= f_n, \\ F_2 &= \gamma_2 f_n + h a_{21} G(y_n, F_1), \\ f_{n+1} &= f_n + h\left(b_1 G(y_n, F_1) + b_2 G(y_n + c_2 h, F_2)\right). \end{aligned} \tag{5.3}$$

The reference sets for internal and external stages are taken $\left\{e^{\lambda_1 y}, e^{\lambda_2 y}\right\}$ and $\left\{1, e^{\lambda_1 y}, e^{\lambda_2 y}\right\}$ respectively. Therefore, the corresponding linear difference operators

$$\begin{aligned} \mathfrak{L}_2[h, \mathbf{a}]f(y) &= f(y + c_2 h) - \gamma_2 f(y) - h a_{21} f'(y), \\ \mathfrak{L}[h, \mathbf{a}]f(y) &= f(y + h) - f(y) - h(b_1 f'(y) + b_2 f'(y + c_2 h)), \end{aligned} \tag{5.4}$$

vanish for the elements of reference sets. After solving the algebraic system

$$\begin{aligned} \mathfrak{L}_2[h, \mathbf{a}] \exp(\lambda_1 y) &= 0, \\ \mathfrak{L}_2[h, \mathbf{a}] \exp(\lambda_2 y) &= 0, \\ \mathfrak{L}[h, \mathbf{a}] \exp(\lambda_1 y) &= 0, \\ \mathfrak{L}[h, \mathbf{a}] \exp(\lambda_2 y) &= 0, \\ \mathfrak{L}[h, \mathbf{a}] 1 &= 0, \end{aligned}$$

the coefficients of the method appear as

$$a_{2,1} = -\frac{-e^{\lambda_1 c_2 h} + e^{\lambda_2 c_2 h}}{h(\lambda_1 - \lambda_2)}, \tag{5.5a}$$

$$\gamma_2 = \frac{e^{\lambda_2 c_2 h}\lambda_1 - \lambda_2 e^{\lambda_1 c_2 h}}{\lambda_1 - \lambda_2}, \tag{5.5b}$$

$$b_2 = -\frac{e^{\lambda_2 h}\lambda_1 - \lambda_1 - e^{\lambda_1 h}\lambda_2 + \lambda_2}{\lambda_1 h\left(-e^{\lambda_2 c_2 h} + e^{\lambda_1 c_2 h}\right)\lambda_2}, \tag{5.5c}$$

$$b_1 = -\frac{\lambda_2 e^{h(\lambda_2 c_2 + \lambda_1)} - e^{\lambda_2 c_2 h}\lambda_2 - \lambda_1 e^{h(\lambda_1 c_2 + \lambda_2)} + e^{\lambda_1 c_2 h}\lambda_1}{\lambda_1 h\left(-e^{\lambda_2 c_2 h} + e^{\lambda_1 c_2 h}\right)\lambda_2}. \tag{5.5d}$$

The local truncation error of the method is given by

$$\begin{aligned}\tau_{i+1}(h) = [(-\frac{1}{4}c_2 + \frac{1}{6})f'''(y_i) + (\frac{1}{4}\lambda_2 c_2 + \frac{1}{4}c_2 G_f(y_i) - \frac{1}{6}\lambda_1 + \frac{1}{4}\lambda_1 c_2 - \frac{1}{6}\lambda_2)f''(y_i)\\ +(-\frac{1}{4}\lambda_1\lambda_2 c_2 + \frac{1}{6}\lambda_1\lambda_2 - \frac{1}{4}\lambda_1 c_2 G_f(y_i) - \frac{1}{4}\lambda_2 c_2 G_f(y_i))f'(y_i) + \frac{1}{4}\lambda_1\lambda_2 c_2 f(y_i)]h^2\\ +O(h^3),\end{aligned}$$

where $\tau_{i+1}(h)$ is defined as (see [103, pp. 317])

$$\tau_{i+1}(h) = \frac{f(y_{i+1}) - f(y_i)}{h} - (b_1 f'(y_i) + b_2 f'(y_i + c_2 h)).$$

If we set $c_2 = 2/3$ as in the classical two stage RK method, the local truncation error becomes

$$\tau_{i+1}(h) = \frac{1}{6}G_f(y_i)h^2\left(f''(y_i) - (\lambda_1 + \lambda_2)f'(y_i) + (\lambda_1\lambda_2)f(y_i)\right) + O(h^3). \tag{5.6}$$

In the next subsection, it can be seen that the selection $c_2 = 2/3$ does not only yield a simple expression for $\tau_{i+1}(h)$, but also reduces computational cost in calculating parameters λ_1 and λ_2 by eliminating the third derivative.

In the case of $\lambda_1, \lambda_2 \to 0$ or $\lambda_1 \to \lambda_2$, the following series expansions of the coefficients may be utilized in order to prevent numerical instabilities.

$$\begin{aligned}a_{2,1} &= \frac{2}{3} + \frac{2}{9}h\left(\lambda_1 + \lambda_2\right) + \frac{4}{81}h^2\left(\lambda_1^2 + \lambda_1\lambda_2 + \lambda_2^2\right) + \frac{2}{243}h^3\left(\lambda_1^3 + \lambda_1^2\lambda_2 + \lambda_1\lambda_2^3 + \lambda_2^3\right)\\ &\quad +O(h^4),\\ \gamma_2 &= 1 - \frac{2}{9}h^2\lambda_1\lambda_2 - \frac{4}{81}h^3\left(\lambda_1^2\lambda_2 + \lambda_1\lambda_2^2\right) + O(h^4),\\ b_1 &= \frac{1}{4} - \frac{1}{144}h^2\left(\lambda_1^2 + \lambda_1\lambda_2 + \lambda_2^2\right) - \frac{1}{2160}h^3\left(2\lambda_1^3 + 7\lambda_1^2\lambda_2 + 7\lambda_1\lambda_2^2 + 2\lambda_2^3\right) + O(h^4),\\ b_2 &= \frac{3}{4} + \frac{1}{144}h^2\left(\lambda_1^2 + \lambda_1\lambda_2 + \lambda_2^2\right) + \frac{1}{2160}h^3\left(2\lambda_1^3 - 3\lambda_1^2\lambda_2 - 3\lambda_1\lambda_2^2 + 2\lambda_2^3\right) + O(h^4).\end{aligned}$$

5.2.2 Selection of the parameters

According to the previous studies on the classical exponentially fitted (EF) methods for $f''(y) = G(f(y))$, there is no unique way of determining fitting parameters. The approaches are usually problem dependent. Some authors assume that the constant value of fitting parameters are known in advance [93, 101]. Another approach is that a formula for fitting parameters can be obtained by minimizing local truncation error [94, 99, 102, 104, 105, 106].

For the problem (5.1), non-constant values of fitting parameters are expected. Therefore the idea of minimizing local truncation error will be used in order to determine the fitting parameters. The construction of the method for (5.1) is illustrated over a first order 2×2 ODE system, i.e.

$$\begin{aligned} u' &= v(y), \\ v' &= G(y, u(y), v(y)), \end{aligned} \tag{5.7}$$

where G has continuous derivatives with respect to y, u and v. Applying the scheme (5.3), for each equation of the system (5.7), yields the following local truncation errors,

$$\begin{aligned} \tau_{i+1,1}(h) &= C_1 h^2 \left(u''(y_i) - (\lambda_1 + \lambda_2)u'(y_i) + (\lambda_1\lambda_2)u(y_i)\right) + O(h^3), \\ \tau_{i+1,2}(h) &= C_2 h^2 \left(v''(y_i) - (\lambda_1 + \lambda_2)v'(y_i) + (\lambda_1\lambda_2)v(y_i)\right) + O(h^3). \end{aligned}$$

Equating the coefficients of h^2 to zero, one increases the order of the method and obtains algebraic equations to get λ_1, λ_2 as well:

$$\begin{aligned} u''(y_i) - (\lambda_1 + \lambda_2)u'(y_i) + (\lambda_1\lambda_2)u(y_i) = 0, \\ v''(y_i) - (\lambda_1 + \lambda_2)v'(y_i) + (\lambda_1\lambda_2)v(y_i) = 0. \end{aligned} \tag{5.8}$$

Since the numerical values of $u(y_i)$, $v(y_i)$, $u'(y_i) = v(y_i)$, $v'(y_i) = u''(y_i) = G(y_i, u(y_i), v(y_i))$, and $v'(y_i) = G_u(y_i, u(y_i), v(y_i))v(y_i) + G_v(y_i, u(y_i), v(y_i))v'(y_i) + G_y(y_i, u(y_i), v(y_i))$ are known by (5.7) at each step in y, (5.8) yields complex or real roots as

$$\lambda_{1,2} = \frac{\beta_i \pm \sqrt{{\beta_i}^2 - 4\alpha_i}}{2},$$

where

$$\alpha_i = \frac{u(y_i)v''(y_i) - u''(y_i)v(y_i)}{u(y_i)v'(y_i) - u'(y_i)v(y_i)}, \qquad \beta_i = \frac{u'(y_i)v''(y_i) - u''(y_i)v'(y_i)}{u(y_i)v'(y_i) - u'(y_i)v(y_i)}.$$

In the case of complex λ's, it is worth mentioning that the coefficients of the method in (5.5) are always real due to complex conjugacy of λ's.

The classical two stage explicit Runge-Kutta methods have local truncation error $O(h^2)$ and second order accuracy [107]. The proposed method is of third order accurate with two stages. The computation of parameters may cause additional computational cost. However, it leads to a more stable, accurate and conservative method. The proposed algorithm is written in *Maple* and it can be found at the end of chapter.

5.3 Numerical Experiments

According to our numerical experiences, the proposed solver behaves like the classical fourth-order Runge-Kutta (ode4) method for such ODEs. However, the ode4 method requires smaller step sizes than EFRK does, in order to keep the solution bounded, especially in oscillatory problems. It is well known that classical integrators do not preserve qualitative properties such as Hamiltonian in the long time simulation if they are not symplectic.

In this section, numerical experiments are performed to verify that the EFRK method is quite flexible in choosing large step sizes and very successful in simulating qualitative behaviours of the equation due to its parameter dependence.

5.3.1 Example 1

We consider a numerical approximation of the asymptotics of the Second Painlevé equation, which has briefly mentioned in Chapter 2,

$$f'' = yf + 2f^3 + \alpha, \tag{5.9}$$

where α is an arbitrary constant. Equation (5.9) is one of the six Painlevé equations whose solutions are called Painlevé transcendents, which generally cannot be governed by elementary functions. These equations are mentioned as most important nonlinear ordinary differential equations by some authors [87, 88, 89, 108]. Besides their mathematical attraction like Painlevé property [89], the Painlevé

equations have arisen in many branches of physics such as mechanics, relativity and optics. The review of previous attempts to analyse Painlevé equations is given in [89] by Clarkson. Clarkson also pointed out that there is need for further numerical and analytical studies of asymptotics of solutions of (5.9).

Rosales [87] considered the second Painlevé equation as a reduction of the (defocusing) mKdV,

$$u_t - 6u^2u_x + u_{xxx} = 0,$$

with the the following form of similarity solutions

$$u(x,t) = (3t)^{-1/3}f(y), \quad y = x/(3t)^{1/3}.$$

Moreover, one can see the connection between the second Painlevé and the KdV,

$$v_t - 6vv_x + v_{xxx} = 0,$$

via the Miura transformation, $v = u_x + u^2$ [17]. Rosales also presented plots of the solutions obtained numerically. Hastings and McLeod [88] proposed asymptotics of the second Painlevé equation as a special case of

$$f'' = yf + 2f|f|^p, \tag{5.10}$$

where $p > 0$. Miles [109, 110] also derived some approximation formulae for asymptotics. The nonlinear Schrödinger equation is mapped to the second Painlevé equation in order to calculate nonlinear eigenfunctions in [111]. Recently, the problem (5.9) has been solved by approximation methods such as homotopy analysis method (HAM) [112], homotopy perturbation method (HPM), Adomian decomposition method (ADM), Legendery-Tau method [113, 114], analytic continuation method, Chebshyev series method [115]. However, the authors of these papers use initial conditions $f(0) = 1$ and $f'(0) = 0$ and seek the solution in a small interval regardless of oscillatory and decaying solutions. The studies in the literature are generally for the case $\alpha = 0$. However, a recent fruitful computational discussion on the second Painlevé with different values of α can be found in [116].

Considering $\alpha = 0$ and the boundary condition,

$$f(y) \to 0 \quad \text{as} \quad y \to \infty, \tag{5.11}$$

Hastings and McLeod [88] give the following theorem:

Theorem 5.1 ([89]). *Any solution of (5.9) with $\alpha = 0$, satisfying $f(y) \to 0$ as $y \to \infty$, is asymptotic to $C\,\mathrm{airy}(y)$, for some C. Conversely, for any C, there is a unique solution $f(y, C)$ of (5.9) with $\alpha = 0$ which is asymptotic to $C\,\mathrm{airy}(y)$ as $y \to +\infty$. If $|C| < 1$, then this solution exists for all real y as $y \to -\infty$, and as $y \to -\infty$*

$$f(y, C) = d\,|y|^{-1/4} \sin\left(\frac{2}{3}\,|y|^{3/2} - \frac{3}{4}d^2 \log(|y|) - \theta_0\right) + o(|y|^{-1/4}),$$

for some constants d and θ_0 which depend on C. If $|C| = 1$ then

$$f(y, C) \sim sgn(C)\sqrt{-\frac{1}{2}y},$$

as $y \to -\infty$. If $|C| > 1$ then $f(y, C)$ has a pole at a finite y^*, dependent on C,

$$f(y, C) \sim sgn(C)(y - y^*)^{-1},$$

as $y \downarrow y^*$. □

The Airy function, $\mathrm{airy}(y)$, is the admissible solution of the linear part of (5.9), $f'' = yf$. Rosales [87] had confirmed the above theorem numerically by employing the fourth-order Runge-Kutta scheme with double precision and small step sizes. One of the numerical challenges of the second Painlevé equation is C sensitivity of any proposed method. In other words an arbitrary ODE solver may blow-up for $|C| = 1 - \epsilon$, where ϵ is small positive real number. It is observed that while *MatLab* solver *ode15s* fails to catch oscillatory motion for constant step size, *ode4*, which is an implementation of the classical fourth-order Runge-Kutta method in the *MatLab Center*, needs relatively small step sizes. Increasing the order of the method or adaptive version of the methods such as *ode45* may be a remedy.

Considering Theorem 5.1, right initial conditions for (5.9) are determined for various values of C as in [87, 109, 110]. In Figure (5-1) the numerical solutions of (5.9) by *ode15s* and *ode4* with right initial conditions $f(5) = C\,\mathrm{airy}(5)$ and $f' = C\,\mathrm{airy}'(5)$ where $C = 1 - 10^{-6}$ are plotted. For step sizes $h = 0.01$ *ode15s* fails to catch oscillatory motion implied in Theorem 5.1 but *ode4* works well.

The proposed method, which is of third order at most, is able to simulate all behaviours explained in Theorem 5.1. In Figure (5-2). the numerical solution,

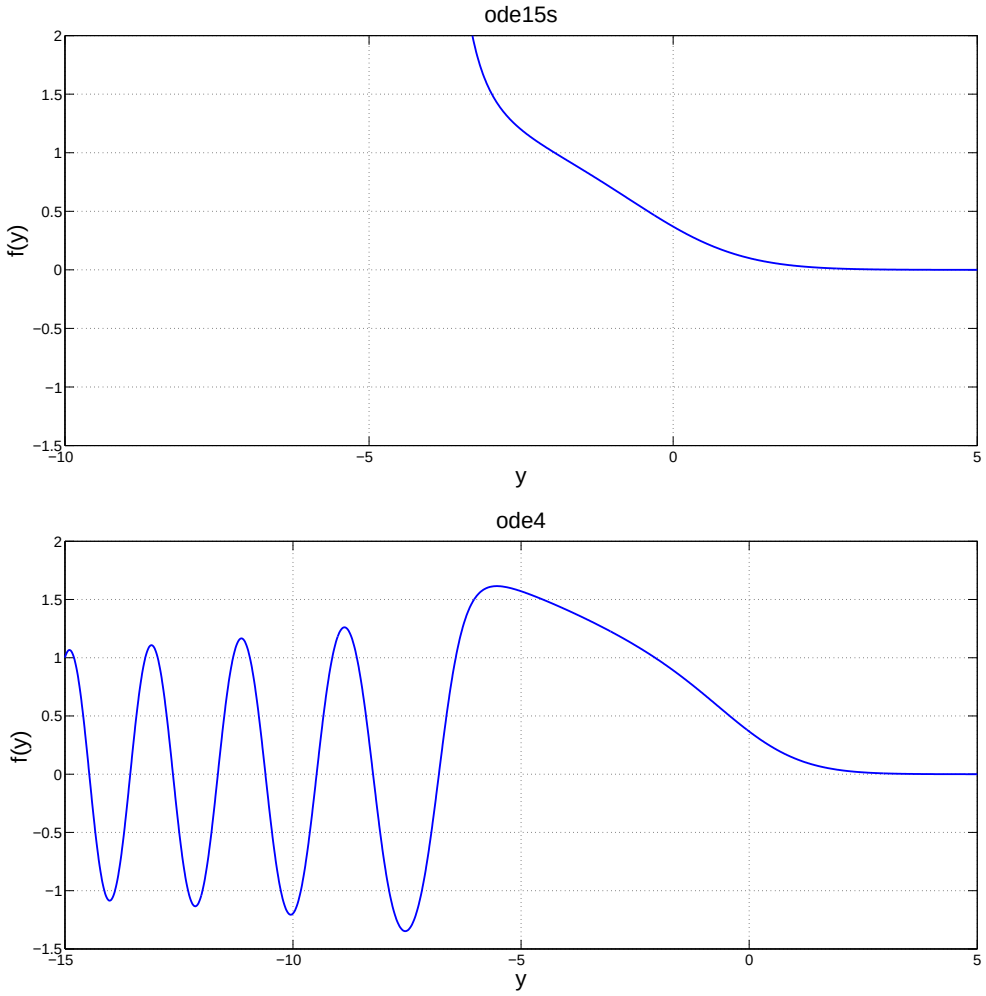

Figure 5-1: ode15s *and* ode4 *solution of (5.9) with* $h = 0.01$ *for* $C = 1 - 10^{-6}$.

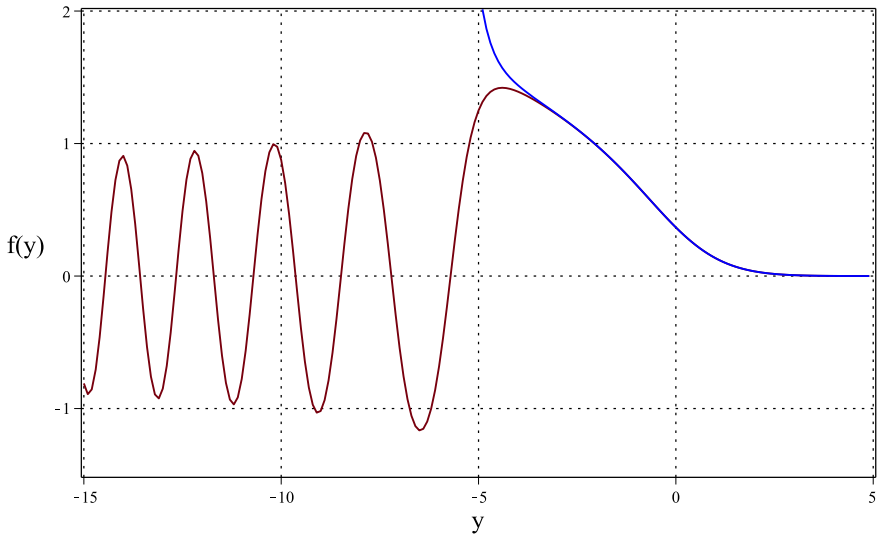

Figure 5-2: *Numerical solution of (5.9) by the present method with* $h = 0.1$ *for* $C = 1 - 10^{-7}$ *(red line) and* $C = 1 + 10^{-4}$ *(blue line).*

by the present exponentially fitted method, is given for $C = 1 - 10^{-7}$ at first. Blow-up motion is also demonstrated for $C = 1 + 10^{-4}$. Here, the step size is taken $h = 0.1$.

The location of the pole can be also investigated by checking the frequencies of the method. As $y \to y^*$, the imaginary parts of the method are zero, which means no oscillation, and real parts are extremely large in magnitude, see Table 5.1. Additionally, since the frequencies are determined by derivatives of the solution in formulae (5.8), frequency computations of the method can be considered as a numerical tool for confirming the location of the pole.

The method is observed to work well even for a coarser mesh, for instance $h = 1.4$. For this step size, *ode4* solver blows up while the EFRK method still remains bounded and oscillates for $|C| < 1$ (see Figure 5-3). Indeed this is the superiority of EF methods to classical methods. When the frequencies are computed accurately, there is no strict restriction on the step sizes of explicit EFRK methods.

On the other hand, the proposed method is efficient and promising for large values of y with $h = 0.1$ and $C = 1 - 10^{-6}$. In Figure 5-4, the present method simulates slow decaying strong oscillation regarding to the asymptotic form in Theorem 5.1. However, *ode4* solver damps the solution early. This may be recovered for smaller step sizes.

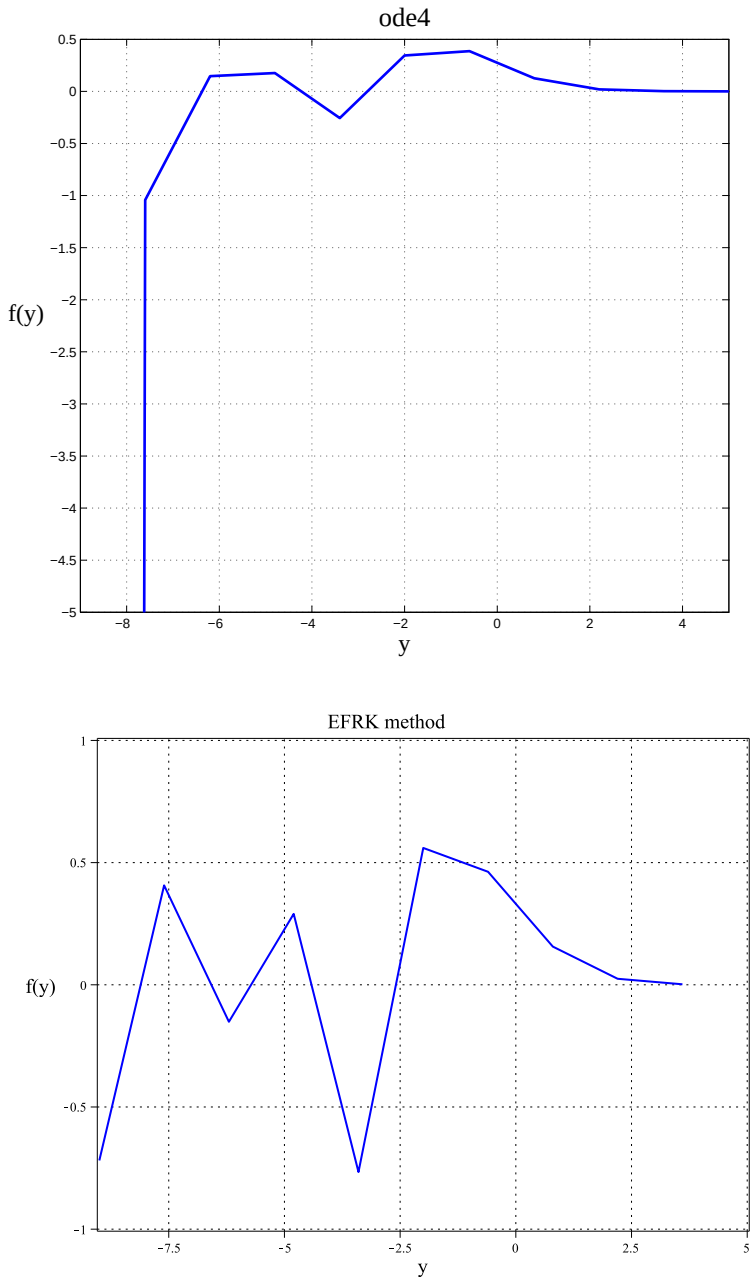

Figure 5-3: *Numerical solutions of (5.9), by the present method and* ode4 *solver, with* $h = 1.4$*, for* $C = 1 - 10^{-6}$.

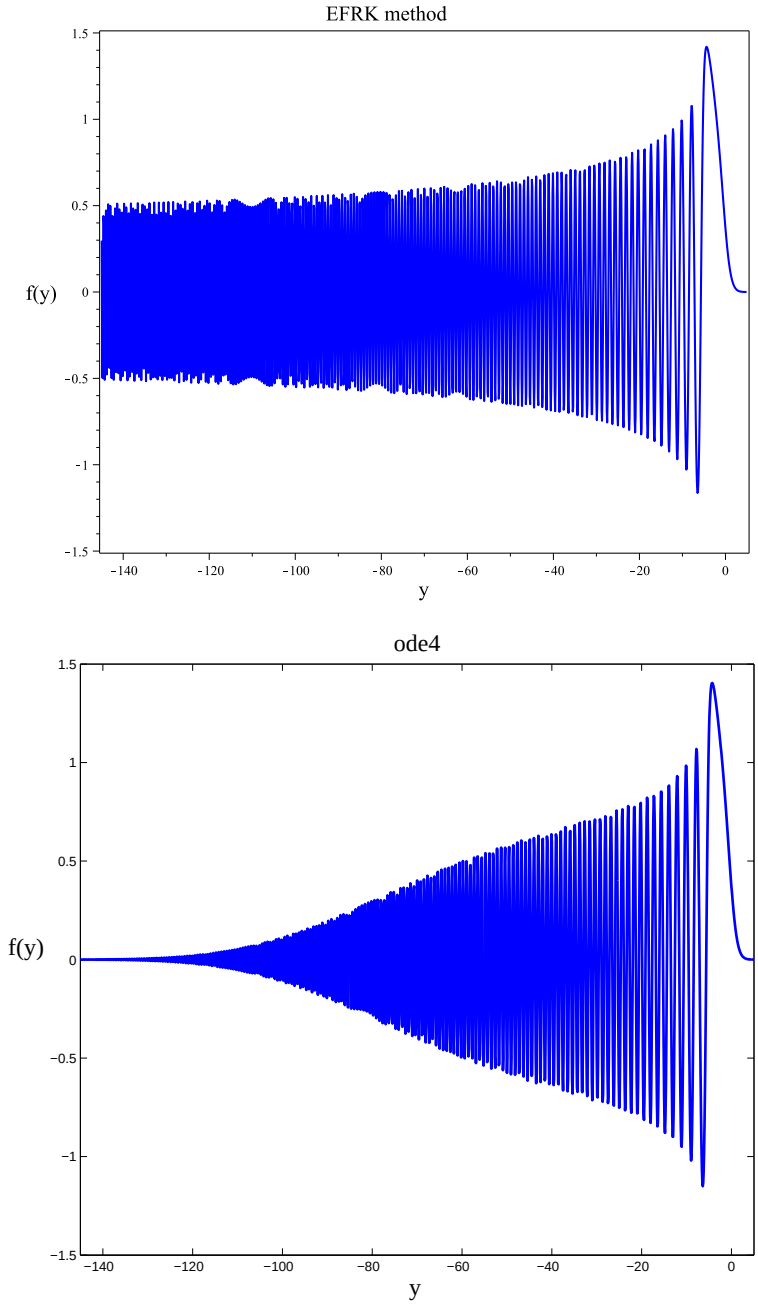

Figure 5-4: *Behaviour of (5.9) for large values of* y*, by the present method and* ode4 *solver, with* $h = 0.1$ *and* $C = 1 - 10^{-6}$.

y	λ_1	λ_2	$f(y)$
-5.39	312.25	53.751	91.145
-5.40	1435.142	237.073	433.454
-5.41	0.270e+9	-0.312e+9	0.118e+9
-5.42	overflow	overflow	overflow

Table 5.1: *Values of the real part of frequencies near the pole for* $C = 1 + 10^{-4}$ *with* $h = 0.01$.

5.3.2 Example 2

Going back to Chapter 4, we now consider the analytical form of (4.8),

$$f'' - \frac{1}{3}yf + 2ff' = 0, \quad -\infty < y < \infty, \tag{5.12}$$

with boundary condition

$$f(y, C) \sim C\,\mathrm{Ai}(y) \quad \text{as} \quad y \to \infty. \tag{5.13}$$

The behaviour of (5.12), when $C < C^*$ and $C > C^*$, where $C^* \approx 0.5911$, are discussed in Chapter 4. In addition to previous studies, we compare the long-time behaviour efficiency of *ode4* and present method for large step sizes. EFRK and *ode4* solutions for $C = 0.591106$ are plotted in Figure 5-5. *ode4* damps the solution in early times for $h = 0.1$. This may be recovered by taking smaller step sizes. However, the present method simulates slow decaying strong oscillation for $h = 0.1$, as mentioned in Chapter 4. One can see Figure 4-1 as a reference to compare the accuracy of the methods for oscillatory tails of the solutions.

The real and imaginary parts of λ_1 and λ_2 versus y are plotted in Figure 5-6, in order to show how parameters affect the solution. Their parallelism with the solution can be seen by comparing Figure 5-5 and 5-6.

5.4 Summary

As a result, an explicit two-stage and third order exponentially fitted Runge-Kutta method to a prototype of second order ODEs is introduced. Since the method has variable coefficients, computational cost is much more than the classical two stage Runge-Kutta method. However, remarkable improvements in accuracy and preservation of qualitative properties are gained. Higher order

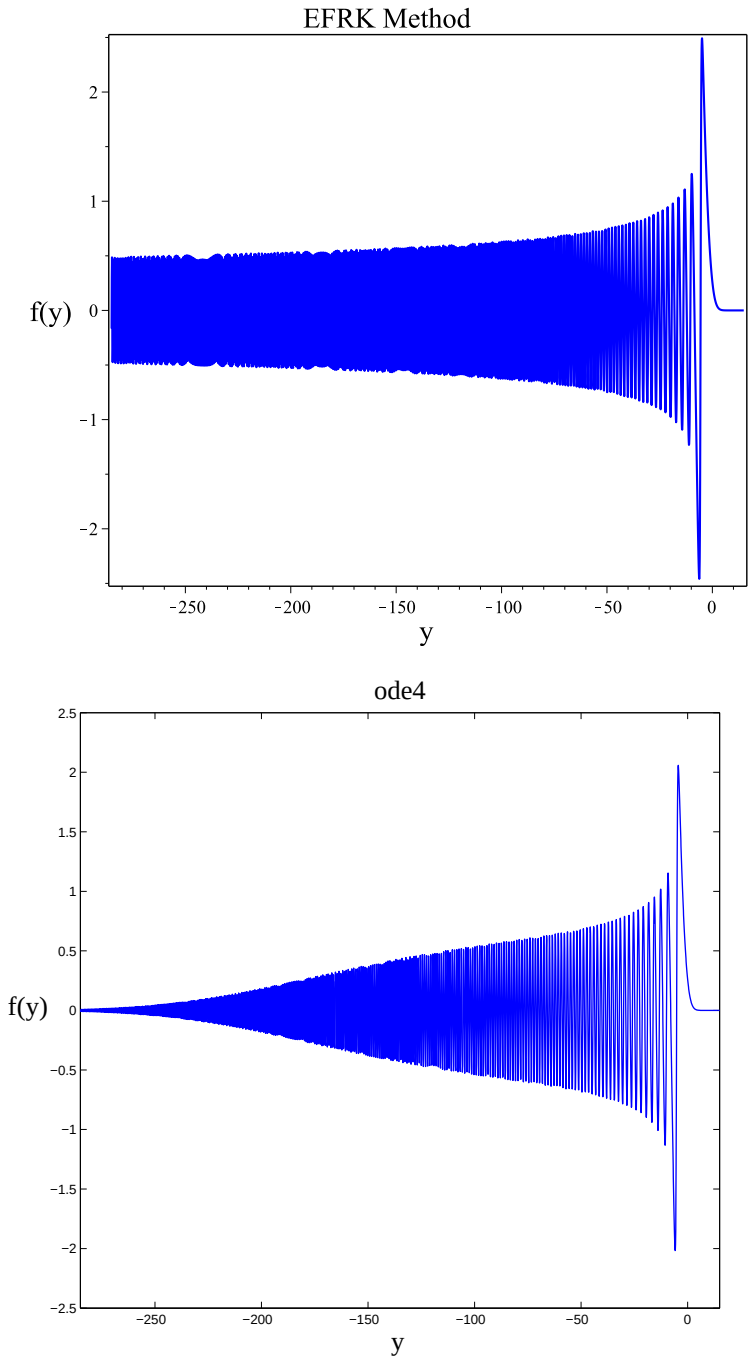

Figure 5-5: *Behaviour of (5.12) with EFRK method and* ode4 *solver for* $h = 0.1$ *and* $C = 0.591106$.

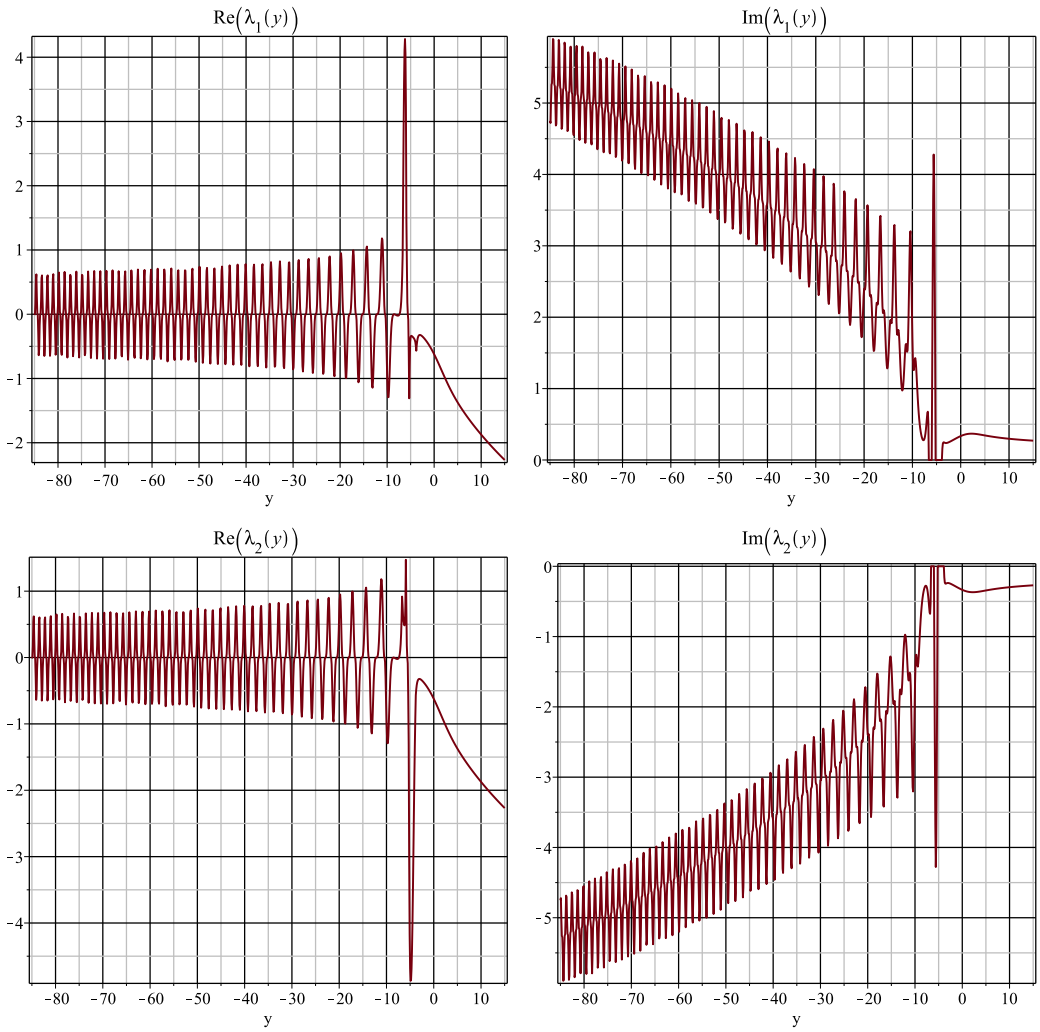

Figure 5-6: *Real and Imaginary parts of the parameters for* $h = 0.1$ *and* $C = 0.591106$.

versions of the method can be obtained by using more stages and other reference sets such as $\{1, y, y^2, ..., y^k, e^{\lambda_1 y}, e^{\lambda_2 y}, ..., y^p e^{\lambda_1 y}, y^p e^{\lambda_2 y}\}$. Exponentially fitted Runge-Kutta-Nyström (EFRKN) methods [96, 117] can also be constructed as an efficient algorithm.

5.5 Algorithm of a two stage EFRK method with two parameters in Maple

One can see that both Example 1 and Example 2 are for the domains decreasing from the initial point. Since the proposed algorithm designed for the domains increasing from the initial point, we have used $y \mapsto -y$ in our examples. After the transformation, the algorithm for Example 2 is given as follows:

```
restart: with(LinearAlgebra):
Digits:=16: # set your digits #
#problem settings begin#
f:=V: #do not change it means  V=U'#
g:=-Y/3*U+2*U*V; #write rhs of your equation as U''=g(Y,U,V)#
#enter the domain and shooting parameter#
initial:=-15; final:=285; C:=0.591106:
#initial must be less than final #
N:=3000; #change number of step#
#enter the initial conditions#
u[0]:=evalf(eval(C*AiryAi(-1/3*3^(2/3)*(Y)),Y=initial));
v[0]:=evalf(eval(diff(C*AiryAi((-1/3*3^(2/3))*Y),Y),Y=initial));
# write rhs of your equation here again#
F:=(U,V,Y)-> <V,-Y*U/3+2*(U)*V>;
#problems settings finished#
c[2]:=2/3:
h:=evalf((final-initial)/N); #steplenght#
U1:=f: V1:=g: U2:=g: V2:=diff(g,U)*f+diff(g,V)*g+diff(g,Y):
alpha:=-(U1*V2-U2*V1)/(-U*V1+V*U1):
beta:=(-U*V2+V*U2)/(-U*V1+V*U1):
y[0]:=<u[0],v[0]>;
for i from 0 to N do
x[i]:=initial+i*h:
```

```
#calculations of the parameters#
denk:=w^2-eval(beta,{U=y[i][1],V=y[i][2],Y=x[i]})*w+eval(alpha,
{U=y[i][1],V=y[i][2],Y=x[i]}):
{solve(denk)}:
mu[1]:=op(1,%):
mu[2]:=op(2,%%):
aa1[i]:=mu[1]: aa2[i]:=mu[2]:
#coefficients of F_2#
g[1] :=Re((exp(mu[2]*c[2]*h)*mu[1]-mu[2]*exp(mu[1]*c[2]*h))
/(mu[1]-mu[2])):
a[2,1] :=Re(-(-exp(mu[1]*c[2]*h)+exp(mu[2]*c[2]*h))/h
/(mu[1]-mu[2])):
Y1:=y[i]:
Y2:=g[1]*y[i]+h*a[2,1]*F(y[i][1],y[i][2],x[i]):
#coefficients of external stage#
b[2] :=Re(-(-exp(mu[2]*h)*mu[1]+mu[1]+exp(mu[1]*h)*mu[2]-mu[2])
/h/mu[1]/(-exp(mu[1]*c[2]*h)+exp(mu[2]*c[2]*h))/mu[2]):
b[1] :=Re((mu[2]*exp(h*(mu[2]*c[2]+mu[1]))-exp(mu[2]*c[2]*h)*
mu[2]-mu[1]*exp(h*(mu[1]*c[2]+mu[2]))+exp(mu[1]*c[2]*h)*mu[1])
/h/mu[1]/(-exp(mu[1]*c[2]*h)+exp(mu[2]*c[2]*h))/mu[2]):
y[i+1]:=y[i]+h*(b[1]*F(Y1[1],Y1[2],x[i])+b[2]*F(Y2[1],Y2[2],x[i]
+c[2]*h)):
end do:
#plot of the original equation#
plot([seq([-x[i],y[i][1]],i=0..N)]);
#real and imaginary parts of parameters(aa1 and aa2) versus y#
plot([seq([-x[i],-Re(aa1[i])],i=0..N)]);
```

Chapter 6

Semilinear Dispersion PDEs: General p's

In this Chapter we focus on the case of general $p > 1$ for the semilinear PDE (1.1). One can see that the rescaled ODEs (3.9) and (4.2) remain truly third-order without conservation. Clearly, it is more complicated than the conservative case, $p = p_0 = 2$. Firstly, we consider the conservation of the first moment which fortunately also yields a second-order ODE with $p = p_1 = 3/2$. We next give the spectral properties of the rescaled linear operator in order to enlighten instabilities in the linearisation of the rescaled PDE for arbitrary values of $p > 1$. However, we do not expect reasonably simple justifications due to the highly oscillatory nature of the eigenfunctions of the problem, in contrast to other evolution equations. Most of our analysis and conclusions for the centre subspace behaviour and bifurcation points remain formal. Therefore, similar to the previous chapters, we rely on numerical results playing an important role in analysing the similarity profiles. We finally use numerics in the ODE and original PDE to clarify such existence and non-existence results. Additionally, some aspects of the semilinear PDE, such as Airy-type radiation conditions at infinity and the extension of solutions beyond blow-up are discussed. With direct simulations to the rescaled PDE, we obtain a non-zero stationary global similarity solution of the '+' case for $p = p_0 = 2$, which is one of the profiles obtained in Chapter 3. We also numerically discuss the behaviour of global and blow-up solutions for $p > 1$.

6.1 Conservation of the first moment: the second critical exponent

As a pleasant surprise, we can also derive a second-order ODE for the second critical exponent $p = p_1 = 3/2$. If we look at conservation of the first moment (we must consider this as an informal procedure, since Airy-type radiation conditions at infinity imply that the first moment is always infinity, but this is not important for such dimension-like analysis only)

$$\frac{\mathrm{d}}{\mathrm{d}t}\int\limits_{\mathbf{R}} xu_S(x,t)\mathrm{d}x = \frac{\mathrm{d}}{\mathrm{d}t}\left[(\sigma(T-t))^{\alpha+2\beta}\int\limits_{\mathbf{R}} yf(y)\mathrm{d}y\right] = 0, \tag{6.1}$$

this gives

$$\alpha + 2\beta = -\frac{1}{3(p-1)} + \frac{2}{3} = 0 \quad \Rightarrow \quad p = p_1 = \frac{3}{2}. \tag{6.2}$$

Thus, the second critical exponent, $p = p_1 = 3/2$, yields the solutions that conserve the first moment for $\int yf \neq 0$. Similar to (3.17), we also have

$$\text{for any} \quad p \neq p_1, \quad \int yf = 0. \tag{6.3}$$

If we use $p = 3/2$ with $\sigma = 1$ in the ODEs (3.9) and (4.2), then we have blow-up self-similar profiles f satisfying

$$f''' - \frac{2}{3}f - \frac{1}{3}f'y \pm (|f|^{1/2}f)'' = 0. \tag{6.4}$$

Unlike the previous chapters, we cannot simply integrate these equations. In order to reduce the order of the ODEs, we first multiply (6.4) by y,

$$f'''y - \frac{2}{3}fy - \frac{1}{3}f'y^2 \pm (|f|^{1/2}f)''y = 0. \tag{6.5}$$

and then integrate by parts

$$f''y - f' - \frac{1}{3}fy^2 \mp |f|^{1/2}f \pm (|f|^{1/2}f)'y = 0. \tag{6.6}$$

Fortunately, a solution of the linear part of (6.6),

$$f''y - f' - \frac{1}{3}fy^2 = 0, \tag{6.7}$$

is the derivative of the Airy function, i.e. $f(y) = \mathrm{Ai}'(y)$. We refer to (3.22) and Figure 3-1 for the asymptotic behaviour of $\mathrm{Ai}'(y)$.

6.1.1 Numerical construction

We now numerically study this special case. In order to obtain an admissible similarity profile, we consider the ODE (6.6),

$$f''y - f' - \frac{1}{3}fy^2 \mp |f|^{1/2}f \pm (|f|^{1/2}f)'y = 0, \quad -\infty < y < \infty,$$

with

$$f(y, C) \sim C\,\mathrm{Ai}'(y) \quad \text{as} \quad y \to \infty, \tag{6.8}$$

where C varies from $-\infty$ to 0. We would like to note that we restrict our attention to $C < 0$ since the solution $f(y, -C)$ is symmetric to $f(y, C)$ with respect to the y-axis, i.e. $f(y, -C) = -f(y, C)$. Similar to Chapter 3 and 4, we use the same methods and notations mentioned in Section 3.4. Additionally, we assign $\mathrm{Ai}''(y) = 3^{-1}y\,\mathrm{airy}(1, 3^{-1/3}y)$. We again choose a relatively large initial point on the right-hand side as $y_0 > 10$, in order to have a reliable initial condition. According to the numerics, we present below the behaviour of $f = f(y, C)$ profiles of the '$-$' and '$+$' case with (6.8) depending on C, respectively.

'$-$' case: We show the behaviour of blow-up similarity profiles f for the different values of C in Figure 6-1. Unlike Section 3.4.2, oscillations are not becoming asymptotically small, which is expected due to zero mass condition when $p \neq p_0$. However, we expect an existence result similar to Conjecture 3.2 but obviously more delicate. It is also worth mentioning for the following studies of arbitrary values $p > 1$ that the oscillatory tails occur symmetric to 0. Figure 6-2 illustrates that $f = f(y, C)$ remains close to $C\mathrm{Ai}'(y)$ for an ever increasing range of y, as $C \to 0^-$. Moreover, Figure 6-3 displays the profile f as an example of large values of $C < 0$.

'$+$' case: Similar to Conjecture 4.2, we expect to face a singularity for any C. Figure 6-4 displays behaviour of $f = f(y, C)$ for $C = -0.05, -0.1, -0.15, ..., -1.1$. The same analysis in Section 4.4.2 can be performed but obviously in a more delicate and detailed way. We represent the behaviour of $f = f(y, C)$ close to C_0^* in Figure 6-5, where $-0.952846354 < C_0^* < -0.952846353$ according to our numerical calculations. Figure 6-6 displays the behaviour of $f = f(y, C)$ compared to $C\mathrm{Ai}'(y)$, when $C = -10^{-3}$.

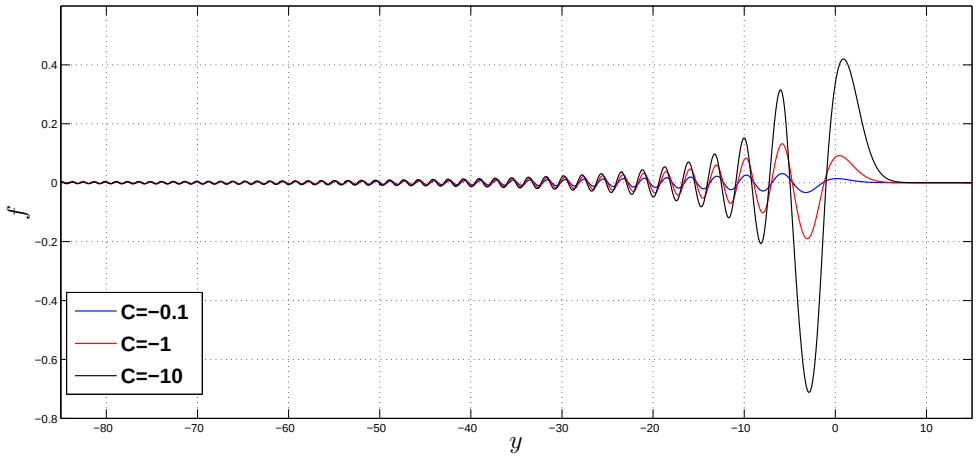

Figure 6-1: *The blow-up similarity profiles f of the '$-$' case for $C = -0.1, -1, -10$.*

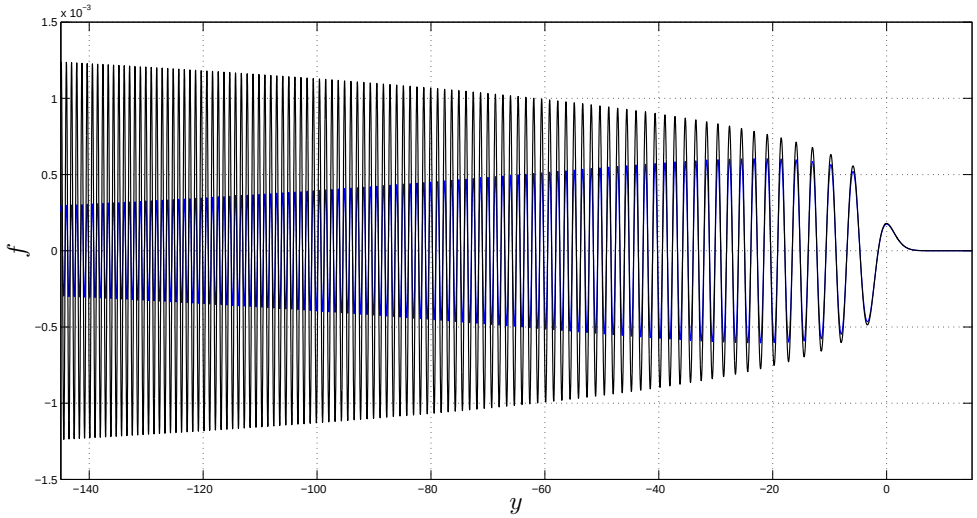

Figure 6-2: *$f = f(y, C)$ of the '$-$' case (blue) and $C\mathrm{Ai}'(y)$ (black) when $C = -10^{-3}$.*

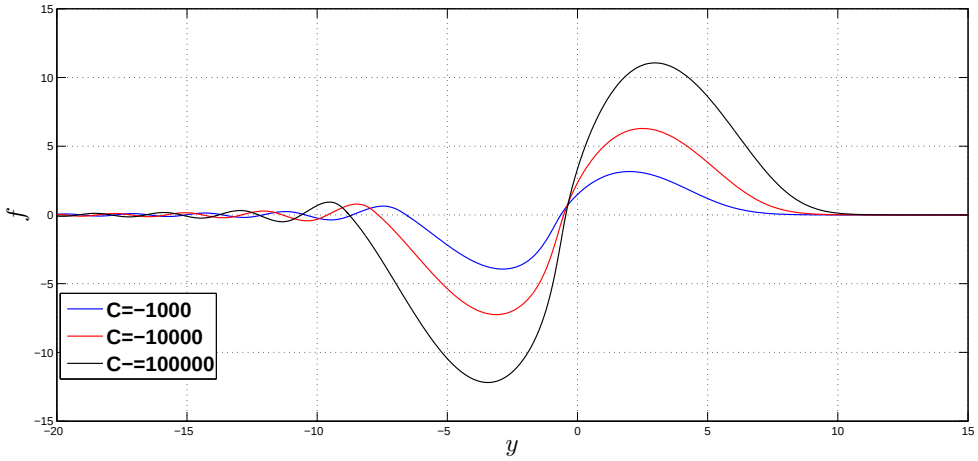

Figure 6-3: *$f = f(y, C)$ of the '$-$' case for $C = -10^3, -10^4, -10^5$.*

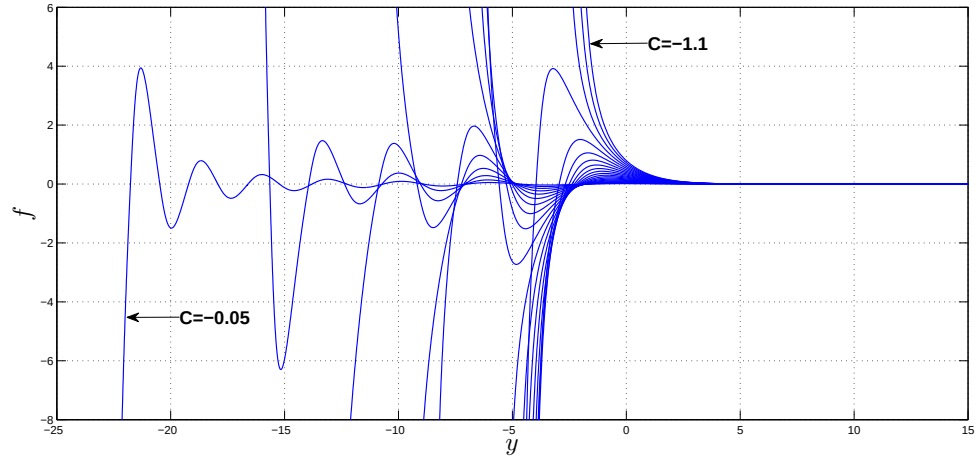

Figure 6-4: *$f = f(y, C)$ of the '$+$' case for $C = -0.05 : -0.05 : -1.1$.*

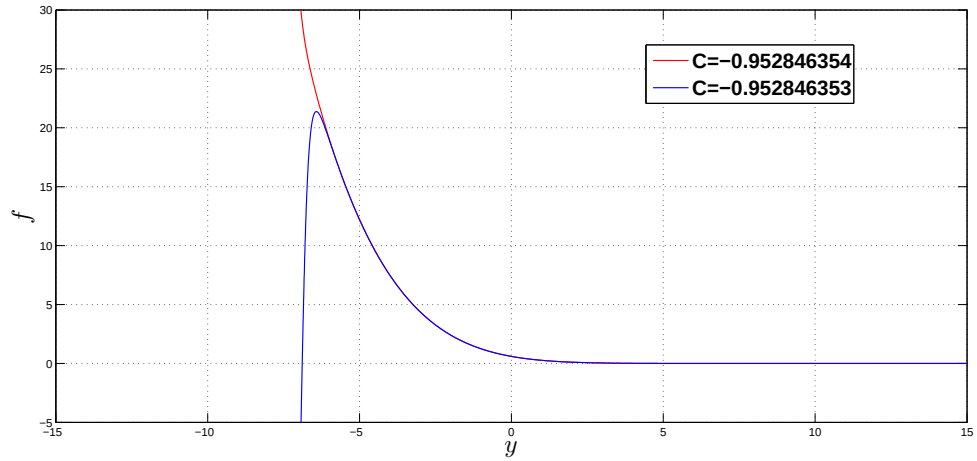

Figure 6-5: *Behaviour of $f = f(y, C)$ of the '+' case when C close to C_0^*.*

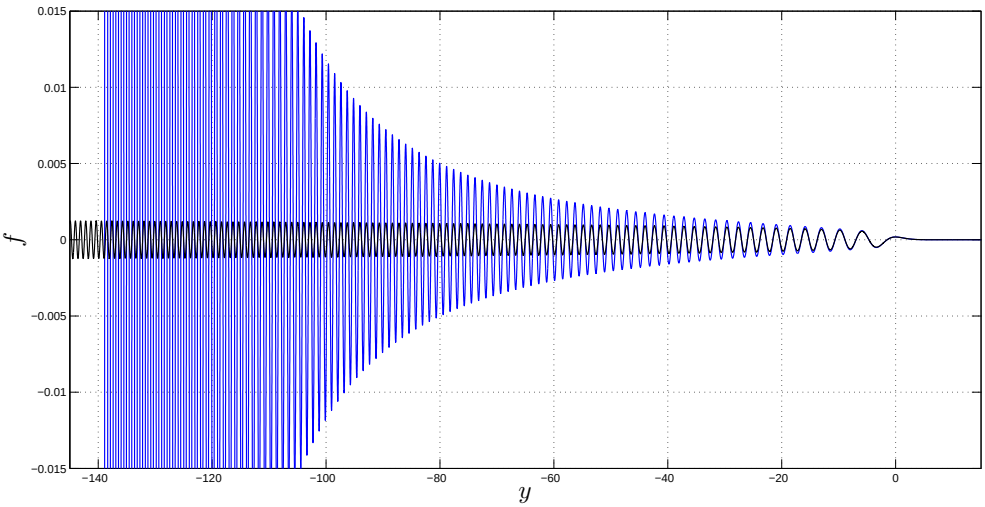

Figure 6-6: *$f = f(y, C)$ of the '+' case (blue) and $C\mathrm{Ai}'(y)$ (black) when $C = -10^{-3}$.*

6.2 The spectral properties of the rescaled linear operator

The spectral theory for linear odd-order operators is well established in [21]. For the completeness of the chapter, we briefly give the auxiliary properties in [21, 45]. These properties will be used for analysing stability and bifurcation points of the semilienar PDE (1.1). Consider equation (3.6) with $\sigma = -1$ (global similarity),

$$\mathbf{A}_{\pm}(f) \equiv f''' + \frac{1}{3(p-1)} f + \frac{1}{3} f' y \pm (|f|^{p-1} f)'' = \mathbf{B}_1 f \pm (|f|^{p-1} f)'' = 0, \quad (6.9)$$

where f decays exponentially as $y \to \infty$ and the linear operator $\mathbf{B}_1$ is defined by

$$\mathbf{B}_1 = \mathbf{B} + c_1 I, \quad \text{where} \quad c_1 = \frac{1}{3(p-1)} - \frac{1}{3} = \frac{p_0 - p}{3(p-1)}. \quad (6.10)$$

Let us now recall the linear dispersion equation (2.3),

$$u_t = u_{xxx} \quad \text{in} \quad \mathbf{R} \times \mathbf{R}_+,$$

and consider its self-similar fundamental solution of the standard similarity form

$$b(x,t) = t^{-1/3} F(y), \quad y = x/t^{1/3}, \quad (6.11)$$

where

$$\mathbf{B}F \equiv F''' + \frac{1}{3} F + \frac{1}{3} F' y = 0 \quad \text{in} \quad \mathbf{R}. \quad (6.12)$$

Here, $\mathbf{B}$ denotes the linear rescaled operator for the linear dispersion equation (2.3). Asymptotic behaviour of the rescaled kernel $F(y) = \mathrm{Ai}(-y)$ for (2.3) can be seen in (3.22) by recalling the reflection $y \mapsto -y$, which satisfies the following estimate [21]:

$$|F(y)| \le \begin{cases} D_0 (1+y^2)^{-1/8} \exp\left(-a_0 |y|^{3/2}\right) & \text{for} \quad y \le 0, \\ D_0 (1+y^2)^{-1/8} & \text{for} \quad y \ge 0, \end{cases}$$

where a_0 is known from (3.22) and D_0 is a positive constant. One can see that $\mathbf{B}_1$ in (6.10) is just a shift of the operator (6.12) for the rescaled fundamental kernel F. Therefore, the spectral properties of $\mathbf{B}$ and the corresponding adjoint operator $\mathbf{B}^*$ occurring for $\sigma = 1$ (blow-up similarity) are key tools in understanding asymptotic behaviour of the nonlinear PDEs. We will use them in the linearised

stability and bifurcation analysis of the semilinear PDEs (1.1).

We would like to point out that $\mathbf{B}$ is non-self-adjoint and not symmetric. $\mathbf{B}$ is naturally defined in the weighted space $L^2_\rho(\mathbf{R})$ with the exponential weight

$$\rho(y) = \begin{cases} \exp\left(a|y|^{3/2}\right) & \text{for} \quad y \leq -1, \\ \exp\left(-ay^{3/2}\right) & \text{for} \quad y \geq 1, \end{cases} \tag{6.13}$$

where $\rho(y)$ is defined to be sufficiently smooth in the complete interval $(-1, 1)$. Here, $\rho(y) > 0$ and $a \in (0, 2a_0)$ is a sufficiently small positive constant, where a_0 is known from (3.22). A Hilbert space of functions $H^3_\rho(\mathbf{R})$ is proposed with the inner product,

$$\langle v, w \rangle_{3,\rho} = \int_{\mathbf{R}} \rho(y) \sum_{k=0}^{3} D_y^k v(y) D_y^k w(y) \mathrm{d}y, \tag{6.14}$$

and the induced norm,

$$||v||^2_{3,\rho} = \int_{\mathbf{R}} \rho(y) \sum_{k=0}^{3} |D_y^k v(y)|^2 \mathrm{d}y, \tag{6.15}$$

where D_y^k denotes the k-th derivative respect to y. So $H^3_\rho \subset L^2_\rho \subset L^2$. Then it is given that $\mathbf{B}$ is a bounded linear operator from $H^3_\rho(\mathbf{R})$ to $L^2_\rho(\mathbf{R})$ with the point spectrum consisting of the real eigenvalues only

$$\sigma(\mathbf{B}) = \left\{ \lambda_\beta = -\frac{\beta}{3}, \beta = 0, 1, 2, ... \right\}, \tag{6.16}$$

and the corresponding eigenfunctions

$$\psi_\beta(y) = \frac{(-1)^\beta}{\sqrt{\beta!}} D_y^\beta F(y). \tag{6.17}$$

Also, the set of eigenfunctions $\Phi = \{\psi_\beta, \beta = 0, 1, 2, ...\}$ is complete in $L^2_\rho(\mathbf{R})$.

Now consider the adjoint operator to $\mathbf{B}$,

$$\mathbf{B}^* = D_y^3 - \frac{1}{3} y D_y, \tag{6.18}$$

in the weighted space $L^2_{\rho^*}$ with exponentially decaying weight

$$\rho^*(y) = \exp\left(-a|y|^{3/2}\right) \quad \text{for} \quad |y| \geq 1, \tag{6.19}$$

where $\rho^*(y) > 0$ and $a \in (0, 2a_0)$ is a sufficiently small positive constant. We would like to point out that $\mathbf{B}^*$ is adjoint to $\mathbf{B}$ in the indefinite metric of $\bar{L}^2(\mathbf{R})$ with the indefinite scalar product

$$\langle v, w \rangle_* = \int_{\mathbf{R}} v(y)\overline{w(-y)}\mathrm{d}y, \tag{6.20}$$

where complex conjugate can be omitted due to the real point spectrum of $\mathbf{B}$ and $\mathbf{B}^*$. So $\mathbf{B}^*$ is a bounded linear operator from $H^3_{\rho^*}(\mathbf{R})$ to $L^2_{\rho^*}(\mathbf{R})$ with the same real point spectrum $\sigma(\mathbf{B}^*) = \sigma(\mathbf{B})$ as in (6.16) and the corresponding eigenfunctions being generalised Hermite polynomials

$$\psi^*_\beta(y) = \frac{1}{\sqrt{\beta!}} \left[y^\beta + \sum_{j=1}^{\lfloor \beta/3 \rfloor} \frac{1}{j!} D^{3j} y^\beta \right], \tag{6.21}$$

where $\lfloor \cdot \rfloor$ denotes the integer part. Additionally, the set of eigenfunctions $\Phi^* = \left\{ \psi^*_\beta, \beta = 0, 1, 2, ... \right\}$ is complete in $L^2_{\rho^*}(\mathbf{R})$.

From this definition of the adjoint operator and eigenfunctions, and the formal calculus of integration by parts, it is given that the orthonormality condition holds,

$$\left\langle \psi_\beta, \psi^*_\gamma \right\rangle_* = \delta_{\beta\gamma} \quad \text{for any} \quad \beta, \gamma \geq 0, \tag{6.22}$$

where $\langle \cdot, \cdot \rangle_*$ denotes the indefinite metric as in (6.20) and $\delta_{\beta\gamma}$ is the Kronecker delta. Moreover, it is known by the definitions that

$$\begin{aligned} \mathbf{B}\psi_\beta &= \lambda_\beta \psi_\beta, \\ \mathbf{B}^*\psi^*_\gamma &= \lambda_\gamma \psi^*_\gamma. \end{aligned} \tag{6.23}$$

Let us also give an explicit representation of the semigroup for $\mathbf{B}$. If one introduces the similarity scaling,

$$u(x,t) = (1+t)^{-1/3} w(y,\tau), \quad y = x/(1+t)^{1/3}, \quad \tau = \ln(1+t) : \mathbf{R}_+ \to \mathbf{R}_+, \tag{6.24}$$

in the linear equation (2.3) with initial data at $t = 0$, i.e., $w_0(y) = u_0(x)$, then the rescaled solution $w(y, \tau)$ satisfying the equation,

$$w_\tau = \mathbf{B}w \quad \text{for} \quad \tau > 0, \tag{6.25}$$

is given by

$$w(y,\tau)=\sum_{(\beta)} e^{\lambda_\beta \tau}\psi_\beta(y)\big\langle w_0(z),\psi^*_\beta(z)\big\rangle_* \equiv e^{\mathbf{B}\tau}w_0. \tag{6.26}$$

6.3 Linearised stability analysis and bifurcation points

We now present some stability/instability results in the linearisation of the rescaled PDE about the zero solution (i.e. for small solutions) with the spectral properties of $\mathbf{B}$. Similar to the linear PDE, for our semilinear PDEs (1.1), if we use the following similarity scaling,

$$u(x,t)=(1+t)^{-1/3(p-1)}v(y,\tau),\quad y=x/(1+t)^{1/3},\quad \tau=\ln(1+t)\geq 0, \tag{6.27}$$

then $v(y,\tau)$ solves the rescaled equation

$$v_\tau=\mathbf{A}_\pm(v)\equiv \mathbf{B}_1 v\pm(|v|^{p-1}v)'', \tag{6.28}$$

where $\mathbf{A}_\pm$ is defined in (6.9) for $\sigma=-1$ and $\mathbf{B}_1$ is known from (6.10). Let us note that the stationary solutions of (6.28) are global similarity profiles ($\sigma=-1$) satisfying (6.9).

6.3.1 Stability of the zero solution

We show that $p=p_0=2$ plays a critical role in the stability/instability of the zero solution, similar to the Fujita critical exponent in the semilinear parabolic equations, e.g. in (2.25).

Proposition 6.1. *The trivial zero solution, $v\equiv 0$, of (6.28) is exponentially linearly unstable for $1<p<p_0=2$ and stable for $p>p_0$ in $H^3_\rho(\boldsymbol{R})$.*

Proof. Let us follow the idea in [21]. If we consider the linearisation of the rescaled equation (6.28) about the zero solution,

$$v_\tau=\mathbf{B}_1 v, \tag{6.29}$$

with (6.10) and (6.16), then the linear operator $\mathbf{B}_1$ has the spectrum

$$\sigma(\mathbf{B}_1)=\left\{\nu_k=c_1-\frac{k}{3}, k=0,1,2,...\right\}. \tag{6.30}$$

For $k = 0$ we have that

$$\nu_0 = c_1 = \frac{p_0 - p}{3(p-1)}, \tag{6.31}$$

where $\nu_0 > 0$ for $1 < p < p_0 = 2$ and $\nu_0 < 0$ for $p > p_0$. Therefore, zero becomes stable for $\nu_0 < 0$ with

$$||v(\tau)||_{3,\rho} \sim e^{\nu_0 \tau} \to 0 \quad \text{as} \quad \tau \to \infty, \tag{6.32}$$

and unstable for $\nu_0 > 0$ with

$$||v(\tau)||_{3,\rho} \sim e^{\nu_0 \tau} \to \infty \quad \text{as} \quad \tau \to \infty, \tag{6.33}$$

in our space using (6.26). □

6.3.2 Centre subspace behaviour

The critical values of p can be obtained from (6.30) by

$$\nu_k = 0 \quad \text{when} \quad p = p_k = 1 + \frac{1}{k+1}, \quad k = 0, 1, 2, ... \tag{6.34}$$

One can also see that $p_k \to 1^+$ as $k \to \infty$. The behaviour of $p_0 = 2$ and $p_1 = 3/2$ with appropriate data has been previously discussed.

Let us consider the rescaled equation (6.28) with the critical exponents $p = p_k$, $k \geq 0$,

$$v_\tau = (\mathbf{B} - \lambda_k)v \pm (|v|^{p-1}v)''. \tag{6.35}$$

In order to study the centre subspace behaviour by the standard invariant manifold theory [118], we look for a solution that takes the form for $\tau \gg 1$,

$$v(\tau) = a_k(\tau)\psi_k + w_k^\perp(\tau), \tag{6.36}$$

where $w_k^\perp$ is asymptotically small and orthogonal to ψ_k, i.e., $\left\langle w_k^\perp, \psi_k^* \right\rangle_* = 0$. If we substitute (6.36) into (6.35) and multiply the equation by the adjoint eigenfunction ψ_k^* in the indefinite metric, using (6.23), we get the asymptotic ODE

$$a_k' = \gamma_k |a_k|^{p-1} a_k (1 + o(1)), \tag{6.37}$$

where $p = p_k = 1 + 1/(k+1)$ and

$$\gamma_k = \pm\big\langle (|\psi_k|^{p-1}\psi_k)'', \psi_k^* \big\rangle_* = \pm\big\langle |\psi_k|^{p-1}\psi_k, (\psi_k^*)'' \big\rangle_*. \tag{6.38}$$

Here, the value of the coefficient γ_k is important. The ODE (6.37) admits unstable (blow-up-like) behaviour for $\gamma_k > 0$ and stable behaviour (global bounded orbits) for $\gamma_k < 0$. Note that $\gamma_0 = \gamma_1 = 0$ since $(\psi_0^*)'' = (\psi_1^*)'' = 0$. Roughly speaking, using this equality in (6.37), for $k = 0, 1$, yields

$$v(y,\tau) \sim C\psi_k(y) \quad \text{as} \quad \tau \to \infty \quad (C \neq 0), \tag{6.39}$$

which is shown by the numerical results for p_0 and p_1 that (6.39) is stable for the '+' case of global similarity with $\sigma = -1$ ('−' case of blow-up similarity with $\sigma = 1$) and unstable for the '−' case of global similarity with $\sigma = -1$ ('+' case of blow-up similarity with $\sigma = 1$).

Proving and calculating $\gamma_k \neq 0$ for $k > 1$ analytically and even numerically is uncertain and not too easy due to the growing oscillatory nature in (6.38). Let us assume that $\big\langle |\psi_k|^{p-1}\psi_k, (\psi_k^*)'' \big\rangle_* < 0$. Then, for the '+' case of global similarity with $\sigma = -1$ ('−' case of blow-up similarity with $\sigma = 1$), we have that the centre subspace behaviour is stable. Integrating the asymptotic ODE (6.37) for $k > 1$ yields

$$a_k(\tau) = \pm\left[(p-1)|\gamma_k|\tau\right]^{-\frac{1}{p-1}}(1 + o(1)) \quad \text{as} \quad \tau \to \infty \quad (p = p_k = 1 + 1/(k+1)). \tag{6.40}$$

So, we have the following centre subspace behaviour of $u(x,t)$ for the '+' case in (6.35) as $t \to \infty$,

$$u(x,t) = \pm(1+t)^{-(k+1)/3}\left(\frac{1}{k+1}|\gamma_k|\ln(1+t)\right)^{-(k+1)}\left[\psi_k\left(x/(1+t)^{1/3}\right) + o(1)\right]. \tag{6.41}$$

Note that there is an extra logarithmic scaling factor. However, the justification of this behaviour with the above crucial assumption is questionable.

Hence, for the case $p > p_k$ (i.e. $\nu_k < 0$), using the linearisation of the rescaled equation (6.28) as in (6.29), one can obtain the stable subspace behaviour by

$$v(y,\tau) = Me^{(\lambda_k + c_1)\tau}\left[\psi_k(y) + o(1)\right] \quad \text{as} \quad \tau \to \infty \quad (M = M(u_0) \neq 0). \tag{6.42}$$

6.3.3 Bifurcation points

We now recall the global similarity profiles f satisfying the (6.9) for $p < p_0$ to formally analyse the stability of the solutions near the critical exponents p_k, $k \geq 0$, particularly using the Lyapunov-Schmidt method in the classical bifurcation theory [119].

In order to check behaviour near the critical exponents, $p \approx p_k$, we set

$$p - p_k = \epsilon \quad \text{where} \quad p = p_k = 1 + \frac{1}{k+1}. \tag{6.43}$$

Thus (6.9) takes the following form:

$$(\mathbf{B} - \lambda_k)f - \epsilon\mu_k f = \mp(|f|^{p-1}f)'' + O(\epsilon^2), \quad \text{where} \quad \mu_k = \frac{(k+1)^2}{3} > 0. \tag{6.44}$$

According to the Lyapunov-Schmidt method, the solution f is given by

$$f = C\psi_k + w^{\perp}(\tau), \tag{6.45}$$

where $w^{\perp}$ is orthogonal to ψ_k, i.e., $\langle w, \psi_k^* \rangle_* = 0$. Using (6.45) in (6.44) and multiplying the equation by the adjoint eigenfunction ψ_k^* in the indefinite metric yields

$$|C|^{p-1} = \frac{\epsilon\mu_k}{\gamma_k}, \tag{6.46}$$

where γ_k is defined as in (6.38). Once again, the value of γ_k is crucial. We know that $\gamma_0 = \gamma_1 = 0$ since $(\psi_0^*)'' = (\psi_1^*)'' = 0$, which yields a vertical line at the bifurcations points p_0 and p_1 in the p-bifurcation diagram suggesting an unbounded continuous family of solutions for the '+' case of global similarity, and non-existence (inconsistent) for the '−' case of global similarity according to the previous numerical results. If we again assume $\left\langle |\psi_k|^{p-1}\psi_k, (\psi_k^*)'' \right\rangle_* < 0$, (6.46) admits a countable number of subcritical pitch-fork bifurcations appearing as $p \to p_k^-$ concentrating to $p = 1^+$ similar to the p-bifurcation diagram in [21] for the '+' case of global similarity and a countable number of supercritical pitch-fork bifurcations appearing as $p \to p_k^+$, similar to the p-bifurcation diagram of the limit unstable Cahn-Hilliard equation in [61], for the '−' case of global similarity. However, analytical and even numerical justification of such behaviour is open because of the assumption. We will rely on numerical results for the ODE and PDE in the following sections, in order to classify the behaviour.

6.4 Algebraic solutions and numerics of the rescaled ODE for arbitrary $p > 1$

Here, numerical experiments on the rescaled ODE (3.6) for $\sigma = 1$ will be used to detect and classify behaviour of the solutions for arbitrary $p > 1$. However, regarding our former discussions, we do not think that we can completely rigorously justify all of the conclusions.

6.4.1 Algebraic solutions

Before pursuing numerical analysis to check the asymptotic behaviour in detail, let us return to the blow-up similarity profiles f satisfying the ODE (3.6) for $\sigma = 1$,

$$f''' - \frac{1}{3(p-1)} f - \frac{1}{3} f' y \pm (|f|^{p-1} f)'' = 0, \quad \text{where} \quad p > 1. \tag{6.47}$$

We already mentioned in the case of $p_0 = 2$ that algebraic decaying solutions play an important role in the asymptotic behaviour of f when the integration constant is non-zero. Locally analysing the ODE (6.47), we detect the algebraic decay,

$$f(y) = \pm \left(\frac{1}{p-1} \right)^{1/(p-1)} |y|^{-1/(p-1)}, \tag{6.48}$$

for $y > 0$ in the '+' case of (6.47) and for $y < 0$ in the '$-$' case. We have seen that the symmetry of oscillatory tails occurs at 0 for p_0 and p_1, where we can integrate the rescaled ODE with zero integration constant. However, we cannot integrate the rescaled ODE for $p > 1$, $p \neq p_0, p_1$. Hence we expect the profiles f of (6.47), especially in the '$-$' case, with positive or negative dominant tails as $y \to -\infty$, which are not admissible according to the conservation law. One can see in (6.48) that symmetry of the oscillatory tails get close to 0 as $p \to 1^+$ in contrast to as $p \to \infty$. We will discuss such behaviour in the next section with the numerical results.

On the other hand, it is known that the linear part of (6.47), for $p = p_0 = 2$,

$$f'' - \frac{1}{3} y f = 0,$$

has two linearly independent solutions,

$$f(y) = C_1 \operatorname{Ai}(y) + C_2 \operatorname{Bi}(y), \tag{6.49}$$

where $\operatorname{Ai}(y)$ is defined as in (3.22) and $\operatorname{Bi}(y)$ is exponentially growing as $y \to \infty$. Let us also point out that the linear part of (6.47) for $p = 3$,

$$f''' - \frac{1}{6}f - \frac{1}{3}f'y = 0, \tag{6.50}$$

has solutions as

$$f(y) = C_1(\operatorname{Ai}(2^{-2/3}y))^2 + C_2 \operatorname{Ai}(2^{-2/3}y)\operatorname{Bi}(2^{-2/3}y) + C_3(\operatorname{Bi}(2^{-2/3}y))^2. \tag{6.51}$$

Moreover, we detect an algebraic solution $f(y) = \pm\sqrt{3}y/6$ satisfying the '+' case of (6.47) for $p = 3$.

6.4.2 Numerical results for the rescaled ODE

Recall that the blow-up similarity ($\sigma = 1$) profiles of the '$-$' case represents the global similarity ($\sigma = -1$) profiles of the '+' case. Also, the blow-up similarity profiles of the '+' case implies the global similarity profiles of the '$-$' case. Therefore, we consider the blow-up self-similar ($\sigma = 1$) profiles f satisfying the rescaled ODE (6.47) with the boundary condition

$$f(y, C) \sim C \operatorname{Ai}(y) \quad \text{as} \quad y \to \infty, \tag{6.52}$$

where we restrict our attention to $C > 0$ since $f(y, -C) = -f(y, C)$. We use the same standard IVP solver supplied by *MatLab* with the same notations given in Section 3.4. In addition to that, we need to use regularization

$$|f|^{p-1}f \mapsto (f^2 + \epsilon^2)^{\frac{p-1}{2}} f. \tag{6.53}$$

Here, ϵ is used to avoid singularities due to $p > 1$ and is small enough to not affect the solutions, where we take $\epsilon = 10^{-6}$ or smaller. We will use some figures to represent behaviour of the numerical results.

'$-$' case: Figures 6-7 and 6-8 display the numerical results for $p > p_0 = 2$ when $C = 1, 10^{-3}, 10^{6}$. It can be seen that the symmetry of oscillatory tails do not occur at 0, which are positive dominant. The symmetry of the tail gets close to 0,

as p gets close to p_0. The effect of the algebraic (non-oscillatory) decay increases as C or p increases for $y < 0$. We have also observed that the oscillatory tail of $p = p_0 = 2$ becomes positive dominant for $C \gg 1$, in contrast to the second order equation with zero integration constant (3.24). We would also like to point out that the profiles are strictly positive for $p > 3$. Figure 6-9 represent the profiles $f = f(y)$ of the '$-$' case in (6.47) with (6.52), for $3/2 = p_1 < p < p_0 = 2$, when $C = 1, 10^6$. In this case, one can see that the tails are negative dominant. So, we can expect this changing behaviour of the tails close to the critical exponents p_k. However, it is not easy to see changes for small values of C since the oscillatory tails become small and symmetric close to 0 as $p > 1$ decreases, see Figure 6-10. Therefore, in Figure 6-11, we display the profiles f close to p_k, where $k = 2, 3, 4$, for $C = 10^6, 10^8$, in order to see that the dominance of the oscillatory tail changes.

'+' case: According to the numerical results, we expect the non-existence of blow-up self-similar solutions for any $p > 1$. All the profiles become unbounded or have positive dominant oscillatory tail (not admissible), see Figure 6-12 for $p = 10, 5, 3, 2, 1.5, 1.25$ and $C = 0.25$. Although there is no need to discuss unbounded solutions, we would like to note that C_0^*, which is described in (4.13), decreases as p increases. Moreover, $C_{k-1}^* - C_k^*$, $k = 1, 2, ...$ decreases as p increases.

6.5 On some aspects of the semilinear PDE and numerics

Conservation and dissipation. Under appropriate decay conditions at infinity, conservation of mass and the first moment are well-known for the Cauchy problem of the linear dispersive equation (2.3) and the porous medium equation (2.13) [6, 36], which are used in determining the critical exponents p_0, p_1 of the semilinear PDE (1.1). Let us also give a formal computation for the L^2-norm. Assuming the solution $u(x,t)$ of the Cauchy problem for the semilinear PDE (1.1) has appropiate decay conditions at infinity, we have

$$\frac{1}{2}\frac{\mathrm{d}}{\mathrm{d}t}\int u^2 \mathrm{d}x = \int u_{xxx} u \mathrm{d}x \pm \int (|u|^{p-1}u)_{xx} u \mathrm{d}x = \mp p \int |u|^{p-1}(u_x)^2 \mathrm{d}x,$$

which implies that the L^2-norm decays or grows with time. Therefore, it is reasonable to look for the global or blow-up solutions of the proposed PDEs in a weak sense.

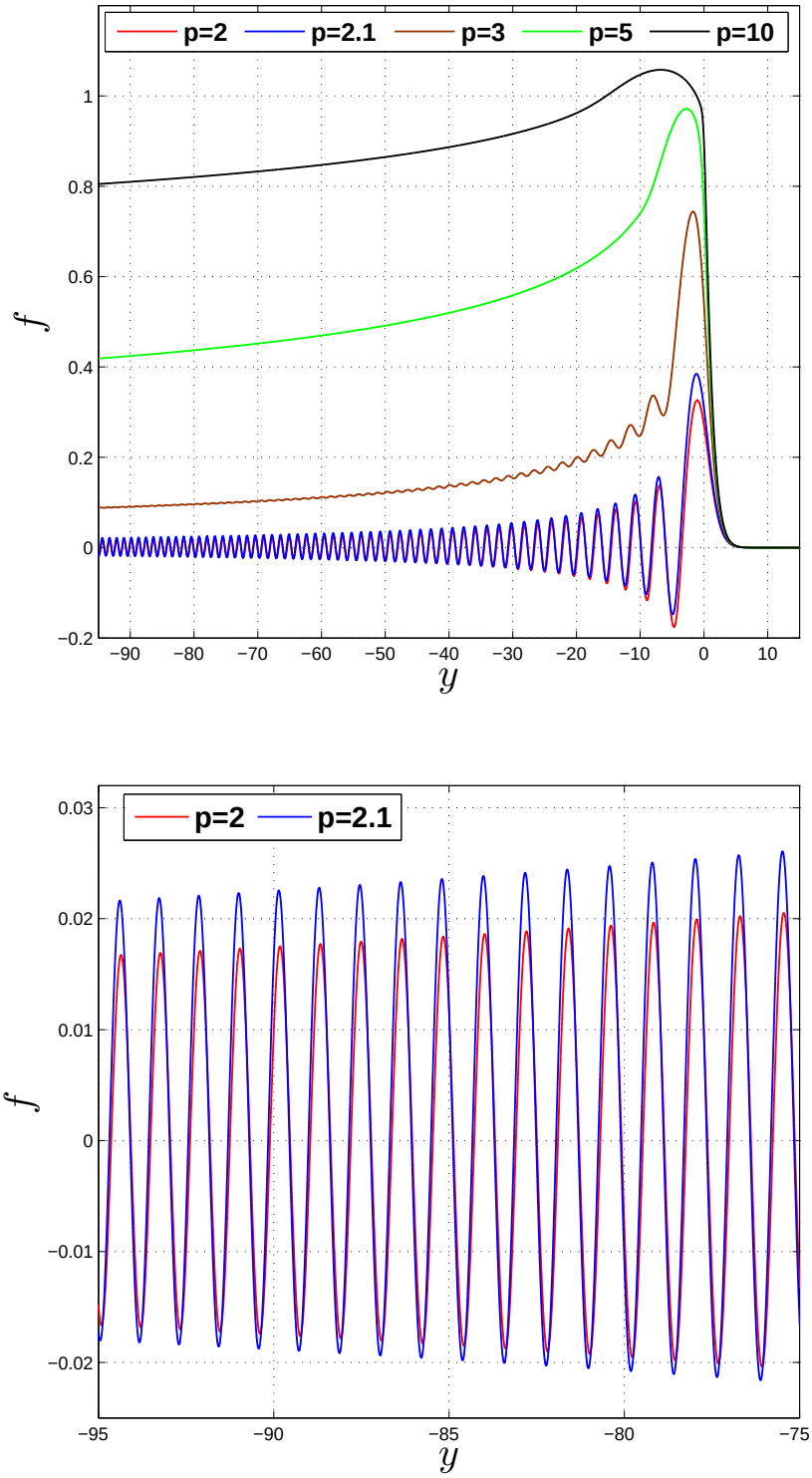

Figure 6-7: *The profiles $f(y)$ for the '$-$' case of (6.47) with (6.52) when $C = 1$ and $p = 2, 2.1, 3, 5, 10$, and the 'tail'.*

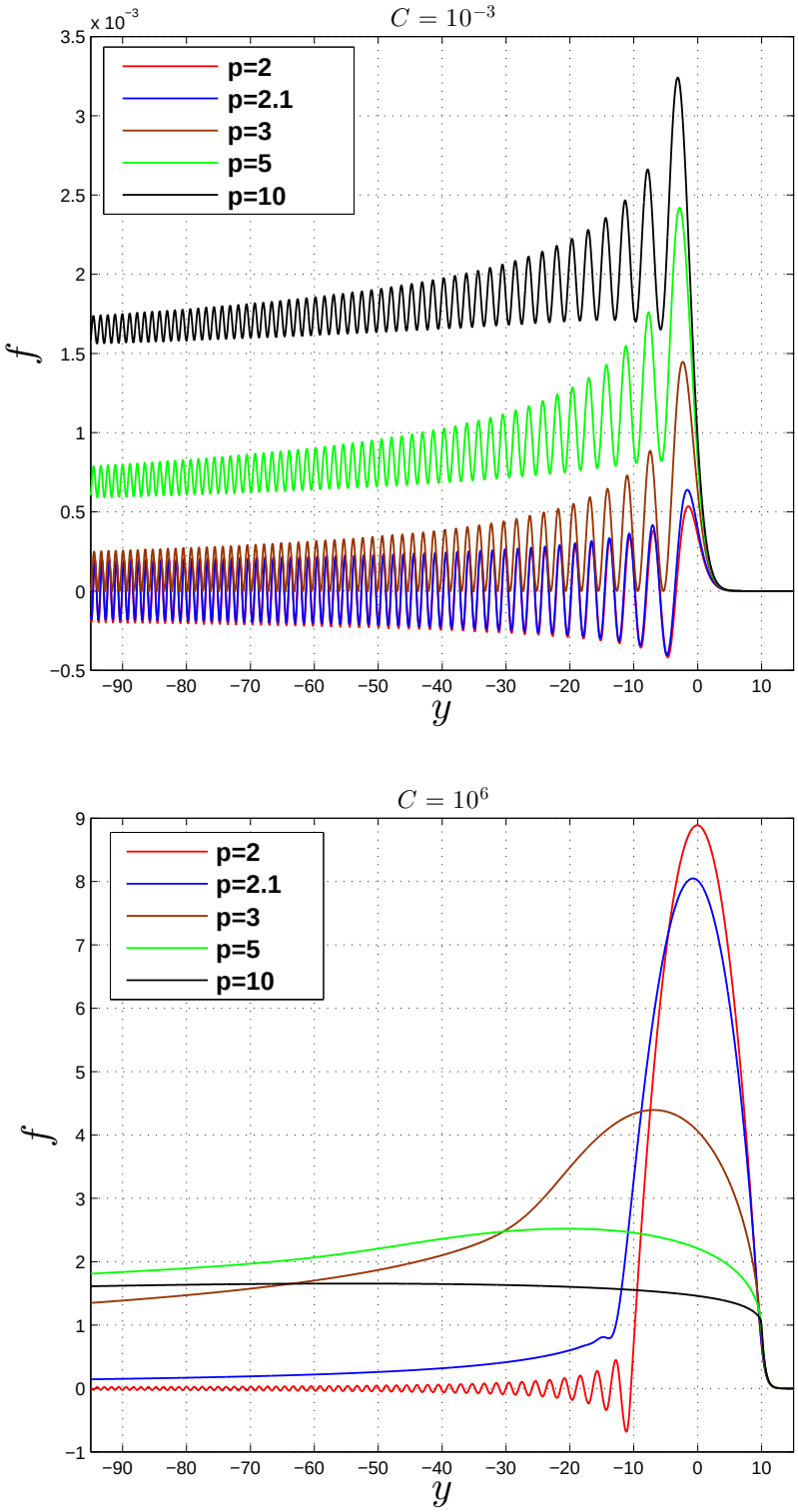

Figure 6-8: *The profiles $f(y)$ for the '$-$' case of (6.47) with (6.52) when $C = 10^{-3}$ and $C = 10^{6}$ for $p = 2, 2.1, 3, 5, 10$.*

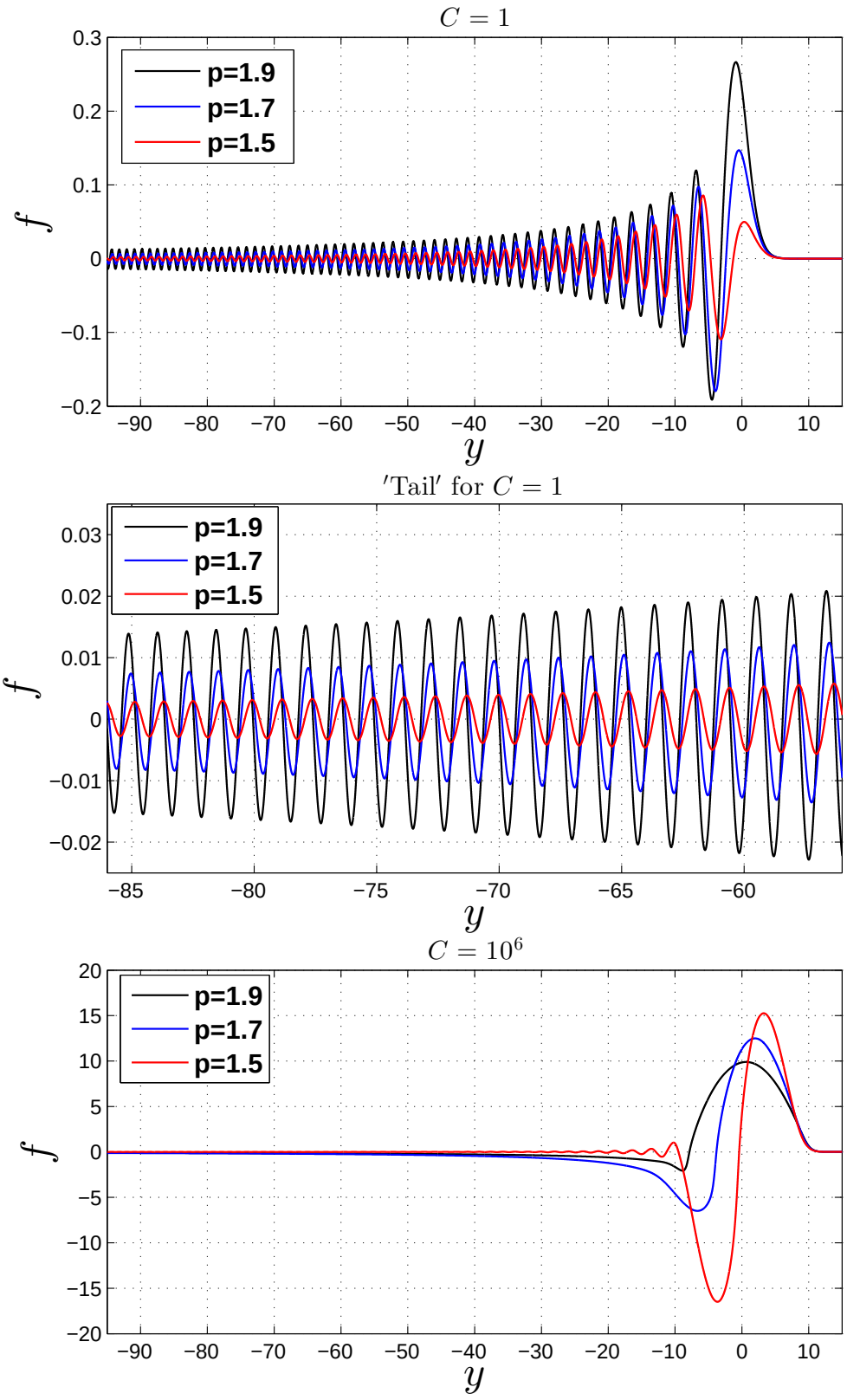

Figure 6-9: *The profiles $f(y)$ for the '$-$' case of (6.47) with (6.52) when $C = 1$ and $C = 10^6$ for $p = 1.9, 1.7, 1.5$.*

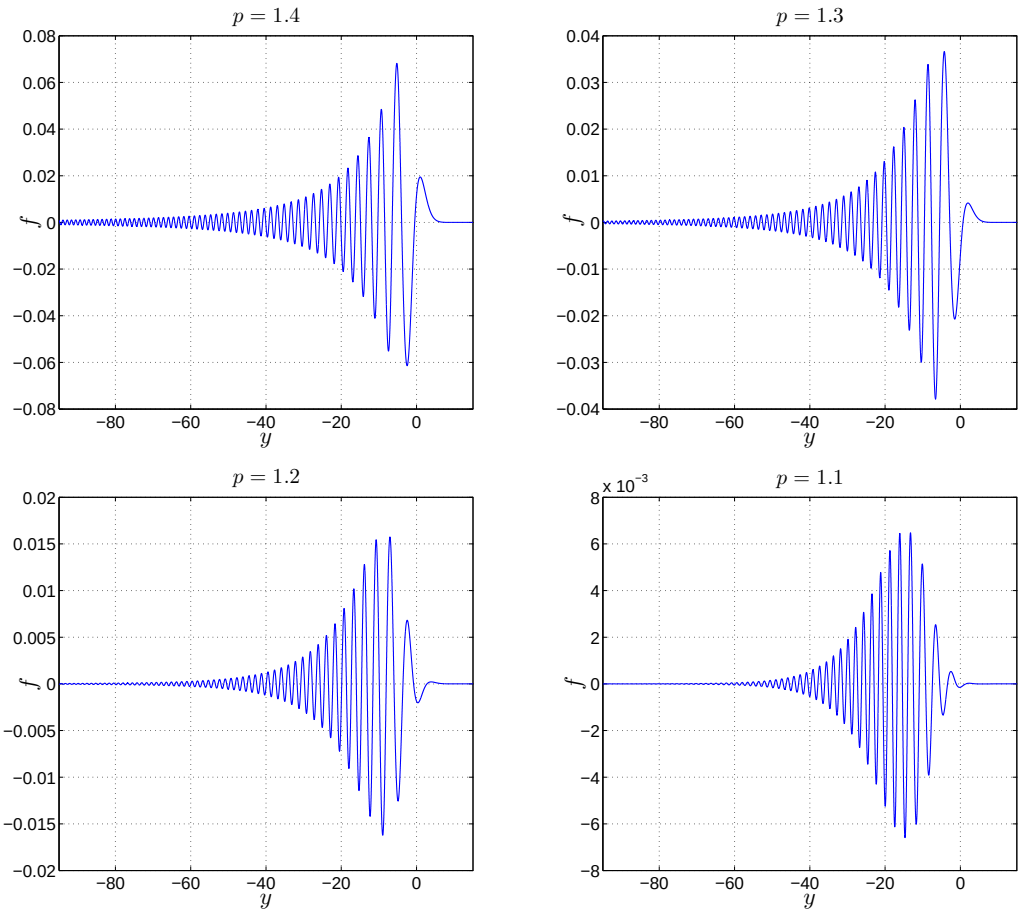

Figure 6-10: *The profiles $f(y)$ for the '$-$' case of (6.47) with (6.52) when $C = 1$ and $p = 1.4, 1.3, 1.2, 1.1$.*

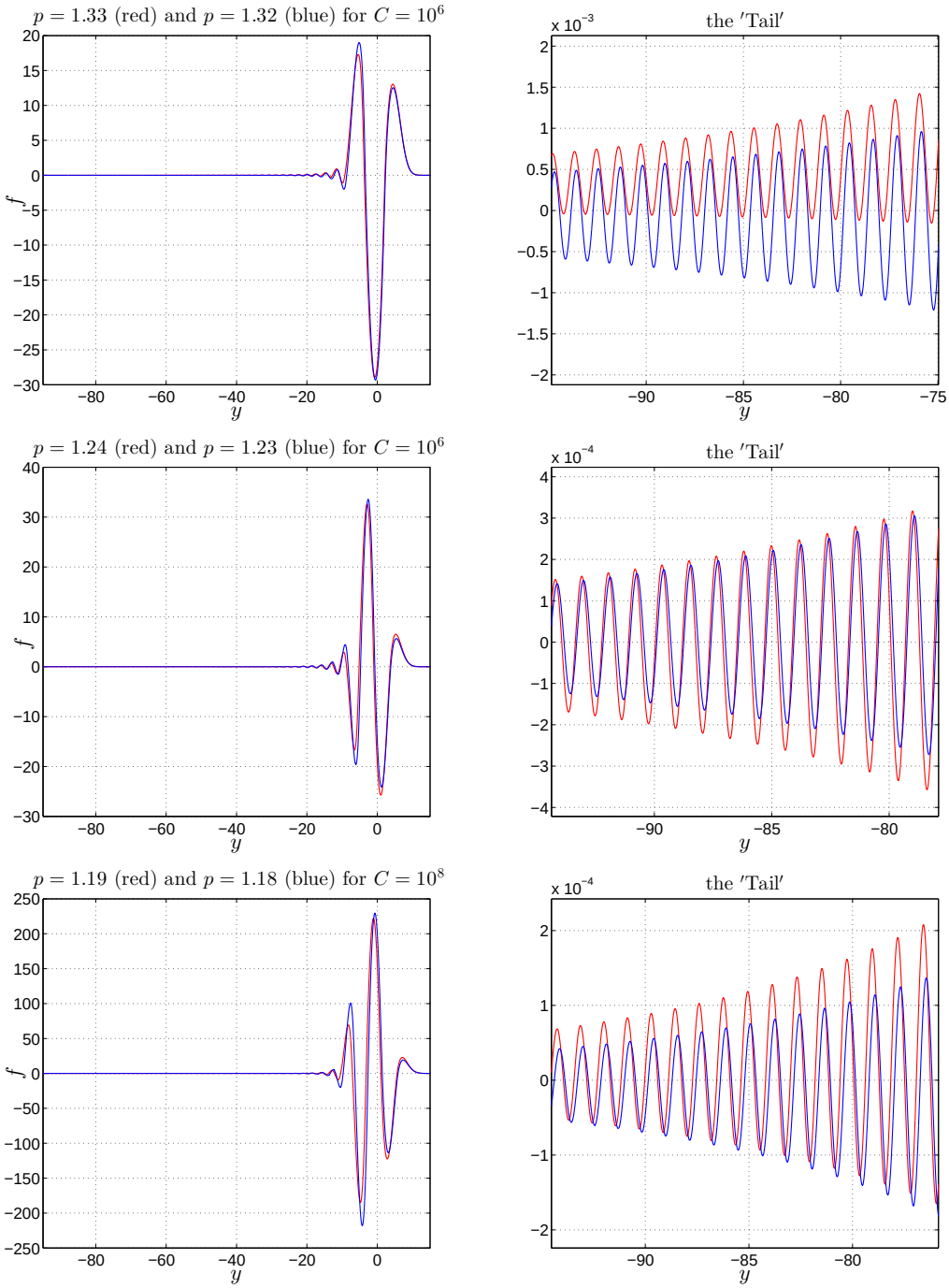

Figure 6-11: *The profiles $f(y)$ for the '$-$' case of (6.47) with (6.52) when p close to p_k, $k = 2, 3, 4$ for large values of C.*

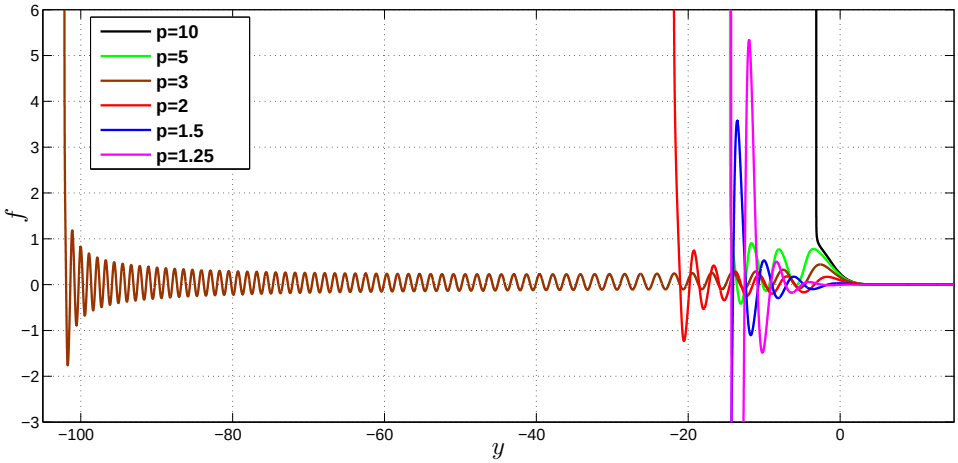

Figure 6-12: *The profiles $f(y)$ for the '+' case of (6.47) with (6.52) when $p = 10, 5, 3, 2, 1.5, 1.25$ and $C = 0.25$,*

On Airy-type radiation conditions at infinity. As we have seen and indicated several times, our ODEs typically admit a 3D bundle at infinity of the form

$$f(y) = \mathrm{Ai}(y) + \frac{A}{y} + \dots,$$

where the first term contains the oscillatory part with two constants $C_{1,2}$ and the second term, though being faster decaying as $y \to \infty$, is not oscillatory. We claimed that, in the true Cauchy problem, one has to have that

$$A = 0.$$

Otherwise, this would correspond not to the Cauchy problems, but a kind of special (IBVP-type) problem with the corresponding conditions at infinity. A possible formulation of such problems includes using a *limit integral operator* of the form, which we formulate now for $y \to -\infty$,

$$\int_{-2a}^{-a} f(y)\mathrm{d}y \to -A \ln 2 \quad \text{as} \quad a \to +\infty.$$

Thus, for $A \neq 0$, we arrive at a problem with quite specific conditions at infinity, and NOT at the Cauchy problem. In other words, for $A \neq 0$, we get a *free-parameter boundary value problem* (cf. a *free-boundary problem* where A plays a role of a "free boundary parameter" but posed at infinity).

This admits a natural re-formulation for the linear dispersion equations (with possible nonlinear perturbations, which are not important and are negligible at infinity), with the same limit integral operator, where

$$A = A(t) \text{ can be an arbitrary given function,}$$

and again, for the Cauchy problem with good initial data, one needs to pose the condition

$$A(t) \equiv 0.$$

An extension of local singular (blow-up) semigroups. This is a well-known problem for the second-order parabolic equations (see, e.g., [48]): what happens after blow-up, for $t > T$. However, for the present third-order dispersion equations, such a mathematical analysis becomes extremely difficult and requires a further detailed and complicated analysis.

The main idea remains the same: for the fully unstable case '$-$', i.e., for the dispersion PDE with the backward porous medium term

$$u_t = u_{xxx} - (|u|u)_{xx},$$

when blow-up occurs always, we construct a sequence $\{u_\epsilon\}$ of global smooth solutions of the same PDEs with a properly truncated nonlinearity given by

$$|u|u \mapsto \frac{|u|u}{1 + \epsilon u^2} \to |u|u,$$

uniformly on bounded u-intervals, and pass to the limit as $\epsilon \to 0^+$, trying to understand how $u_\epsilon(x,t)$ behaves in this limit for $t > T$. This could lead (in any weak and/or partial limit sense) to a construction of an extension of solutions beyond blow-up.

Unfortunately, we have yet to get any mathematical justification and convincing results.

However, our numerical experiments for not that small $\epsilon \sim 10^{-1}$ or 10^{-2} show that the global smooth classical solutions $u_\epsilon(x,t)$ become highly oscillatory for $t > T$ everywhere in x.

Thus, our preliminary conclusion is as follows:

in the above unstable '$-$' case, blow-up is complete,

and no proper continuation for $t > T$ is possible. Recall that this is quite surprising, recalling the conservation of mass in this problem (for both u and u_ϵ), also meaning that huge oscillations from $-\infty$ to $+\infty$ in x after blow-up have the average *zero* mass.

6.5.1 Numerics for the PDE

In this section we present numerical illustrations of the original PDE (1.1) for $p > 1$. We use *pde15s* solver of *Chebfun* package [120, 121], which is written in *MatLab*. The idea of the *pde15s* is to replace the spatial derivatives in a given PDE with Chebyshev spectral discretisation and solve the corresponding ODE in time using *ode15s* of *MatLab*, i.e., a 'method of lines (MOL)' type technique. We set $x \mapsto -x$ in the PDE (1.1) in order to have similar structure represented for the rescaled ODEs, such as fast decay behaviour at the right-hand side and oscillatory behaviour at the left-hand side. We take the initial condition

$$u_0(x,0) = u_0(x) = Ce^{-x^2}, \quad C = const. \neq 0. \tag{6.54}$$

Setting a fixed interval, u and u' are taken to be zero at the right-hand boundary point, u is taken to be zero at the left-hand boundary point, as boundary conditions. We also set tolerance to $1e-2$, which is '*eps*' in *Chebfun* terminology.

In Figures 6-13 and 6-14, we show the behaviour for the global in time solution $u(x,t)$ of the '+' case of (1.1) with (6.54) for different values of C and $p > 1$. Here, the evolution of the global solutions is stable as expected (see comments below for the similarity solutions). Figure 6-15 shows the evolution of the initial data close to the blow-up point for the solution $u(x,t)$ of the '$-$' case of (1.1) with (6.54). Unlike the global solutions, we do not have much hope of easily finding stable evolution of blow-up solutions due to the unstable porous medium operator, which can create different special singularity formation phenomena. Here, in most cases, the actual blow-up rate is much faster than the similarity rate.

Let us recall the rescaled PDE (6.28),

$$v_\tau = v_{yyy} + \frac{1}{3(p-1)}v + \frac{1}{3}yv_y \pm (|v|^{p-1}v)_{yy},$$

which is obtained by global similarity scaling (6.27). According to the non-existence of the global similarity profiles of the '$-$' case of (6.28) in Chapter 4 for

$p = p_0 = 2$, we expect that large-time behaviour cannot converge to a non-zero steady state. Namely, there can be blow-up or convergence to $f = f(y) = 0$ trivial solution. On the other hand, the existence of the global similarity profiles of the '+' case of (6.28) is proposed in Chapter 3 for $p = p_0 = 2$. Therefore, we expect that solutions converge in τ on compact subsets of y to a non-zero equilibrium f observed in Chapter 3. With direct simulations to the rescaled PDE (6.28), for $p = p_0 = 2$ and $C = 1$ in (6.54) (i.e. $v(y, 0) = v_0(y) = e^{-y^2}$), we have that the solution converges to the global self-similar profile (Figure 3-12) of the rescaled ODE (3.24) for $C \approx 196.5$ in (3.25), see Figure 6-16 and 6-17. Here, the solution reaches its steady state after $\tau \approx 250$ and its structure does not change. For the second critical exponent $p = p_1 = 3/2$ (the first moment conservative case), we observe that the solution $v(y, \tau)$ does not converge to an equilibrum, in contrast to the first critical exponent $p = p_0 = 2$, see Figure 6-18 for the initial data $v_0(y) = e^{-y^2}$ and Figure 6-19 for $v_0(y) = -2ye^{-y^2}$. Here, the first hump grows. This unstable behaviour is same for all $1 < p < p_0 = 2$. Such behaviour remains open. More delicate analysis using new theoretical and numerical tools are still needed for proposed odd-order PDE, which is relatively untouched.

Let us particularly point out that, regarding the existence of global similarity profiles and non-existence of blow-up similarity profiles for the '+' case with $p = p_0 = 2$ in Chapter 3 and 4, we numerically confirm that large-time behaviour of global solution for the '+' case of the rescaled PDE converges to a non-zero similarity profile in Chapter 3, but large-time behaviour of blow-up solution cannot converge to a non-zero steady state.

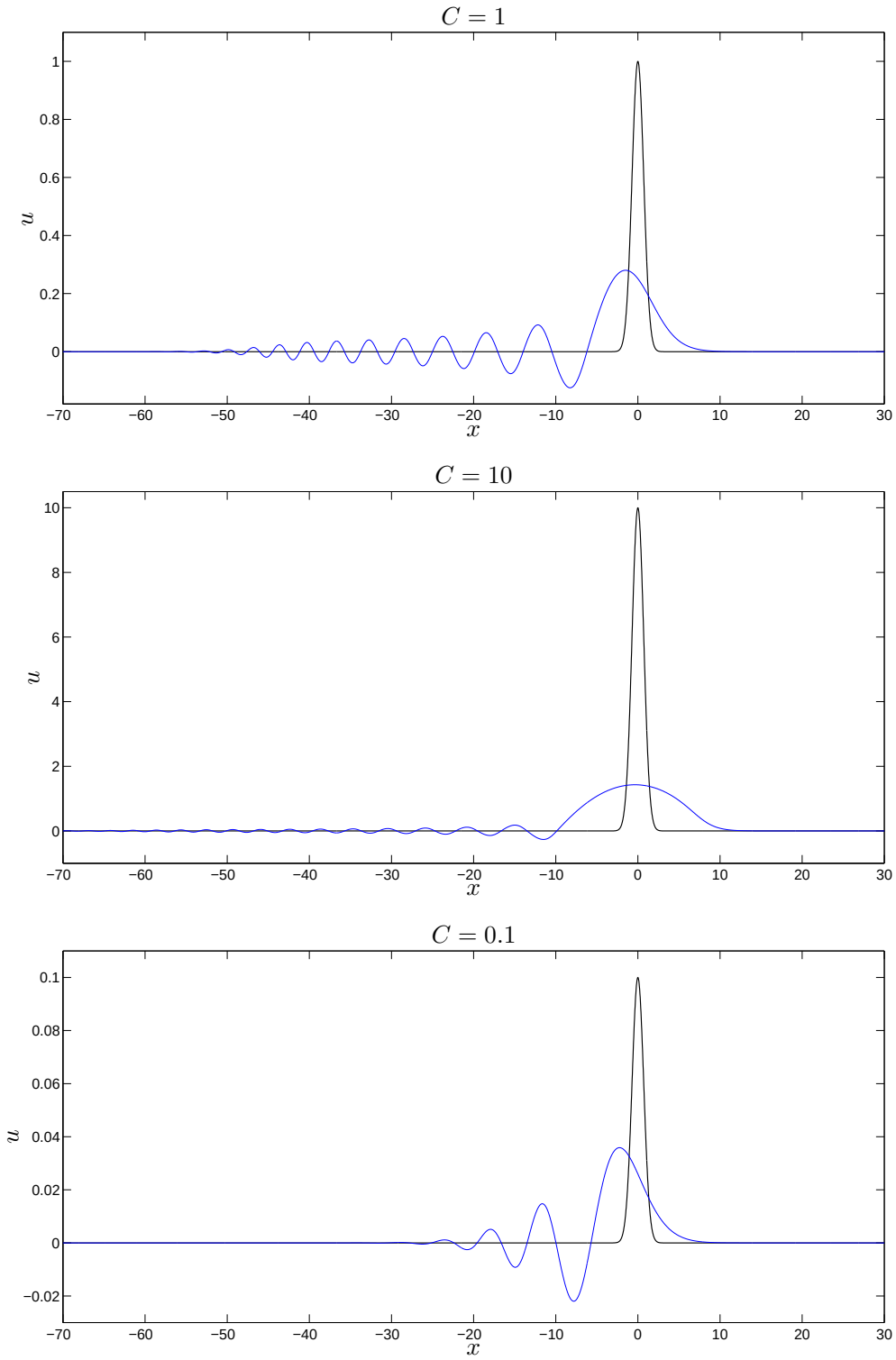

Figure 6-13: *$u(x,t)$ of the '+' case of (1.1) with (6.54) for $C = 1, 10, 0.1$ and $p = 2$, when $t = 0$ (black) and $t = 5$ (blue).*

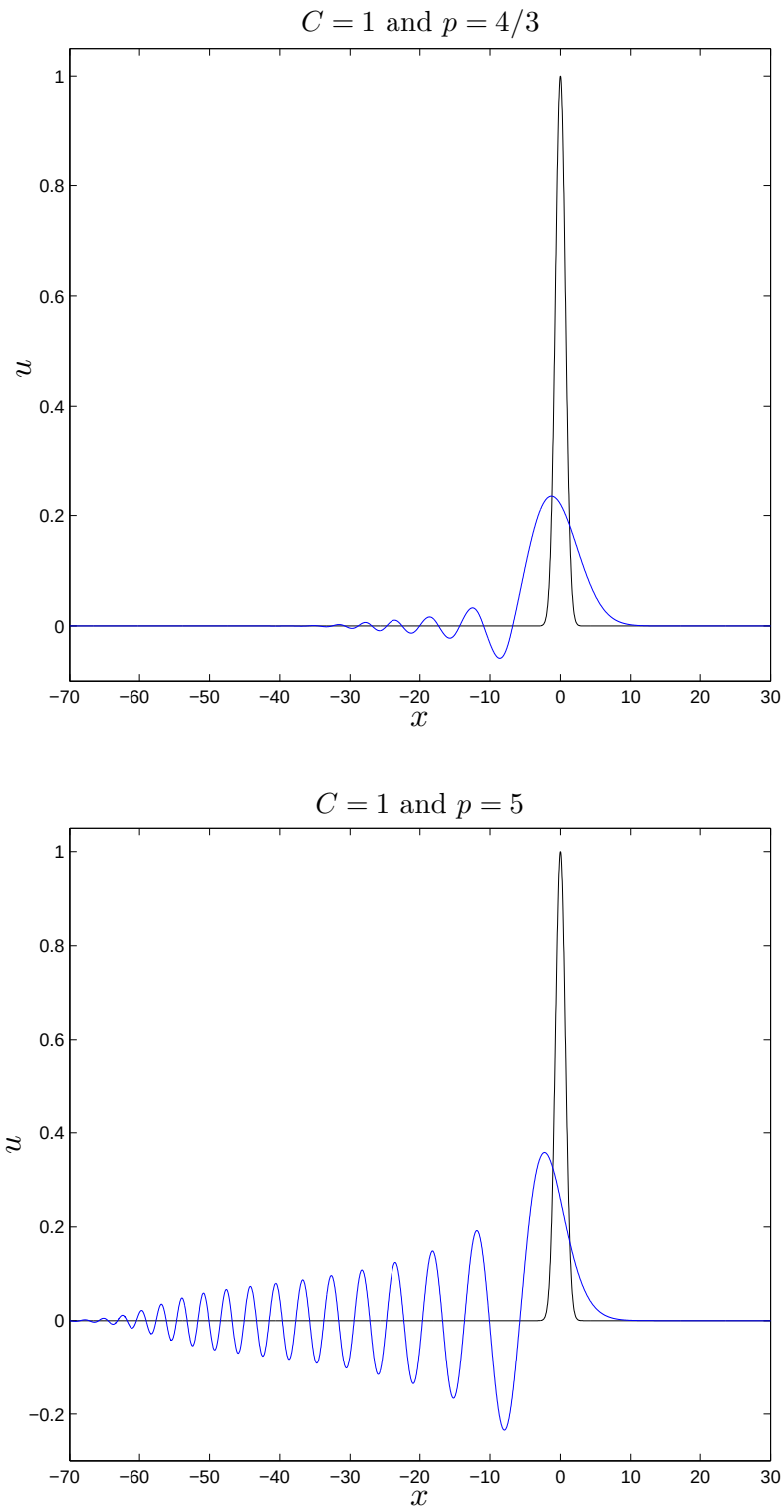

Figure 6-14: *$u(x,t)$ of the '+' case of (1.1) with (6.54) for $C = 1$ and $p = 4/3, 5$, when $t = 0$ (black) and $t = 5$ (blue).*

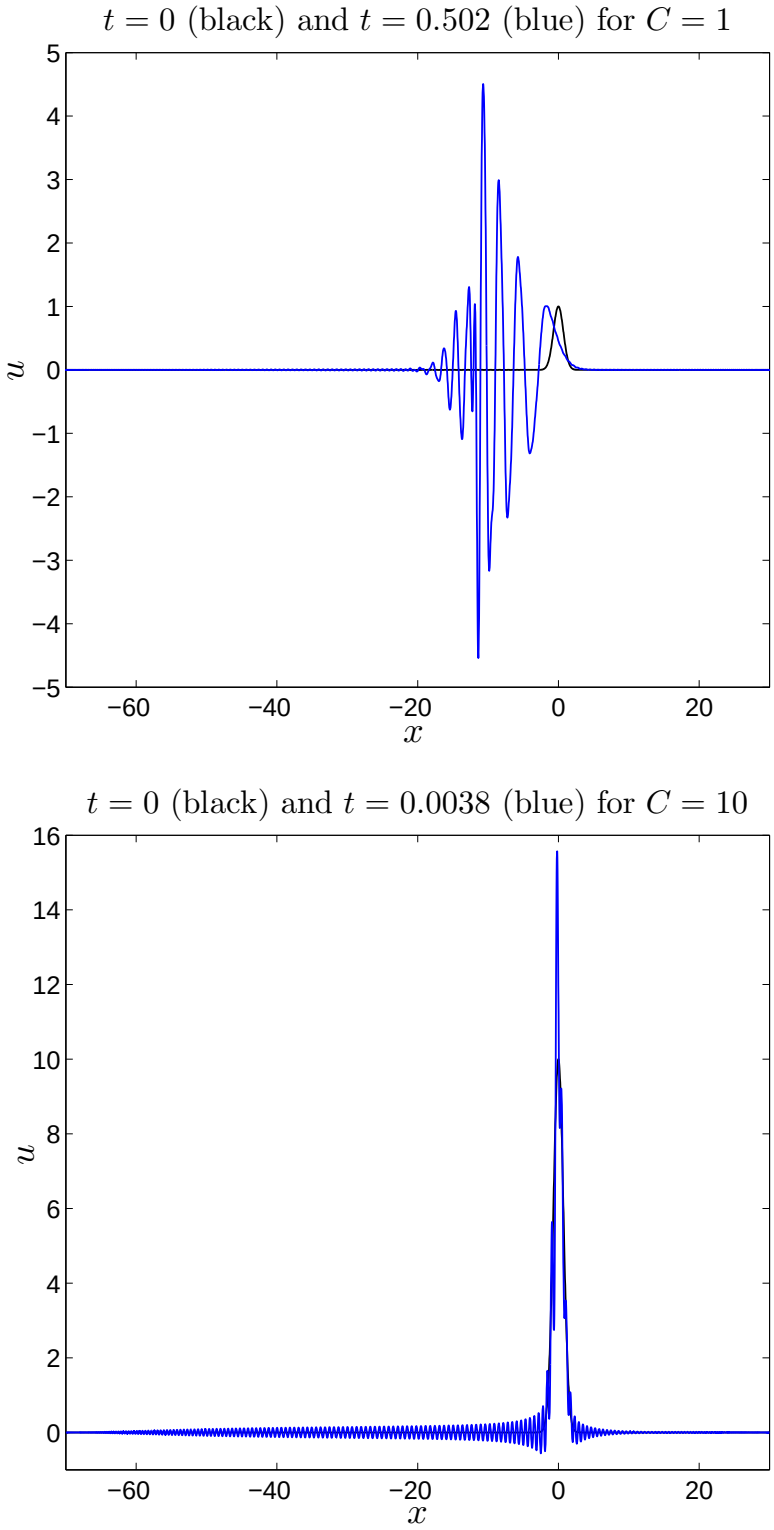

Figure 6-15: *$u(x,t)$ of the '$-$' case of (1.1) with (6.54) for $C = 1, 10$ and $p = 2$, when $t = 0$ (black) and t close to blow-up point.*

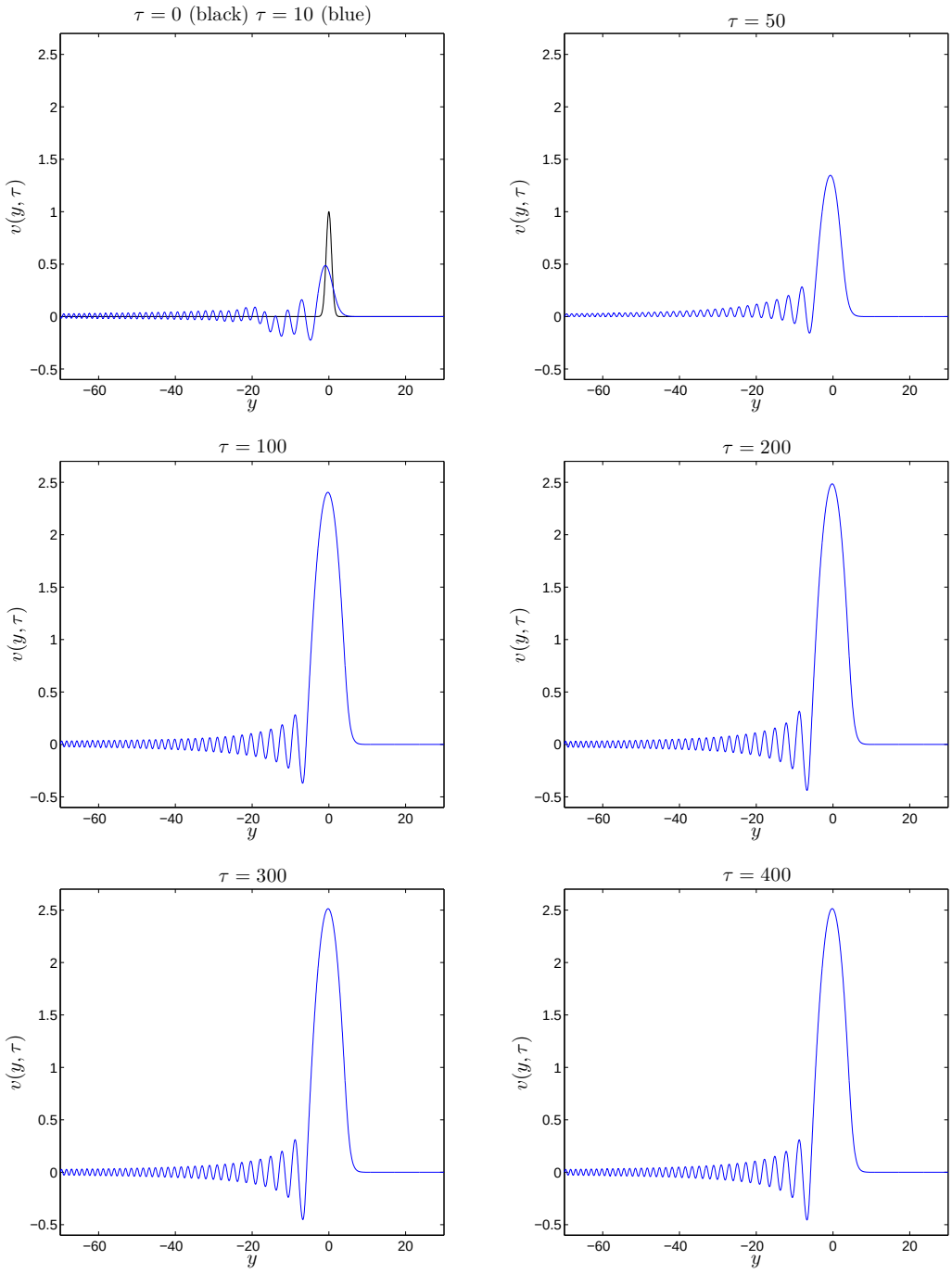

Figure 6-16: *$v(y,\tau)$ of the '+' case of (6.28) with (6.54) for $C = 1$ and $p = 2$, when $\tau = 0, 50, 100, 200, 300, 400$.*

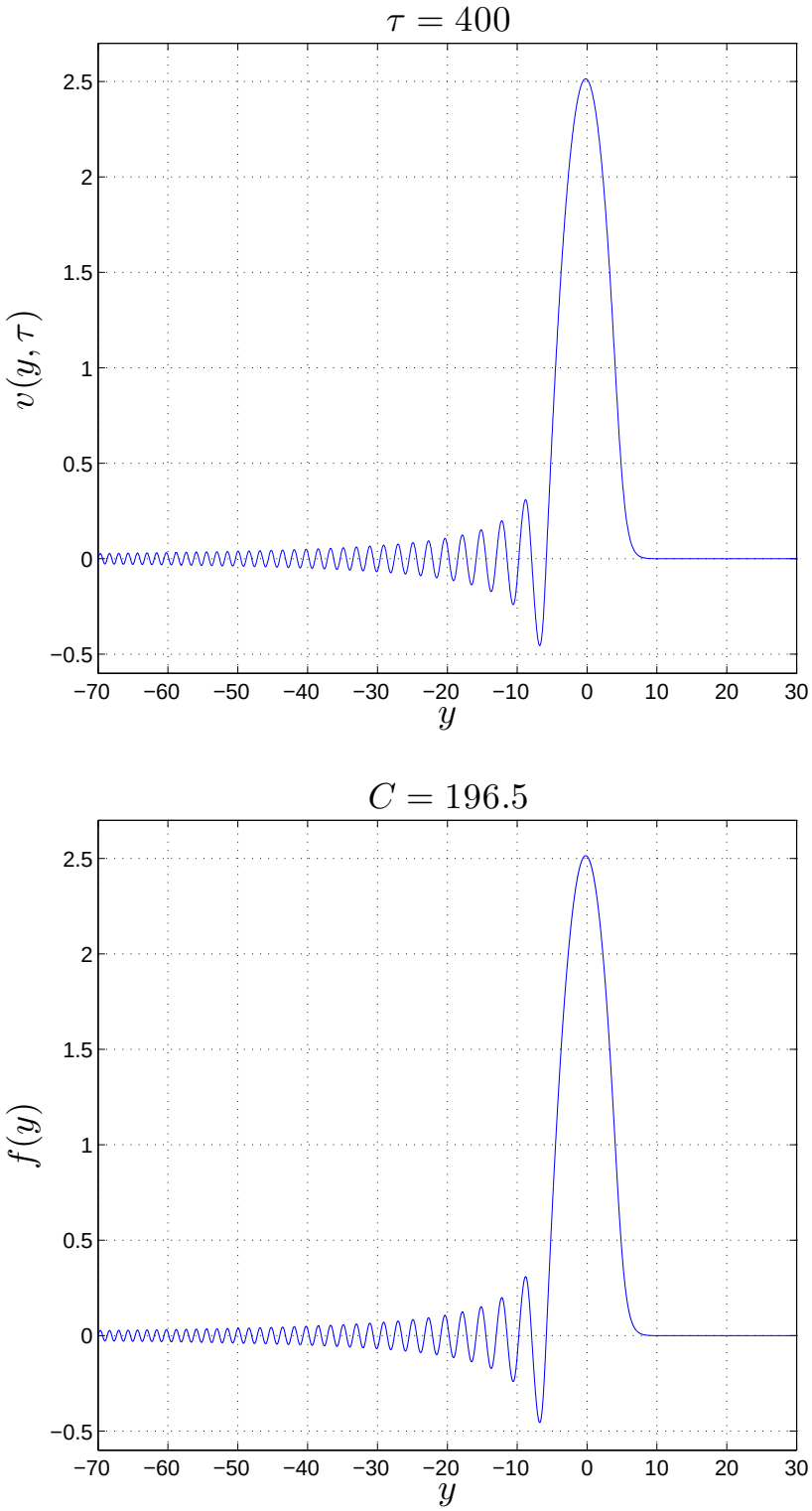

Figure 6-17: *$v(y,\tau)$ of the '+' case of (6.28) with (6.54) for $C = 1$ and $p = 2$ when $\tau = 400$, and the similarity profile $f(y)$ of (3.24) and (3.25) when $C = 196.5$.*

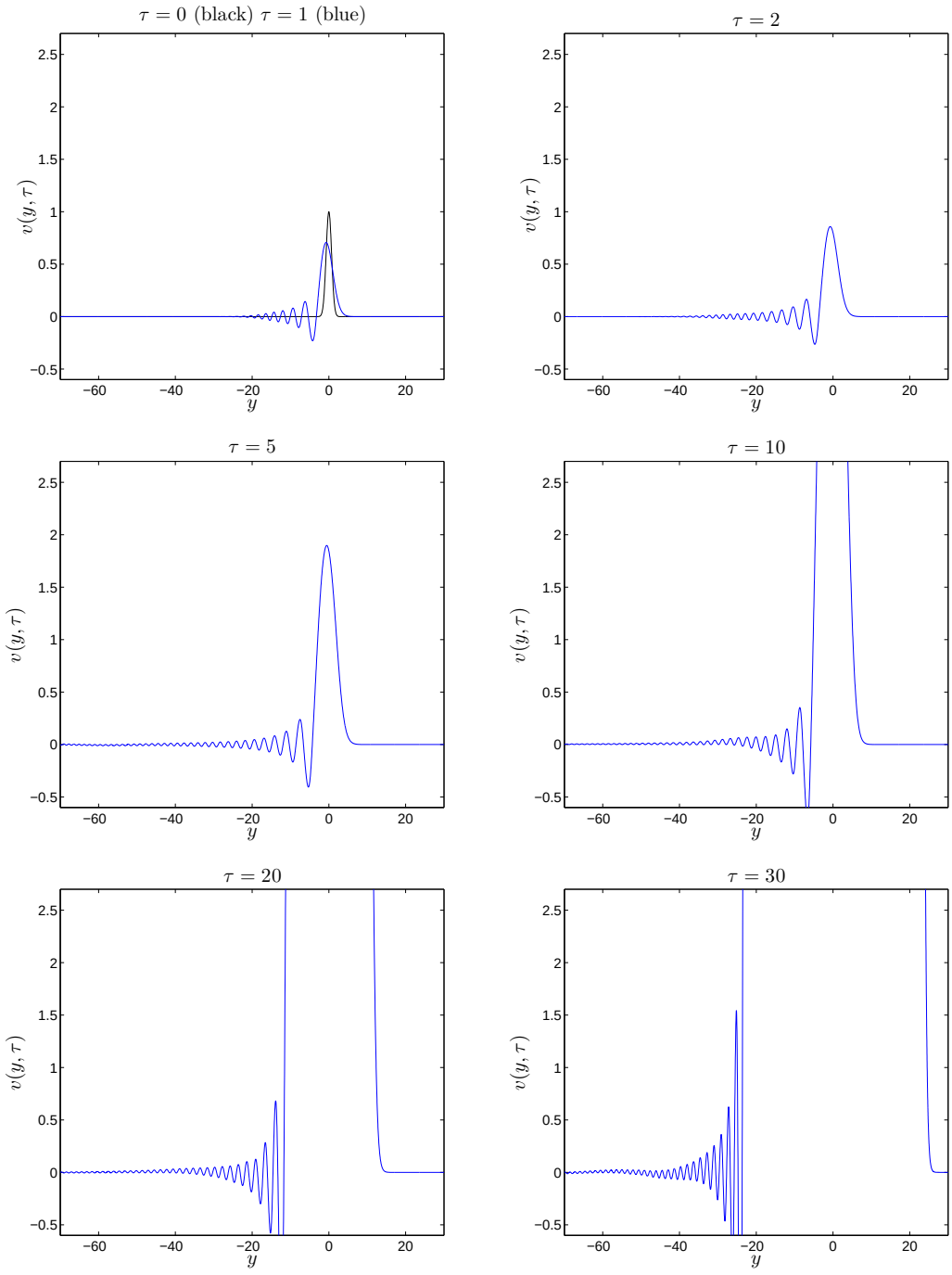

Figure 6-18: *$v(y,\tau)$ of the '+' case of (6.28) with (6.54) for $C = 1$ and $p = 1/2$, when $\tau = 0, 1, 2, 5, 10, 20, 30$.*

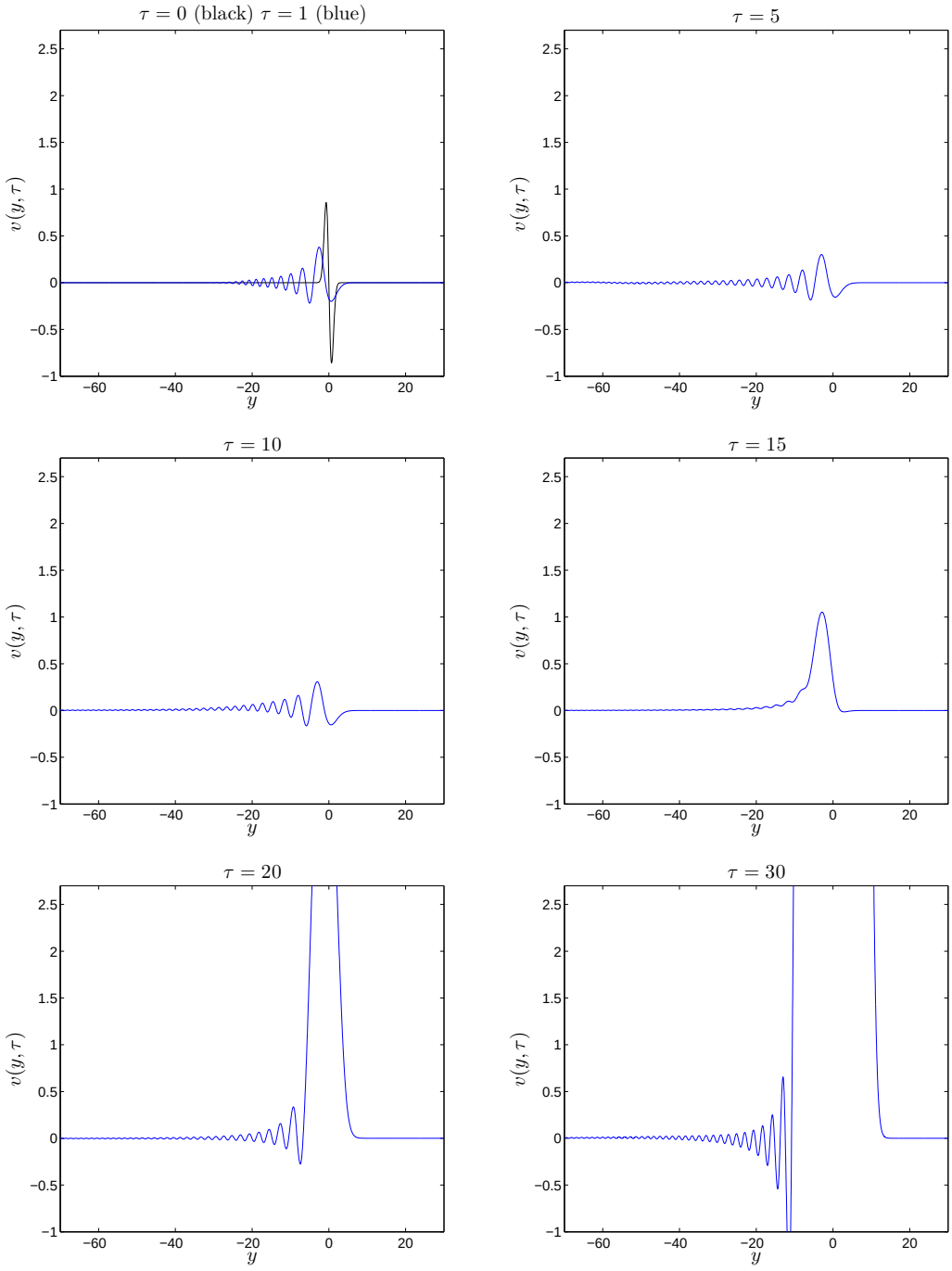

Figure 6-19: *$v(y,\tau)$ of the '+' case of (6.28) with $v(y,0) = v_0(y) = -2ye^{-y^2}$ and $p = 3/2$, when $\tau = 0, 1, 5, 10, 15, 20, 30$.*

Chapter 7

The Similarity Solutions of Nonlinear Dispersion Equation

This final chapter very briefly looks at the behaviour for similarity solutions of the NDE (1.6),

$$u_t = (|u|^n u)_{xxx} \pm (|u|^{p-1}u)_{xx} \quad \text{in} \quad \mathbf{R} \times \mathbf{R}_+, \quad n > 0 \quad \text{and} \quad p > n+1,$$

and attempts to give some aspects. One can easily see that the NDE (1.6) is more complicated and hence more difficult than the semilinear equation (1.1). Therefore, it is not expected at this stage to rigorously present key aspects analytically and even numerically. We will particularly pay attention to $p = n + 2$, which helps us to simplify the rescaled nonlinear equation and compare with semilinear ones studied in previous chapters. Before looking at the similarity solutions of the NDE (1.6), it is worth mentioning some examples of the third-order NDEs.

7.1 Nonlinear Dispersion Equations (NDEs)

The first model we put forward is the following third-order equation,

$$u_t = u^n u_{xxx}, \tag{7.1}$$

where $n \in \mathbf{R}$. For $n = 3$, (7.1) is known as the *Harry Dym* equation that is an integrable soliton equation and has direct links to the KdV equation. A more detailed survey can be found in [23, Chapter 4]. Let us also visit a canonical model

$$u_t = (uu_x)_{xx}, \tag{7.2}$$

which is the third-order quadratic NDE (NDE-3). Several blow-up and global similarity solutions of (7.2) with locally integrable initial data demonstrating shock and rarefaction waves are well studied in [42]. We have already mentioned in Chapter 2 that global similarity solutions governed by nonlinear eigenfunctions of the nonlinear dispersive equation,

$$u_t = (|u|^n u)_{xxx} \quad \text{in} \quad \mathbf{R} \times \mathbf{R}_+, \tag{7.3}$$

are constructed in [22], where global existence and uniqueness of the similarity profiles are also established in order to justify numerical construction.

An important aspect of NDEs is the compacton phenomenon, which arises in scientific applications, such as formation of drops. Compactly supported solitary waves are called *compactons*, which are also known as solitons with finite wavelength or solitons free of exponential wings [25, 122]. Considering $K(n,n)$ in (2.9) we have

$$u_t + a(u^n)_x + (u^n)_{xxx} = 0, \quad n > 1, \tag{7.4}$$

which is the well known as *Rosenau-Hyman* equation when $a = 1$ and $n = 2$. For $a > 0$ (i.e. the focusing branch), the equation (7.4) possesses the explicit compacton [25, 124]

$$u(x,t) = \begin{cases} \left\{ \frac{2cn}{a(n+1)} \cos^2 \left[\frac{\sqrt{a}(n-1)}{2n}(x-ct) \right] \right\}^{\frac{1}{n-1}}, & |x-ct| < \frac{n\pi}{\sqrt{a}(n-1)}, \\ 0, & \text{otherwise.} \end{cases} \tag{7.5}$$

However, for $a < 0$ (i.e. the defocusing branch), the equation (7.4) has the solitary pattern solutions having cusps or infinite slopes [123, 124]

$$u(x,t) = \left\{ \frac{2cn}{a(n+1)} \cosh^2 \left[\frac{\sqrt{-a}(n-1)}{2n}(x-ct) \right] \right\}^{\frac{1}{n-1}}. \tag{7.6}$$

Moreover, let us consider $DD(1,n,n)$ in (2.8) as

$$u_t + a(u^n)_x + (u^n)_{xxx} + \mu u_{xx} = 0, \quad a, \mu = \text{consts.}, \tag{7.7}$$

which is also known as the $K(n,n)$-Burger equation [124]. Note that there is an additional dissipative term u_{xx} in comparing to the $K(n,n)$ equation (7.4). A

family of solutions is given in [124] as

$$u(x,t)=\left\{\frac{\sqrt{-a}}{2\mu}\left(1+\tanh\left[-\frac{\sqrt{-a}(n-1)}{2n}x+\frac{a\mu(n-1)}{2n}t\right]\right)\right\}^{\frac{-1}{n-1}}, \qquad (7.8)$$

where complex solutions occur for $a>0$. One can see that the mix of dispersion and dissipation changed the compactons (7.5) and solitary pattern solutions (7.6). This changing in the structure is intriguing for its physical sense.

We would like to note that we have applied proposed methods of [46, 124], such as the tanh method, exp-function method and Riccati equation based method that are efficient tools to find explicit solutions of various even and odd-order PDEs, for our models (1.1) and (1.6) with appropriate exponents. We have also used the *TWSolutions* tool in *Maple*. However, these methods are not helpful for our main models since they only give trivial or stationary solutions (e.g. $u(x,t)=C_1\tanh(\pm x)$ and $u(x,t)=C_2\tan(\mp x)$ for $p=2$ in (1.5)), which is also confirmed by Wazwaz [125]. Investigations on the exact solution of our models (if at all) will be one of our future research titles.

7.2 Similarity and the rescaled equation

Using the similarity form

$$u_S(x,t)=(\sigma(T-t))^{\alpha}f(y),\quad y=x/(\sigma(T-t))^{\beta},$$

where

$$\alpha=-\frac{1}{3(p-(n+1))+n}<0\quad\text{and}\quad\beta=\frac{p-(n+1)}{3(p-(n+1))+n}>0, \qquad (7.9)$$

in the NDE (1.6) for $n>0$, $p>n+1$ yields the ODE

$$(|f|^n f)'''+\sigma\alpha f-\sigma\beta f'y\pm(|f|^{p-1}f)''=0. \qquad (7.10)$$

One can naturally see that we have the semilinear equation (1.1) for $n=0$. Similar to the semilinear PDE, using the reflections (3.3), the blow-up similarity ($\sigma=1$) profiles of the '$-$' case will also be representing the global similarity ($\sigma=-1$) profiles of the '$+$' case, where we take $T=0$ for convenience. Moreover, the blow-up similarity profiles of the '$+$' case will represent the global similarity

profiles of the '$-$' case. Therefore, we restrict our attention to the blow-up similarity profiles satisfying the ODE

$$(|f|^n f)''' - \frac{1}{3(p-(n+1))+n} f - \frac{p-(n+1)}{3(p-(n+1))+n} f' y \pm (|f|^{p-1} f)'' = 0. \quad (7.11)$$

We recall the usual settings for (7.11) that are an admissible oscillatory behaviour as $y \to -\infty$ and a suitable decaying behaviour as $y \to \infty$.

Carefully looking at the ODE (7.11), fortunately, we can simply integrate the equation for $p_0 = p = n+2 > n+1$, where $n > 0$. Therefore, substituting $p = n+2$ in (7.11) and integrating once with the zero integration constant gives

$$(|f|^n f)'' - \frac{1}{n+3} f y \pm (|f|^{n+1} f)' = 0 \quad \text{in} \quad \mathbf{R}. \quad (7.12)$$

In order to remove the nonlinearity in the third-order derivative in (7.12), let us use the natural setting

$$Y = |f|^n f \quad \Rightarrow \quad f = |Y|^{-\frac{n}{n+1}} Y. \quad (7.13)$$

So substituting (7.13) into (7.12) yields

$$Y'' - \frac{1}{n+3} |Y|^{-\frac{n}{n+1}} Y y \pm (|Y|^{\frac{1}{n+1}} Y)' = 0 \quad \text{in} \quad \mathbf{R}. \quad (7.14)$$

Here, let us mention that the first nonlinear eigenfunction, which appears as a solution of

$$Y'' - \frac{1}{n+3} |Y|^{-\frac{n}{n+1}} Y y = 0 \quad \text{in} \quad \mathbf{R}, \quad (7.15)$$

related to (7.3), is numerically constructed with local existence and uniqueness justification using asymptotic analysis in [22]. They proposed that all the solutions of the ODE (7.15) with a fixed interface point $y_0 > 0$ are oscillatory as $y \to -\infty$, by recalling $y \mapsto -y$ see [22].

We will give some numerical results of (7.14) for different values of n. Especially, the behaviour for $n \ll 1$ and $n \gg 1$ are interesting. Here, as $n \to 0^+$ ($p = n+2 \to 2^+$), we expect a connection of the similarity profiles $f(y)$ for (7.14) with the semilinear ones studied in the previous chapters, which implies a 'homotopy' connection (or 'homotopy' limit) [21, 22, 48]. In the case of the opposite 'nonlinear' limit $n \to \infty$, for the class of uniformly bounded solutions,

let us briefly give a formal analysis. If we substitute

$$Y = (n+3)^{-\frac{n+1}{n}}\widehat{Y} \tag{7.16}$$

into (7.14), then we have

$$\widehat{Y}'' - |\widehat{Y}|^{-\frac{n}{n+1}}\widehat{Y}y \pm (n+3)^{-\frac{1}{n}}(|\widehat{Y}|^{\frac{1}{n+1}}\widehat{Y})' = 0. \tag{7.17}$$

We now pass to the limit $n \to \infty$, using $(n+3)^{-\frac{1}{n}} \to 1$ and $-\frac{n}{n+1} \to -1$, which yields

$$\widehat{Y}'' - \operatorname{sgn}\widehat{Y}y \pm \widehat{Y}' = 0. \tag{7.18}$$

Solving (7.18), we obtain the following algebraic treatment of the profile $\widehat{Y}$ as $n \to \infty$,

$$\begin{aligned} \widehat{Y} > 0: &\quad \widehat{Y}_+ = \pm\frac{1}{2}y^2 - y \mp c_1 e^{\mp y} + c_2, \\ \widehat{Y} < 0: &\quad \widehat{Y}_- = \mp\frac{1}{2}y^2 + y \mp d_1 e^{\mp y} + d_2, \end{aligned} \tag{7.19}$$

where c_1, c_2, d_1, d_2 are constants. Let us point out that $\widehat{Y}_+ = \widehat{Y}_-$ and $\widehat{Y}'_+ = \widehat{Y}'_-$, when $\widehat{Y} = 0$, according to the continuity conditions for the function $\widehat{Y}(y)$. In the next section, we will illustrate such behaviours using numerics.

7.2.1 Numerical construction

We consider the blow-up self-similar ($\sigma = 1$) profiles Y satisfying the rescaled ODE (7.14) with the initial condition at the finite point $y_0 > 0$,

$$Y(y_0, C) = C\,\mathrm{Ai}(y_0), \quad Y'(y_0, C) = C\,\mathrm{Ai}'(y_0). \tag{7.20}$$

For small solutions of (7.15), [22] suggested the expansion

$$Y(y) = \left(\frac{n^2 y_0}{2(n+1)(n+2)(n+3)}\right)^{\frac{n+1}{n}} |y - y_0|^{\frac{2(n+1)}{n}}(1 + o(1)) \tag{7.21}$$

as $y \to y_0^- > 0$. They looked at some point $y_0 - \epsilon$, where $\epsilon = 10^{-3}$, and used this point in (7.21) as the initial condition. However, they were not able to efficiently compare behaviour for different values of n, especially for $n \ll 1$, because Y and Y' have become very small, e.g. $Y \sim 10^{-45}$ for $y_0 = 10$ and $n = 0.2$, so they had to

take a relatively large initial point. In order to give some efficient comparison for different values of n, we use (7.20) in our calculations, where $y_0 = 15$. We again use the same standard IVP solver supplied by *MatLab* with the same notations given in Section 3.4.

'−' case: In Figure 7-1, we show the behaviour for $Y(y)$ of (7.14) with (7.20) when $n = 0, 0.01, 0.1, 0.5, 1, 2, 10, 100$ and $C = 1$. We expect that all the similarity profiles $Y = Y(y)$ are bounded and have decaying oscillatory tail symmetric to $Y = 0$, hence they are admissible similarity profiles. One can see the connection of $Y(y)$ with the semilinear one in Chapter 3, as $n \to 0^+$, see Figure 3-12 in the case of semilinear one, where $n = 0$. As n increases, the first 'hump' becomes wider, hence we suggest taking larger initial point y_0. Note that the numerical results presented here are constructed as in Section 3.4.

'+' case: Figure 7-2 display the behaviour for $Y(y)$ of (7.14) with (7.20) when $n = 0, 0.01, 0.1, 0.5, 1, 2, 10, 100$ and $C = 0.1$. We expect that all the profiles here are unbounded similar to semilinear one in Chapter 4. We refer to Figure 4-3 for $n = 0$.

Studies in this chapter can be extended to the different values of $p > n+1$ and $n > 0$, but are obviously more delicate since the nonlinear equation (7.10) remains third order, which means we expect to face many more numerical challenges. However, similar to $p_1 = 3/2$ for the semilinear equation, we can simplify (7.10) when $p_1 = n + 3/2$. On the other hand, one can also check the behaviour for the profiles of (7.10), for the critical values $p = p_k = n + 1 + 1/(k+1)$, $k = 0, 1, 2, ...$

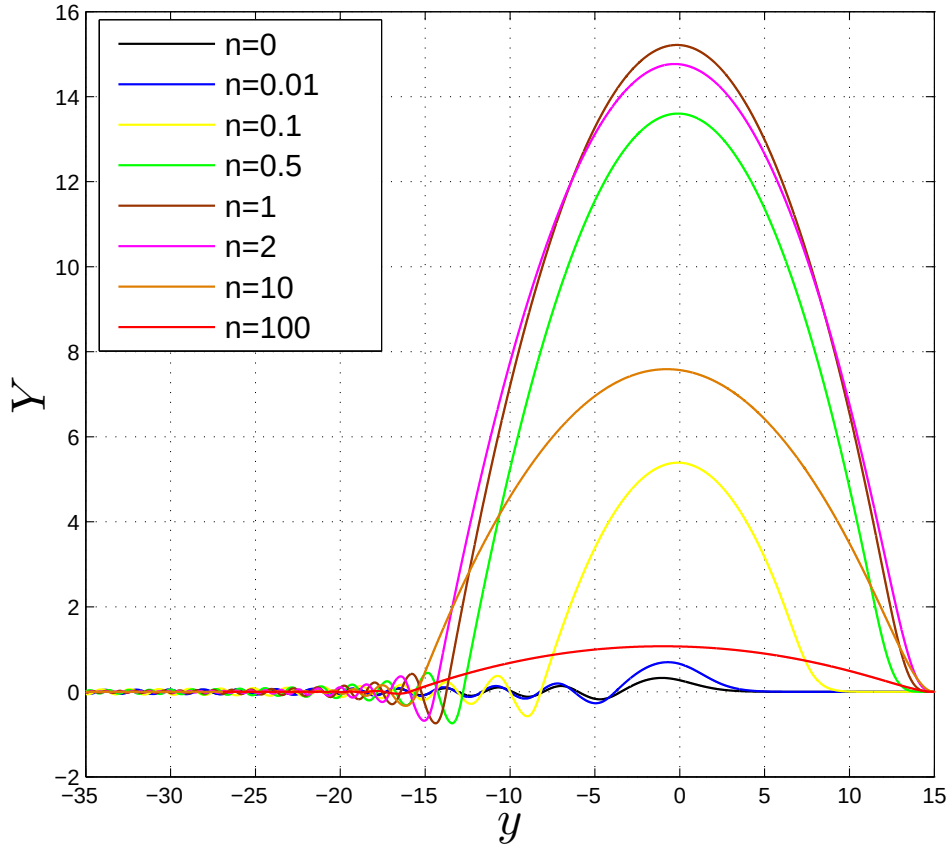

Figure 7-1: *The profiles* $Y(y)$ *for the '−' case of (7.14) with (7.20) when* $n = 0, 0.01, 0.1, 0.5, 1, 2, 10, 100$ *and* $C = 1$.

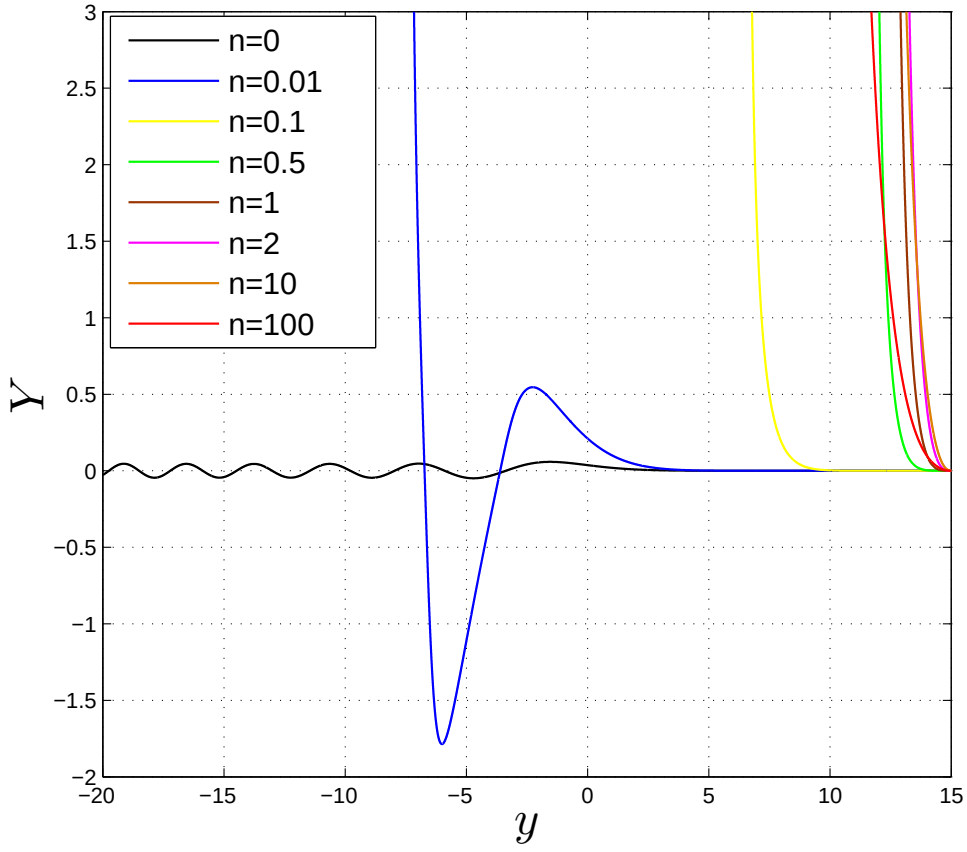

Figure 7-2: *The profiles* $Y(y)$ *for the '+' case of (7.14) with (7.20) when* $n = 0, 0.01, 0.1, 0.5, 1, 2, 10, 100$ *and* $C = 0.1$.

Chapter 8

Conclusions and Further Work

8.1 Conclusions

The key structure of this thesis has been based on understanding and classifying the asymptotic behaviour of the proposed PDEs using analytical and numerical tools, where the asymptotic behaviour, as $t \to T^-$ or $t \to \infty$, are governed by similarity solutions.

Chapter 3 has studied the blow-up self-similar profiles of the '$-$' case of the semilinear dispersion PDE (1.1) for the first critical (mass conservative) case $p = p_0 = 2$, which also implies the global self-similar profiles of the '$+$' case. We have been able to integrate the rescaled third-order ODE for $p = p_0 = 2$. We have presented explicit solutions of the corresponding rescaled ODEs and discussed the effect of such solutions. According to the numerical and perturbation results, an unbounded continuous family of admissible similarity solutions (i.e. the profiles have finite mass) parameterized by C (initial mass) have been observed for the signed form of the second-order rescaled ODE with zero integration constant. For the analytical form of the second-order rescaled ODE with zero integration constant, such existence is valid for $C > C^*$, where $C^* \approx -0.5911$ has been numerically obtained. We have displayed the behaviour of the profiles for different values of C. Asymmetric (to 0) oscillatory tails have been observed for the rescaled ODEs with the non-zero integration constant, which are not admissible due to the conservation law, i.e. the profiles do not have finite mass. We have also briefly discussed expected behaviour for the case $1 < p \neq 2$. Finally, the signed and analytical form of the rescaled second-order ODE has been displayed

for the same values of C, in order to show the signed form damps to zero faster than the analytical form.

Chapter 4 has looked at the blow-up self-similar profiles of the '+' case of the semilinear dispersion PDE (1.1) for the first critical case $p = p_0 = 2$, which also represent the global self-similar profiles of the '−' case. Similar to Chapter 3, the rescaled third-order ODE has been integrated for $p = p_0 = 2$. We have given explicit solutions of the corresponding ODEs, in order to discuss the effect of such solutions. Unlike Chapter 3, according the numerical and perturbation results, there have been no admissible self-similar solutions of the signed form of the rescaled second order ODE with zero integration constant, i.e. we have not been not able to obtain any bounded profile. The behaviour of the profiles for different values of C has been displayed and explained. For the analytical form of the rescaled second order ODE with zero integration constant, using $f \mapsto -f$, we have reminded reader that the corresponding rescaled ODE was same with the analytical form in Chapter 3, i.e. the existence is valid for $C < C^*$, where $C^* \approx 0.5911$. Moreover, for the signed form of the rescaled ODE with the non-zero integration constant, we have shown that all profiles became unbounded.

In short, for the first critical case $p = p_0 = 2$, existence of blow-up similarity profiles of the '−' case and global similarity profiles of the '+' case for all $C \neq 0$ has been observed. On the other hand, non-existence of blow-up similarity profiles of the '+' case and global similarity profiles of the '−' case has been achieved. We have summarized such results by using Table 4.1 at the end of Chapter 4. Unlike the first critical exponent $p = p_0 = 2$, it has been not expected to easily find and classify admissible similarity profiles for $1 < p \neq 2$ since the rescaled ODE has been third order, which has been discussed in Chapter 6.

Chapter 5 has proposed an exponentially fitted Runge-Kutta method for Airy-type initial value problems, similar to the rescaled ODEs in Chapter 3 and 4. Efficiency of the technique for large step sizes has been presented by using two examples, the second Painlevé equation and the analytical form of the rescaled ODE with zero integration in Chapter 4. It has been observed that the technique is reliable in giving certain behaviours even for large step sizes, in comparison to the classical fourth-order Runge-Kutta (*ode4*) method. However, the computational time is more than *ode4* due to calculation of the 'fitting' parameters in each step.

In Chapter 6, we have first looked at the similarity profiles of the semilinear PDE (1.1) for the second critical exponent $p = p_1 = 3/2$, which has been obtained

by the conservation of the first moment. Fortunately, we have been able to integrate the rescaled third-order ODE for $p = p_1 = 3/2$. According to the numerical and perturbation results, similar conclusions about existence as in Chapter 3 and 4 have been obtained for the '$-$' and '$+$' case. Then, in order to give characteristics of the rescaled profiles, we have analysed the invariant subspace behaviour and bifurcation points by using the spectral properties of the rescaled linear operator. However, we have not managed to give rigorous proof due to the absence of integral computation. Algebraic solutions of the rescaled third-order ODE have been given in order to explain asymmetric (to 0) oscillatory tails obtained in the numerical results section for arbitrary values of $p > 1$. According to the numerical experiments for the rescaled ODE, admissible similarity profiles have been expected close to the critical exponents $p = p_k = 1 + 1/(k+1)$, $k = 2, 3, ...$, where the dominancy of the tails change sign. However, the justification of these profiles is questionable. We have also given some aspects of the original PDE with numerical experiments, where we do not expect any proper continuation after blow-up, which means complete blow-up, due to existence/non-existence results for the signed form of the rescaled ODE in Chapter 3 and 4. However, one can expect incomplete blow-up, which means a proper continuation after blow-up, according to the existence results of blow-up and global similarity profiles for the analytical form of the rescaled ODE when $0 < C < |C^*|$. Additionally, according to our experiments with the non-zero integration constant for $p = p_0 = 2$ in Chapter 3 and 4, and the rescaled third-order ODE for $p > 1$, where $p \neq p_0, p_1$, in Section 6.4, which yield asymmetric (to 0) oscillatory tails, we have claimed that we had to omit algebraic decay in the true Cauchy Problem. Otherwise, we have arrived at a problem with specific conditions at infinity, i.e. a free-parameter boundary value problem. Finally, we have numerically observed that the global similarity profile satisfying the signed rescaled ODE in Chapter 3 govern the global in time dynamics for the '$+$' case of the original signed PDE, for $p = p_0 = 2$. However, large-time behaviour of the blow-up solution for the '$+$' case of the original PDE cannot converge to a non-zero steady state, regarding the non-existence result in Chapter 4. For the '$-$' case of the original PDE, unstable evolution of blow-up solutions have been observed due to the unstable porous medium operator, which can yield different special singularity formation phenomena. On the other hand, for the '$+$' case of the original rescaled PDE with $1 < p < p_0 = 2$, the global solutions have not been able to reach its steady state. According to the existence results for $p = p_1 = 3/2$ in Section 6.1, such behaviour remains open. Therefore,

we have seen that more delicate analysis using new numerical and theoretical tools are still needed for such relatively untouched odd-order PDE.

Chapter 7 has briefly looked at the similarity solutions of the nonlinear dispersion PDE (1.6) for $p = n+2$, $n > 0$. Mathematical and numerical approaches have been used to understand behaviour of the similarity solutions of the problem for various values of $n > 0$. Especially, the behaviour for $n \ll 1$ and $n \gg 1$ has been discussed. As $n \to 0^+$, the connection of the similarity profiles for the nonlinear equation with the semilinear ones has been displayed. Moreover, $n \to \infty$ case has been analysed. The existence for the blow-up similarity profiles of the '$-$' case and the non-existence for the '$+$' case has been numerically proposed and displayed.

8.2 Further work

There is surely still much that can be studied for our models since these models have not been investigated much in the literature. Although the behaviour of solutions for the rescaled equations is well understood, there are still some results that remain unproven. Especially, some analysis in the invariant subspaces and bifurcation points remain formal because of some open questions in functional settings of the linear dispersion PDE and highly oscillatory tail of the eigenfunctions. More qualitative and quantitative tools are needed since the current techniques are insufficient.

In the case of the semilinear PDE, we would like to have obtained the asymptotic solution of the rescaled ODE, particularly for $p = p_0 = 2$, similar to the Hastings-Mcleod solution of the second Painlevé equation. Carefully looking at the asymptotics of solutions to the linear dispersion equation and the second Painlevé equation, we may motivate the asymptotics of solutions to the rescaled second-order ODE as follows:

$$f(y,C) \sim \begin{cases} C\,\mathrm{Ai}\,(y) & \text{as} \quad y \to +\infty, \\ d|y|^{-1/4}\sin\left(|y|^{3/2} + g(y,C) + \theta_0\right) & \text{as} \quad y \to -\infty, \end{cases}$$

where d and θ_0 are constants depending on C, and $g(x,C)$ is a suitably chosen function. On the other hand, the dependence of singularity point y^* on shooting parameter C for the rescaled ODE is intriguing. Currently there might not be a scientific application of proposed third-order PDEs, however we would also like to look at the "singular" case $p < 1$ related to the Fast Diffusion equation (2.13).

Moreover, the higher-odd-order analogy of these models is also interesting, i.e.

$$u_t = (-1)^{k+1} D_x^{2k+1} u \pm (|u|^{p-1}u)_{xx} \quad \text{in} \quad \mathbf{R} \times \mathbf{R}_+, \quad k = 1, 2, ..., \tag{8.1}$$

where the first critical exponent is $p = p_0 = 2k$. The asymptotic behaviour of rescaled kernel $f(y) = \mathrm{Ai}_{2k+1}(y)$ of the fundamental solution for the linear part of (8.1) is well constructed in [21], see (3.22) for $k = 1$. It is worth mentioning that the decay of oscillations increases as k increases, i.e. from $y^{-1/4}$, for $k = 1$, to $\sim y^{-1/2}$ as $k \to \infty$.

For the NDE, numerical and analytical techniques can be extended to the different values of p and n, in order to classify behaviour of similarity solutions, but are obviously more delicate. Particularly, the similarity profiles for $1 < p < n + 1$ and $p = n + 1$ can be investigated. Although there is not much hope regarding to open questions in the semilinear case, a formal local "nonlinear" bifurcation analysis based on comparison of linear and nonlinear eigenfunctions can also be done in order to justify numerical results. Using the idea of the studies on the NDE in Chapter 7, a nonlinear extension of the KdV equation,

$$u_t = (|u|^n u)_{xxx} \pm (|u|^{p-1}u)_x \quad \text{in} \quad \mathbf{R} \times \mathbf{R}_+,$$

where $p = n + 3$, $n > 0$, is intriguing, in order to look at the KdV equation by homotopy connection, as $n \to 0^+$.

On the other hand, the investigation into exact solutions of these models for appropriate exponents is also intriguing, if there is an exact solution at all. A delicate numerical study for the original PDE having both second and third-order derivatives can also be done constructing a reliable method. Moreover, we bear in mind that the proposed models can be extended to be multi-dimensional $\mathbf{R}^N \times \mathbf{R}_+$, where we can still use some basic theory.

For the prototype of the second order ODEs studied in Chapter 5, we can use more stages or other reference sets $\{1, y, y^2, ..., y^k, e^{\lambda_1 y}, e^{\lambda_2 y}, ..., y^p e^{\lambda_1 y}, y^p e^{\lambda_2 y}\}$, as hinted before, in order to efficiently catch a much longer range of behaviour for larger step sizes, in comparison to the classical fourth order Runge-Kutta method. On the other hand, a reliable splitting method applied to the non-autonomous problems [126, 127] is under consideration with U. Erdoğan and M. Seydaoğlu for the rescaled ODE (3.24),

$$f'' - \frac{1}{3} yf - 2|f|f' = 0.$$

This equation can be written as a first order system of equations

$$\frac{\mathrm{d}}{\mathrm{d}y}\begin{Bmatrix} f \\ g \end{Bmatrix} = \begin{pmatrix} 0 & 1 \\ y/3 & 0 \end{pmatrix}\begin{Bmatrix} f \\ g \end{Bmatrix} + \begin{Bmatrix} 0 \\ 2\,|f|\,g \end{Bmatrix}$$

which we split as follows

$$\frac{\mathrm{d}}{\mathrm{d}y}\begin{Bmatrix} f \\ g \end{Bmatrix} = \begin{pmatrix} 0 & 1 \\ y_1/3 & 0 \end{pmatrix}\begin{Bmatrix} f \\ g \end{Bmatrix}, \qquad \frac{\mathrm{d}y_1}{\mathrm{d}y} = 1,$$

and

$$\frac{\mathrm{d}}{\mathrm{d}y}\begin{Bmatrix} f \\ g \end{Bmatrix} = \begin{Bmatrix} 0 \\ 2\,|f|\,g \end{Bmatrix},$$

where we can now apply the scheme of the splitting method for the non-autonomous equation [126, 127].

Appendix A

Comment on the Semilinear Dispersive PDE with Absorption, and with Source

Let us recall the semilinear dispersion equation with absorption (2.4),

$$u_t = u_{xxx} - |u|^{p-1}u, \quad p > 1,$$

in order to very briefly give additional comments and illustrations for the behaviour of the problem. A similarity (VSS) solution has the form

$$u(x,t) = t^{-1/(p-1)} f(y), \quad y = x/t^{1/3},$$

where f satisfies the rescaled ODE,

$$f''' + \frac{1}{p-1} f + \frac{1}{3} f' y - |f|^{p-1} f = 0 \quad \text{in} \quad \mathbf{R}. \tag{A.1}$$

For the semilinear dispersive equation with source,

$$u_t = u_{xxx} + |u|^{p-1}u, \quad p > 1, \tag{A.2}$$

if we construct the blow-up similarity solutions that have the form

$$u(x,t) = (-t)^{-1/(p-1)} f(y), \quad y = -x/(-t)^{1/3}, \tag{A.3}$$

then f satisfies the same rescaled ODE (A.1). One can see that the ODE (A.1) cannot be simplified by integration for $p = p_0 = 4$, in contrast to our problem. As

we mentioned in Chapter 2, bifurcation analysis admits a countable number of similarity solutions for the critical exponents $p = p_k = 1+3/(k+1)$, $k = 0, 1, 2, ...$ [21]. However, numerical studies for the ODE (A.1) in [21] did not manage to show any reliable similarity profiles, since obtained oscillatory tails are not symmetric to $f = 0$. Also, the behaviour for $p > p_0 = 4$ is not given numerically. Here, we would first like to clarify the non-symmetric (to $f = 0$) tails. If we carefully look at the ODE, the profiles are actually affected by algebraic decay,

$$f(y) = \pm \left(\frac{3(p+2)(2p+1)}{(p-1)^3} \right)^{1/(p-1)} |y|^{-3/(p-1)}. \tag{A.4}$$

Moreover, constructing the same numerics (recalling $x \mapsto -x$) with the same initial condition (6.54), which is proposed in Chapter 6 to our semilinear PDE (1.1), for the above semilinear PDEs, we illustrate the behaviour of the problem, see Figures A-1 and A-2. It is still curious that the stable similarity profiles satisfying the ODE (A.1) may govern the global in time or blow-up dynamics for appropriate values of $p > 1$. Also, simulations to the semilinear dispersion PDE with source (A.2) suggest that global in time solutions occur for $p > p_0$ with sufficiently small initial mass. Here, $p = p_0 = 4$ actually plays a critical role, similar to the Fujita exponent for the semilinear heat equation (2.25). Hence, more detailed and delicate analysis for the blow-up and global in time dynamics, governed by similarity solutions, of such dispersion PDEs are needed, which will be one of the future research interests. As we have seen in this thesis several times, there is still much that can be studied for the third-order PDEs, requiring more qualitative and quantitative approaches.

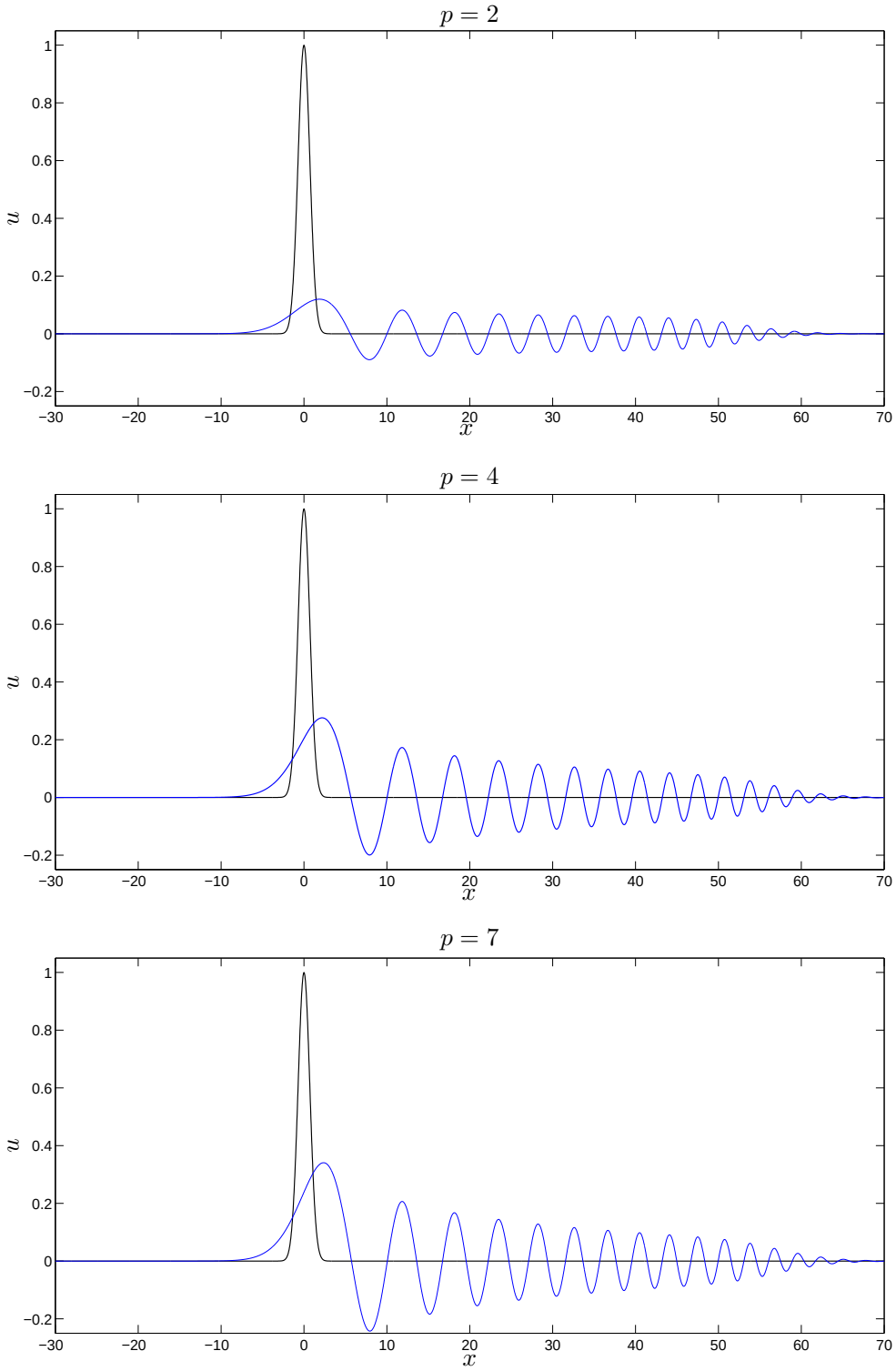

Figure A-1: *$u(x,t)$ of the semilinear PDE with absorption for $C = 1$ and $p = 2, 4, 7$, when $t = 0$ (black) and $t = 5$ (blue).*

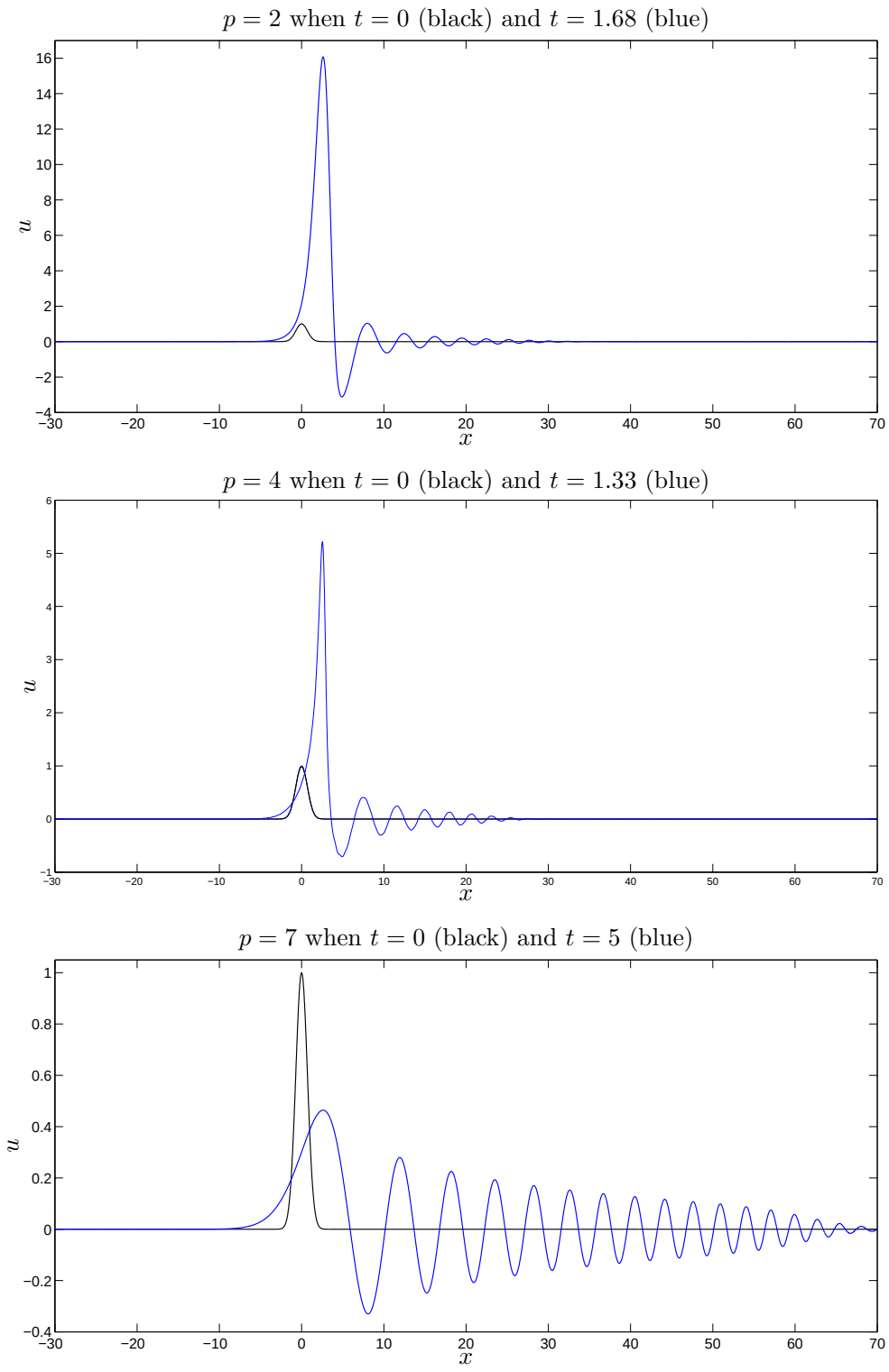

Figure A-2: *$u(x,t)$ of the semilinear PDE with source for $C = 1$ and $p = 2, 4, 7$.*

Bibliography

[1] P. A. Clarkson, A. S. Fokas, M. J. Ablowitz, *Hodograph transformations of linearizable partial differential equations*, SIAM J. Appl. Math., 49 (1989), pp. 1188–1209.

[2] P. Gungor, V. I. Lahno, R. Z. Zhdanov, *Symmetry classification of KdV-type nonlinear evolution equations*, J. Math. Phys., 45 (2004), pp. 2280–2313.

[3] J. S. Russel, *Report on Waves*, Report of the fourteenth meeting of the British Association for the Advancement of Science, York, September (1844), pp. 311–390.

[4] J. Boussinesq, *Théorie des ondes et des remous qui se propagent le long d'un canal rectangulaire horizontal, en communiquant au liquide continu dans ce canal des vitesses sensiblement pareilles de la surface au fond*, J. Math. Pures Appl, 17 (1872), pp. 55–108.

[5] D. J. Korteweg, G. de Vries, *On the change of form of long waves advancing in a rectangular canal and on a new type of long stationary waves*, Philos. Mag., 539 (1895), pp. 422–443.

[6] T. Tao, *Why are solitons stable?*, Bull. Amer. Math. Soc., 46 (2009), pp. 1–33.

[7] T. Tao, *Global behaviour of nonlinear dispersive and wave equations*, Current Developments in Mathematics, 2006 (2008), pp. 255–340.

[8] R. Cote, *Construction of solutions to the subcritical gKdV equations with a given asymptotical behavior*, J. Func. Anal., 241 (2006), pp. 143–211.

[9] C. E. Kenig, G. Ponce, L. Vega, *Well-posedness and scattering result for the generalized Korteweg-De Vries equation via contraction principle*, Commun. Pur. Appl Anal., 46 (1993), pp. 527–620.

[10] F. Merle, *Existence of blow-up solutions in the energy space for the critical generalized Korteweg-de Vries equation*, J. Amer. Math. Soc., 14 (2001), pp. 555–578.

[11] J. L. Bona, V. A. Dougalis, O. A. Karakashian, W. R. McKinney, *Conservative, High-Order Numerical Schemes for the Generalized Korteweg-de Vries Equation*, Phil. Trans. R. Soc. Lond. A, 351 (1995), pp. 107–164.

[12] J. L. Bona, F. B. Weissler, *Similarity solutions of the generalized Korteweg-de Vries equation*, Mat. Proc. Cambridge Philos. Soc., 127 (1999), pp. 323–351.

[13] D. B. Dix, W. R. McKinney, *Numerical computations of self-similar blow-up solutions of the generalized Korteweg-de Vries equation*, Differ. Integral Equ., 11 (1998), pp. 679–723.

[14] C. Klein, R. Peter, *Numerical study of blow-up in solutions to generalized Korteweg-de Vries equations*, arXiv:1307.0603 [math-ph], 2013.

[15] H. Koch, *Self-similar solutions to super-critical gKdV*, arXiv:1404.4591 [math.AP], 2014.

[16] N. Strunk, *Well-posedness for the supercritical gKdV equation*, Commun. Pure Appl. Anal., 13 (2014), pp. 527–542.

[17] R. M. Miura, *The Korteweg-de Vries equation: a survey of results*, SIAM Review, 18 (1976), pp. 412–459.

[18] E. M. de Jager, *On the origin of the Korteweg-de Vries equation*, Forum der Berliner Mathematischen Gesellschaft, 19 (2011), pp. 171–195.

[19] N. Tzvetkov, *On the long time behavior of KdV type equations (after Martel-Merle)*, Séminaire Bourbaki, 46 (2003-2004), pp. 219–248.

[20] K. Brauer, *The Korteweg-de Vries equation: history, exact solutions, and graphical representation*, University of Osnabrück, May 2000.

[21] R. S. Fernandes, V. A. Galaktionov, *Very singular similarity solutions and Hermitian spectral theory for semilinear odd-order PDEs*, J. Part. Diff. Eq., 24 (2011), pp. 207–263.

[22] R. S. Fernandes, V. A. Galaktionov, *Eigenfunctions and very singular similarity solutions of odd-order nonlinear dispersion PDEs: toward a 'nonlinear Airy function' and others*, Stud. Appl. Math., 129 (2012), pp. 163–219.

[23] V. A. Galaktionov, S. R. Svirshchevskii, *Exact Solutions and Invariant Subspaces of Nonlinear Partial Differential Equations in Mechanics and Physics*, Chapman and Hall/CRC, Florida, 2007.

[24] P. Rosenau, *On a class of nonlinear dispersive-dissipative interactions*, Phys. D, 123 (1998), pp. 525–546.

[25] P. Rosenau, J. M. Hyman, *Compactons: solitons with finite wavelength*, Phys. Rev. Lett., 70 (1993), pp. 564–567.

[26] R. S. Johnson, *A nonlinear equation incorporating damping and dispersion*, J. Fluid Mech., 42 (1970), pp. 49–60.

[27] T. Kawahara, *Weak Nonlinear Magneto-Acoustic Waves in a Cold Plasma in the Presence of Effective Electron-Ion Collisions*, J. Phys. Soc. Jpn., 28 (1970), pp. 1321–1329.

[28] L. van Wijngaarden, *On the motion of gas bubbles in a perfect fluid*, Ann. Rev. Fluid Mech., 4 (1972), pp. 369–373.

[29] G. Gao, *A theory of interaction between dissipation and dispersion of turbulence*, Sci. Sinica (Ser. A), 28 (1985), pp. 616–627.

[30] Y. N. Zayko, I. S. Nefedov, *New class of solutions of the Korteweg-de Vries-Burgers equation*, Appl. Math. Lett., 14 (2001), pp. 115–121.

[31] Z. Feng, *An exact solution to the Korteweg-de Vries-Burgers equation*, Appl. Math. Lett., 18 (2005), pp. 733–737.

[32] A. S. Sharma, H. Tasso, *Connection between wave envelope and explicit solution of a nonlinear dispersive equation*, Report IPP 6/158, 1977.

[33] P. J. Olver, *Evolution equations possessing infinitely many symmetries*, J. Math. Phys., 18 (1977), pp. 1212–1216.

[34] Z. Lian, S. Y. Lou, *Symmetries and exact solutions of the Sharma-Tasso-Olver equation*, Nonlinear Analysis: Theory, Methods and Applications, 63 (2005), pp. 1167–1177.

[35] A. M. Wazwaz, *Integrable couplings of the Burgers equation and the Sharma-Tasso-Olver equation*, Romanian Reports in Physics, 65 (2013), pp. 383–390.

[36] J. L. Vazquez, *Smoothing and Decay Estimates for Nonlinear Parabolic Equations of Porous Medium Type*, Oxford Univ. Press, Oxford, 2006.

[37] H. A. Levine, L. E. Payne, *Nonexistence theorems for the heat equation with nonlinear boundary conditions and for the porous medium equation backward in time*, J. Differ. Equat., 16 (1974), pp. 319–334.

[38] W. Craig, J. Goodman, *Linear dispersive equations of Airy type*, J. Differ. Equat., 87 (1990), pp. 38–61.

[39] H. Cai, *Dispersive smoothing effects for KdV type equations*, J. Differ. Equat., 136 (1997), pp. 191–221.

[40] W. Craig, T. Kappeler, W. Strauss, *Gain of regularity for equations of KdV type*, Ann. Inst. H. Poincare, 9 (1992), pp. 147–186.

[41] A. M. Wazwaz, *Travelling wave solutions of generalized forms of Burgers, Burgers-KdV and Burgers-Huxley equations*, Appl. Math. Comput., 169 (2005), pp. 639–656.

[42] V. A. Galaktionov, S. I. Pohozaev, *Third-order nonlinear dispersive equations: shocks, rarefaction, and blowup waves*, Comp. Math. Math. Phys., 48 (2008), pp. 1784–1810.

[43] C. E. Kenig, G. Ponce, L. Vega, *Higher-order nonlinear dispersive equations*, Proc. Amer. Math. Soc., 122 (1994), pp. 157–166.

[44] L. L. Dawson, *Uniqueness properties of higher order dispersive equations*, J. Differ. Equat., 236 (2007), pp. 199–236.

[45] R. S. Fernandes, *Very Singular Solutions of Odd-Order PDEs, with Linear and Nonlinear Dispersion*, PhD thesis, University of Bath, Nov 2008.

[46] G. W. Griffiths, W. E. Schiesser, *Traveling Wave analysis of Partial Differential Equations: Numerical and Analytical Methods with MATLAB and MAPLE*, Academic Press, New York, 2011.

[47] V. A. Galaktionov, E. L. Miditieri, S. I. Pohozaev, *Blow-up for Higher-Order Parabolic, Hyperbolic, Dispersion and Schrödinger Equations (Monographs and Research Notes in Mathematics)*, Chapman and Hall/CRC, Boca Raton, 2014.

[48] J. D. Evans, V. A. Galaktionov, J. R. King, *Unstable sixth-order thin film equation: I. Blow-up similarity solutions*, Nonlinearity, 20 (2007), pp. 1799–1841.

[49] V. A. Galaktionov, J. L. Vazquez, *The problem of blow-up in nonlinear parabolic equations*, Discr. Cont. Dyn. Syst., 8 (2002), pp. 399–433.

[50] A. A. Samarskii, V. A. Galaktionov, S. P. Kurdyumov, A. P. Mikhailov, *Blow-up in Quasilinear Parabolic Equations*, De Gruyter, New York, 1995.

[51] W. M. Ni, P. E. Sacks, J. Tavantzis, *On the asymptotic behavior of solutions of certain quasilinear parabolic equations*, J. Differ. Equat., 54 (1984), pp. 97–120.

[52] V. A. Galaktionov, *Single point gradient blow-up and nonuniqueness for a third-order nonlinear dispersion equation*, Stud. Appl. Math., 126 (2011), pp. 103–143.

[53] M. A. Herrero, J. L. Vazquez, *Singularity formation on the one-dimensional supercooled Stefan problem*, Euro J. Appl. Math., 7 (1996), pp. 119–150.

[54] J. M. Ball, *Remarks on blow-up and nonexistence theorems for nonlinear evolution equations*, Quart. J. Math. Oxford, 28 (1977), pp. 473–486.

[55] C. Bandle, H. Brunner, *Blow-up in diffusion equations: a survey*, J. Comp. Appl. Math., 97 (1998), pp. 3–22.

[56] K. Deng, H. A. Levine, *The Role of Critical Exponents in Blow-Up Theorems: The Sequel*, J. Math. Anal. Appl., 243 (2000), pp. 85–126.

[57] T. Suzuki, *The Blowup Mechanism in Nonlinear Partial Differential Equations: Scaling and Variation*, Partial Differential Equations: Theory, Analysis and Applications, Mathematics Research Developments (2011), pp. 339–345.

[58] B. Hu, *Blow-up Theories for Semilinear Parabolic Equations*, Springer-Verlag, New York, 2011.

[59] V. A. Galaktionov, *Incomplete self-similar blow-up in a semilinear fourth-order reaction-diffusion equation*, Stud. Appl. Math., 124 (2010), pp. 347–381.

[60] V. A. Galaktionov, *Vast Multiplicity of Very Singular Self-Similar Solutions of a Semilinear Higher-Order Diffusion Equation with Time-Dependent Absorption*, J. Math. Sci. Univ. Tokyo, 17 (2010), pp. 323–358.

[61] J. D. Evans, V. A. Galaktionov, J. F. Williams, *Blow-up and global asymptotics of the limit unstable Cahn-Hilliard equation*, SIAM J. Math. Anal., 38 (2006), pp. 64–102.

[62] J. D. Evans, V. A. Galaktionov, J. R. King, *Blow-up similarity solutions of the fourth-order unstable thin film equation*, Euro J. Appl. Math., 18 (2007), pp. 195–231.

[63] J. D. Evans, V. A. Galaktionov, J. R. King, *Unstable sixth-order thin film equation: II. Global similarity patterns*, Nonlinearity, 20 (2007), pp. 1843–1881.

[64] C. J. Budd, V. A. Galaktionov, J. F. Williams, *Self-similiar blow-up in higher-order semilinear parabolic equations*, SIAM J. Math. Anal., 64 (2004), pp. 1775–1809.

[65] F. Merle, P. Raphael, J. Szeftel, *Stable self-similar blow-up dynamics for slightly L^2 super-critical NLS equations*, Geom. Funct. Anal., 20 (2010), pp. 1028–1071.

[66] T. Cazenave, *Finite-time blowup for a family of nonlinear parabolic equations*, Lecture notes prepared for VI ENAMA, Aracaju, Brazil, Nov 2012.

[67] S. Kaplan, *On the growth of solutions of quasilinear parabolic equations*, Comm. Pure Appl. Math., 16 (1963), pp. 305–330.

[68] H. A. Levine, *Some nonexistence and instability theorems for formally parabolic equations of the form* $Pu_t = -Au + f(u)$, Arc. Ration. Mech. Anal., 51 (1973), pp. 371–386.

[69] B. Hu, H. M. Yin, *The profile near blow-up time for solution of the heat equation with a nonlinear boundary condition*, Trans. Am. Math. Soc., 346 (1994), pp. 117–135.

[70] R. T. Glassey, *: On the blowing up of solutions to the Cauchy problem for nonlinear Schrödinger equations*, J. Math. Phys., 18 (1977), pp. 1794–1797.

[71] H. Fujita, *: On the blowing up of solutions to the Cauchy problem for* $u_t = \Delta u + u^\alpha$, J. Fac. Sci. Univ. Tokyo Sect. A. Math., 16 (1966), pp. 105–113.

[72] G. I. Barenblatt, *Scaling, Self-similarity, and Intermediate Asymptotics*, Cambridge University Press, Cambridge, 1996.

[73] J. Eggers, M. A. Fontelos, *The role of self-similarity in singularities of partial differential equations*, Nonlinearity, 22 (2009), pp. R1–R44.

[74] W. F. Osgood, *Beweis der Existenz einer Lösung der Differentialgleichung* $dy/dx = f(x, y)$ *ohne Hinzunahme der Cauchy-Lipschitz'schen Bedingung (German)*, Monatsh. Math. Phys., 9 (1898), pp. 331–345.

[75] K. Hayakawa, *On the nonexistence of global solutions of some semilinear parabolic equations*, Proc. Japan Acad., 49 (1973), pp. 503–525.

[76] K. Kobayashi, T. Sirao, H. Tanaka, *On the blowing up problem for semilinear heat equations*, J. Math. Soc. Japan, 29 (1977), pp. 407–424.

[77] D. Aronson, H. F. Weinberger, *Multidimensional nonlinear diffusion arising in population genetics*, Adv. Math., 30 (1978), pp. 33–76.

[78] Y. Giga, R. V. Kohn, *Asymsptotic self-similar blow-up of semilinear heat equation*, Comm. Pure Appl. Math., 38 (1985), pp. 297–319.

[79] J. F. Williams, *Scaling and singularities in higher-order nonlinear differential equations*, PhD thesis, University of Bath, 2003.

[80] V. A. Galaktionov, J. L. Vazquez, *Continuation of blow-up solutions of nonlinear heat equations in several space dimensions*, Comm. Pure Appl. Math., 50 (1997), pp. 1–68.

[81] M. Fila, *Blow-up of solutions of semilinear parabolic equations*, Special lectures at Tohoku University, 9-12 May, 2006.

[82] A. A. Lacey, D. E. Tzanetis, *Global, Unbounded Solutions to a Parabolic Equation*, J. Diff. Eq., 101 (1993), pp. 80–102.

[83] Y. Martel, F. Merle, *Nonexistence of blow-up solution with minimal L^2-mass for the critical gKdV equation*, Duke Math. J., 115 (2002), pp. 385–408.

[84] J. L. Bona, P. E. Souganidis, W. A. Strauss, *Stability and instability of solitary waves of Korteweg-de Vries type*, Proc. R. Soc. Lond. A, 411 (1987), pp. 395–412.

[85] U. Erdoğan, H. Koçak, *Numerical study of the asymptotic of the second Painlevé equation by a functional fitting method*, Math. Meth. Appl. Sci., 36 (2013), pp. 2347–2352.

[86] U. Erdoğan, H. Koçak, *A reliable scheme with large time steps for second order initial value problems*, Submitted.

[87] R. R. Rosales, *The similarity solution for the Korteweg-de Vries equation and the related Painlevé transcendent*, Proc. R. Soc. Lond. A., 361 (1978), pp. 265–275.

[88] S. P. Hastings, J. B. McLeod, *A boundary value problem associated with the second Painlevé transcendent and the Korteweg-de Vries equation*, Arch. Rat. Mech. Anal., 73 (1980), pp. 31–51.

[89] P. A. Clarkson, *Asymptotics of the second Painlevé transcendent*, Special functions and orthogonal polynomials, Contemp. Math., 471 (2008), pp. 69–83.

[90] E. A. Coddington, N. Levinson, *Theory of Ordinary Differential Equations*, McGraw-Hill Book Company, Inc., New York/London, 1955.

[91] U. Erdoğan, *On the Numerical Solution of Differential Equations by Exponentially Fitted (EF) Methods*, PhD Thesis, Ege University, 2012.

[92] G. V. Berghe, H. D. Meyer, M. V. Daele, T. V. Hecke, *Exponentially-fitted explicit Runge-Kutta methods*, Comp. Phys. Comm., 123 (1999), pp. 7–15.

[93] G. V. Berghe, H. D. Meyer, M. V. Daele, T. V. Hecke, *Exponentially fitted Runge-Kutta methods*, J. Comput. Appl. Math., 125 (2000), pp. 107–115.

[94] G. V. Berghe, L. G. Ixaru, H. D. Meyer, *Frequency determination and step-length control for exponentially-fitted Runge-Kutta methods*, J. Comput. Appl. Math., 132 (2001), pp. 95–105.

[95] G. V. Berghe, L. G. Ixaru, M. V. Daele, *Optimal implicit exponentially-fitted Runge-Kutta methods*, Comp. Phys. Comm., 140 (2001), pp. 346–357.

[96] X. Wu, B. Wang, J. Xia, *Explicit symplectic multidimensional exponential fitting modified Runge-Kutta-Nyström methods*, BIT Numer. Math., 52 (2012), pp. 773–795.

[97] T. Ozis, U. Erdogan, *Efficient exponential fitting algorithm with two fitting parameters for oscillation problem*, AIP Conf. Proc., 1389 (2013), pp. 1594–1596.

[98] A. Konguetsof, T. Simos, *An exponentially-fitted and trigonometrically-fitted method for the numerical solution of periodic initial-value paroblems*, Comp. Math. Appl., 45 (2003), pp. 547–554.

[99] H. V. de Vyver, *Frequency evaluation for exponentially fitted Runge-Kutta methods*, J. Comput. Appl. Math., 184 (2005), pp. 442–463.

[100] P. Williams, T. Simos, *A new family of exponentially fitted methods*, Math. Comput. Model., 38 (2003), pp. 571–584.

[101] G. V. Berghe, M. V. Daele, H. V. Vyver, *Exponentially fitted Runge-Kutta methods of collocation type: fixed or variable know points?*, J. Comput. Appl. Math., 159 (2003), pp. 217–239.

[102] U. Erdogan, T. Ozis, *A smart nonstandard finite difference scheme for second order nonlinear boundary value problems*, J. Comp. Phys., 230 (2011), pp. 6464–6474.

[103] E. Süli, D. F. Mayers, *An Introduction to Numerical Analysis*, Cambridge University Press, Cambridge, UK, 2003.

[104] J. P. Coleman, L. G. Ixaru, *Truncation errors in exponential fitting for oscillatory problems*, SIAM J. Numer. Anal., 44 (2006), pp. 1441–1465.

[105] L. G. Ixaru, G. V. Berghe, H. D. Meyer, *Frequency evaluation in exponential fitting multistep algorithms for ODEs*, J. Comput. Appl. Math., 140 (2002), pp. 561–599.

[106] H. Ramos, J. Vigo-Aguiar, *On the frequency choice in trigonometrically fitted methods*, Appl. Math. Lett., 23 (2010), pp. 1378–1381.

[107] J. Butcher, J. Vigo-Aguiar, *Numerical Methods for Ordinary Differential Equations*, John Wiley&Sons, UK, 2003.

[108] K. Iwasaki, H. Kimura, S. Shimomura, M. Yoshida, *From Gauss to Painlevé: a Modern Theory of Special Functions*, Vol. 16, Aspects of Mathematics E, Viewag, Braunschweig, Germany, 1991

[109] J. W. Miles, *On the second Painlevé Transcendent*, Proc. R. Soc. Lond. A, 361 (1978), pp. 277-291.

[110] J. W. Miles, *The second Painlevé transcendent: a nonlinear Airy function*, Mechanics Today, 5 (1980), pp. 297-313.

[111] D. Witthaut, H. J. Korsch, *Uniform semiclassical approximations of the nonlinear Schrödinger equation by a Painlevé mapping*, J. Phys. A: Math. Gen, 39 (2006), pp. 14687-14697.

[112] E. Hesameddini, H. Latifizadeh, *Homotopy analysis method to obtain numerical solutions of the Painlevé equations*, Math. Meth. Appl. Sci., 35 (2012), pp. 1423–1433.

[113] M. Dehghan, F. Shakeri, *The numerical solution of the second painlevé equation*, Numer Meth. Part. Diff. Eq., 25 (2009), pp. 1238–1259.

[114] R. Ellahi, S. Abbasbandy, T. Hayat, A. Zeeshan, *On comparison of series and numerical solutions for second Painlevé Equation*, Numer Meth. Part. Diff. Eq., 26 (2010), pp. 1070–1078.

[115] E. Hesameddini, A. Peyrovi, *Homotopy perturbation method for second Painlevé equation and comparisons with analytic continuation extension and Chebyshev series method*, International Mathematical Forum, 5 (2010), pp. 629–637.

[116] B. Fornberg, J. A. C. Weideman, *A computational exploration of the second Painlevé equation*, Foundations of Computational Mathematics, 14 (2014), pp. 985–1016.

[117] T. E. Simos, *Exponentially fitted Runge-Kutta-Nyström method for the numerical solution of initial-value problems with oscillating solutions*, Appl. Math. Lett., 15 (2002), pp. 217–225.

[118] A. Lunardi, *Analytic Semigroups and Optimal Regularity in Parabolic Problems*, Birkhäuser, Berlin, 1995.

[119] M. A. Krasnosel'skii, P. P. Zabreiko, *Geometrical Methods of Nonlinear Analysis*, Springer-Verlag, Berlin/Tokyo, 1984.

[120] T. A. Driscoll, N. Halem, L. N. Trefethen, *Chebfun Guide*, Pafnuty Pubblications, Oxford, 2014.

[121] L. N. Trefethen et al., *Chebfun Version 5.1*, The Chebfun Development Team, (2014), http://www.chebfun.org/.

[122] A. M. Wazwaz, *The sine-cosine method for obtaining solutions with compact and noncompact structures*, Appl. Math. Comput., 159 (2004), pp. 559–576.

[123] P. Rosenau, *On nonanalytic solitary waves formed by a nonlinear dispersion*, Phys. Lett. A, 23 (1997), pp. 305–318.

[124] A. M. Wazwaz, *The tanh method for compact and noncompact solutions for variants of the KdV-Burger and the $K(n,n)$-Burger equations*, Physica D, 213 (2006), pp. 147–151.

[125] A. M. Wazwaz, *Private Communication.*

[126] S. Blanes, F. D. C. Maragni, S. Ragni, *Splitting and composition methods for explicit time dependence in separable dynamical systems*, J. Comput. Appl. Math., 235 (2010), pp. 646–659.

[127] M. Seydaoğlu, S. Blanes, *High-order splitting methods for separable non-autonomous parabolic equations*, Appl. Numer. Math., 84 (2014), pp. 22–32.